

CALIFORNIA INSTITUTE OF TECHNOLOGY

DANIEL AND FLORENCE GUGGENHEIM JET PROPULSION CENTER

ANALYTICAL STUDIES OF STEADY AND NON-STEADY MOTIONS OF A BUBBLY LIQUID

by
William A. Symington

May 1978

SUPPORTED THROUGH CONTRACT NUMBER EX-76-G-03-1305
U. S. DEPARTMENT OF ENERGY

CALIFORNIA INSTITUTE OF TECHNOLOGY
Division of Engineering and Applied Science
Daniel and Florence Guggenheim Jet Propulsion Center
Kármán Laboratory of Fluid Mechanics and Jet Propulsion

ANALYTICAL STUDIES OF STEADY AND NON-STEADY
MOTIONS OF A BUBBLY LIQUID

William A. Symington

May 1978

Performed With the Support of the
U. S. Department of Energy
Contract EX-76-G-03-1305

ABSTRACT

A consistent set of continuum-like equations which describe, under certain limitations, the flow of bubbly gas-liquid mixtures is applied in the solution of a few problems that bear on technological issues of nuclear reactor safety. The solutions of these problems illustrate the significance of the ratio between the viscous relaxation time of the bubbles and the characteristic time of the flow, in scaling experimental results.

The choked flow of a bubbly mixture through a contraction in a one-dimensional duct is treated. It is found that in many cases the ratio of the contraction residence time to the viscous relaxation time is small, indicating the motion of the bubbles will be dictated largely by the dynamic forces on them. The one-dimensional equations are solved approximately for small values of this ratio.

A rudimentary experiment on choked bubbly flow through a contraction was conducted using a contraction with gradual changes in area, making the experimental situation amenable to a one-dimensional analysis. Distributions of pressure and mass flow rates of liquid and gas were measured. The results compare favorably with theoretical calculations.

The rise through a liquid of a uniform cloud of bubbles is also analyzed. Self-preserving wave solutions of the non-linear equations are found to exist and have the form of transitions between a region of high void fraction below and a region of lower void fraction above. These waves are unstable to small disturbances in response to which they will steepen, developing

into clumps of bubbles above which are regions of low void fraction. The fact that the bubbles in these clumps may coalesce presents a mechanism for a change in flow regime from bubbly to some other, perhaps slug or annular flow. The effect of bubble-bubble interactions in impeding the formation of these clumps is speculated upon.

Finally, the flow of a bubbly mixture over a wavy wall is analyzed. The solution illustrates some of the important deviations from one-dimensional flow and shows the manner in which phase separation tends to make use of the strict one-dimensional flow assumption more limited than in single phase flow. The solution is incomplete in the sense that the effect of interactions between bubbles and solid boundaries is lacking.

TABLE OF CONTENTS

Chapter	Title	Page
	Abstract	ii
	Table of Contents	iv
	List of Illustrations	vi
	List of Tables	ix
1	Introduction	1
	References	7
2	The Equations Governing Bubbly Two-Phase Flow	10
	References	22
	Notation for Chapter 2	23
3	One-Dimensional Flow in a Duct	25
	References	46
	Notation for Chapter 3	47
4	Experiments on One-Dimensional Duct Flow	57
	References	65
5	The Rise of a Cloud of Bubbles Through a Liquid	80
	5.1 Statement of the Problem	80
	5.2 Linear Analysis of the Growth of a Disturbance	83
	5.3 Non-Linear Analysis of the Growth of a Disturbance	91
	5.4 Speculation on the Effect on Bubble-Bubble Interactions	99

TABLE OF CONTENTS (Cont'd.)

Chapter	Title	Page
	References	104
	Notation for Chapter 5	105
6	Bubbly Flow over a Wavy Wall	120
	References	130
	Notation for Chapter 6	131
7	Concluding Remarks	133

LIST OF ILLUSTRATIONS

Figure Number	Caption	Page
2.1	Geometry and Notation for Calculation of Forces on a Single Bubble	24
4.1	Photograph of the Contraction	67
4.2	Dimensions of the Contraction	68
4.3	Photograph of the Bubble Injection Tubes	69
4.4	Schematic of Flow System	70
4.5	Photographs of the Flow in the Contraction; Upstream Void Fraction Approximately 0.1	71
4.6	Area (Normalized by Throat Area) vs. Pressure (Normalized by Upstream Pressure); Experiment and Theory - Run 3; Upstream Void Fraction = 0.175	72
4.7	Area (Normalized by Throat Area) vs. Pressure (Normalized by Upstream Pressure); Experiment and Theory - Run 4; Upstream Void Fraction = 0.120	73
4.8	Area (Normalized by Throat Area) vs. Pressure (Normalized by Upstream Pressure); Experiment and Theory - Run 5; Upstream Void Fraction = 0.211	74
4.9	Area (Normalized by Throat Area) vs. Pressure (Normalized by Upstream Pressure); Experiment and Theory - Run 6; Upstream Void Fraction = 0.307	75
4.10	Area (Normalized by Throat Area) vs. Pressure (Normalized by Upstream Pressure); Experiment and Theory - Run 8; Upstream Void Fraction = 0.149	76
4.11	Area (Normalized by Throat Area) vs. Pressure (Normalized by Upstream Pressure); Experiment and Theory - Run 17; Upstream Void Fraction = 0.096	77

LIST OF ILLUSTRATIONS (Cont'd.)

Figure Number	Caption	Page
4.12	Dimensionless Throat Pressure, p_{th}/p_0 , vs. Upstream Void Fraction, α_0 , for a Choked Contraction; Experiment and Theory	78
4.13	Critical Pressure Ratio, p^*/p_0 , vs. Upstream Volume Flow Fraction, β ; Comparison of Theory to Data of Reference 4.2	79
5.1	Geometry and Notation for One-Dimensional Analysis of a Disturbance to a Uniform Bubble Cloud	110
5.2	Normalized Phase Speed $\frac{-(1+3\gamma)b_{\pm}(k)}{3\gamma k}$ vs. Wave Number, k	111
5.3	Solution of Linearized Equations for One-Dimensional Disturbance; Void Fraction Perturbation	112
5.4	Solution of Linearized Equations for One-Dimensional Disturbance; Gas Velocity Perturbation	113
5.5	Solution of Linearized Equations for One-Dimensional Disturbance; Liquid Velocity Perturbation	114
5.6	Solution of Linearized Equations for One-Dimensional Disturbance; Pressure Perturbation	115
5.7	A Permanent Wave Solution, Void Fraction, α , vs. ETA, $\frac{y + u_0 t}{V_0 \tau_v}$	116
5.8	A Solution of the Burger's Equation for a One-Dimensional Disturbance	117
5.9	Development of a Long Length Scale Disturbance	118
5.10	Geometry and Notation for Bubble-Bubble Interaction Calculation	119

LIST OF ILLUSTRATIONS (Cont'd.)

Figure Number	Caption	Page
6.1	Geometry and Notation for Bubbly Flow over a Wavy Wall	132

LIST OF TABLES

Table Number	Title	Page
3.1	Computed Solution for a Choked Contraction - Zeroth Order	48
3.2	Computed Solution for a Choked Contraction - Zeroth Order	49
3.3	Computed Solution for a Choked Contraction - Zeroth Order	50
3.4	Computed Solution for a Choked Nozzle - Zeroth and First Orders	51
3.5	Computed Solution for a Choked Nozzle - Zeroth and First Orders	53
3.6	Computed Solution for a Choked Nozzle - Zeroth and First Orders	55
4.1	Summary of Experimental Data	66
5.1	Pertinent Data on 1/32" Diameter Air Bubbles Rising in Water	107
5.2	Computed Values of the Functions $a_{\pm}(k)$ and $b_{\pm}(k)$	108
5.3	Computed Values of the Functions $a_{\pm}(k)$ and $b_{\pm}(k)$	109

CHAPTER 1

Introduction

In recent years the difficulties in our understanding of two-phase flow systems have become apparent, largely through our concern over the safety of nuclear power plants. In the so-called Loss of Coolant Accident, considered to be one of the most troublesome problems for a nuclear reactor, the pipe supplying the cooling fluid to the reactor is assumed to break allowing the reactor to depressurize rapidly. Because of this rapid depressurization vapor would be generated in the reactor, and the ensuing flow of coolant from the reactor would almost certainly be a bubbly one, at least initially.

One peculiarity of such bubbly flows is that the fluid, considered as a continuum, supports a system of acoustic waves that move with velocities that may be less than 40 m/sec. Such flows exhibit some features of gas dynamic flow fields in addition to their other complexities. It is the purpose of this thesis to examine some of the properties of bubbly flows by solving some relatively elementary problems which, although perhaps not of great technological interest in themselves, contribute to the understanding of more complex flow fields.

In an early investigation, Tangren, Dodge and Seifert (1.1), 1949, used a homogeneous flow model to analyze the choked flow of a bubbly mixture through a nozzle. Isbin, Moy and DaCruz (1.2), 1957, performed an experiment on the choked flow of a steam-water mixture. They found that the homogeneous flow model did not

describe the situation adequately. Muir and Eichhorn (1.3), 1963, performed an extensive experimental investigation on the choked flow of an air-water mixture. The use of an air-water mixture removed complications due to phase change. Muir and Eichhorn concluded that the inability to account for slip between the phases of the homogeneous flow model of Tangren, Dodge and Seifert was a major factor in accounting for the differences in the theoretical and experimental results. Experiments very similar to those of Muir and Eichhorn were performed by Henry (1.4), 1971 and Baum (1.5), 1972. Their motivation was to ascertain whether a choked nozzle could be used to measure the gas content in liquid sodium, as described by Henry (1.6), 1970. The analytical models of Zivi (1.7), 1964, Moody (1.8), 1965, Cruver and Moulton (1.9), 1967 and Fauske (1.10) 1964 attempt to account for slip between the phases by using the slip ratio as a parameter with respect to which different physical quantities are maximized. The correctness of such a model is questionable. Levy (1.11), 1965, accounts for the slip between the phases in a separated flow by neglecting friction between the two phases, and using a momentum equation for each phase. Models based on the idea that a sound wave cannot propagate upstream through the throat of a choked nozzle have been presented by D'Arcy (1.12), 1971 and Baum and Horn (1.13), 1971. The difficulty with these models lies in postulating the relationship between the differential changes in gas and liquid velocity across a sound wave. For a separated flow Giot and Fritte (1.14), 1972, demonstrated that the slip must be determined

from a momentum equation for each phase and that interphase friction and heat transfer is important in determining the critical flow rate. Bouré, Fritte, Giot and Réocreux (1.15), 1976, have recently pointed out the similarities between two-phase and single-phase critical flow and have postulated the possible importance of gradient dependant interphase transport mechanisms in the former. Restricting their attention to bubbly flow, Prosperatti and Van Wijngaarden (1.16), 1976, have offered an explanation of critical flow in terms of the characteristics of the equations of motion. A great deal of the analytical work mentioned here is discussed in more detail in the book by Hsu and Graham (1.17), 1976.

Analytical studies of situations where compressibility is not an important feature have usually either assumed that the flow is homogeneous, as did Gonzalez and Lahey (1.18), 1973, or used a drift flux model. Drift flux models are described in detail in the book by Wallis (1.19), 1969. Zuber and Staub (1.20), 1967, analyzed a two-phase boiling system using a drift flux model and showed it to be a form of the theory of kinematic waves (1.21, 1.22), 1955. They also verified experimentally the accuracy of their analysis (1.23, 1.24), 1966, 1967. Of course these models are only accurate for low frequency transients.

In Chapter 2 of this thesis we derive equations which, under certain approximations, describe the flow of a bubbly mixture in three dimensions. These equations state mathematically that the mass of both gas and liquid are separately conserved, that the momentum of the mixture is conserved, and that the sum of the

forces on each of the bubbles is equal to its mass times its acceleration. The first three of these have appeared in the literature before (1.25) and are well accepted. The fourth has apparently entered the literature only recently (1.26) in a less general form.

In Chapter 3 we consider the choked flow of a bubbly mixture through a contraction in a one-dimensional duct, accounting for the relative motion of the two phases. It is found that in many instances the relative motion between the bubbles and liquid is almost wholly determined by the dynamic forces on the bubbles and that the viscous forces are unimportant. A perturbation solution of the governing equations is presented, in which the small parameter is the ratio between the residence time of a bubble in the contraction and the time associated with the action of viscosity in slowing down the bubbles.

It is easily shown that the restrictions guaranteeing the accuracy of one-dimensional flow are more severe for bubbly flow than for homogeneous liquids. As a consequence, there is considerable doubt whether the experiment of Muir and Eichhorn can be well described by a one-dimensional analysis. Therefore, some rudimentary experiments on the choked flow of a bubbly mixture through a contraction were performed using a duct with very gradual area changes. The results of these experiments, described in Chapter 4, are compared with the theoretical solution presented in Chapter 3. The comparison is quite reasonable even for void fractions as high as .3 or .4. This indicates that the

flow is still bubbly at these high void fractions, probably because the bubbles are created not very far upstream of the contraction. This implies that in the blow down of a reactor vessel, if the bubbles are nucleated homogeneously, the flow may remain bubbly to void fractions higher than previously expected.

In Chapter 5 we study the motion and stability of a cloud of gas bubbles rising through a liquid; the goal being to describe the development of a disturbance to the uniform void fraction. Although the resulting problem is mathematically ill-posed, we find that we may still describe the growth of such a disturbance quite reasonably. Both a solution of the linearized equations and singular perturbation analysis applicable to long length scale disturbances are presented. The results suggest that the growth of these disturbances may be a mechanism for a change in the flow regime from bubbly to some other, perhaps slug or annular flow. A question posed by the results of this analysis is: whether or not bubble-bubble interactions may impede the growth of a disturbance and hence prevent such a change of flow regime.

Chapter 6 deals with the flow of a bubbly mixture over a wavy wall. It is found that when the waves in the wall are of small amplitude both the gas and liquid velocity fields may be described by potentials. The governing equations are then solved in linearized form. The solution illustrates clearly the basic character of the motion of the bubbles; reacting more quickly to a pressure gradient than the liquid. Also, being a two-dimensional problem, it demonstrates directly the consequences of our inability

to prescribe a boundary condition on the gas velocity field at a solid boundary. This difficulty arises due to our neglect of forces due to interactions with boundaries in deriving the equation of motion for the bubbles. It results in our solution being invalid in a thin layer near the wall which is of a thickness on the order of the range of these interaction forces.

This work was supported in part by U. S. Department of Energy Contract EX-76-G-03-1305; the opinions expressed here are not necessarily those of the U. S. Department of Energy.

REFERENCES

- 1.1 R.H. Tangren, C.H. Dodge and H. S. Seifert, "Compressibility Effects in Two-Phase Flow", Journal of Applied Physics Volume 20, Number 7, July 1949, pp. 637 - 645.
- 1.2 H. S. Isbin, J. E. Moy and A. J. R. DaCruz, "Two-Phase Steam Water Critical Flow", AIChE Journal Volume 3, 1957, pp. 361 - 365.
- 1.3 T. F. Muir and R. Eichhorn, "Compressible Flow of an Air-Water Mixture Through a Vertical Two-Dimensional Converging - Diverging Nozzle", Proceedings of the 1963 Heat Transfer and Fluid Mechanics Institute, Stanford University, 1963, Stanford University Press, pp. 183 - 204.
- 1.4 R. E. Henry, "Experiments on Entrained Gas Detection", Transactions of the American Nuclear Society Volume 14, 1971, p. 277.
- 1.5 M. R. Baum, "An Experimental Study of Adiabatic Choked Gas-Liquid Bubble Flow in a Convergent-Divergent Nozzle", Trans. Instn. Chem. Engrs. Volume 50, 1972, pp. 293 - 299.
- 1.6 R. E. Henry, "Gas Detection with a Choked Converging-Diverging Nozzle", Transactions of the American Nuclear Society Volume 13, 1970, pp. 794 - 795.
- 1.7 S. M. Zivi, "Estimation of Steady State Steam Void Fraction by Means of the Principle of Minimum Entropy Production", Journal of Heat Transfer, Trans. ASME Volume 86, 1964, pp. 247 - 252.
- 1.8 F. J. Moody, "Maximum Flow Rate of a Single Component Two Phase Mixture", Journal of Heat Transfer Volume 87, Trans ASME 1965, pp. 134 - 142.
- 1.9 J. E. Cruver, R. W. Moulton, "Critical Flow of Liquid-Vapor Mixtures", AIChE Journal Volume 13, 1967, pp. 52 - 60.
- 1.10 H. K. Fauske, "Some Ideas About the Mechanisms Causing Two-Phase Critical Flow", Applied Scientific Research A13, 1964, pp. 149 - 160.
- 1.11 S. Levy, "Prediction of the Two-Phase Critical Flow Rate", Journal of Heat Transfer Trans. ASME Volume 87, 1965, pp. 53 - 58.
- 1.12 D. F. D'Arcy, "On Acoustic Propagation and Critical Mass Flux in Two-Phase Flow", Journal of Heat Transfer Trans. ASME Volume 93, 1971, pp. 413 - 421.

- 1.13 M. R. Baum and G. Horn, "The Speed of Sound in Non-Equilibrium-Gas Liquid Flow: Predicting the Onset of Choked Flow in a Sodium-Water Heat Exchanger", Nuclear Engineering and Design Volume 16, 1971, pp. 193 - 203
- 1.14 M. Giot and A. Fritte, "Two Phase Two and One Component Critical Flows with the Variable Slip Model", Progress in Heat and Mass Transfer Volume 6, 1972, pp. 651 - 670.
- 1.15 J. A. Bouré, A. A. Fritte, M. M. Giot and M. L. Réocreux, "Highlights of Two-Phase Critical Flow", Int. Journal of Multiphase Flow Volume 3, 1976, pp. 1 - 22.
- 1.16 A. Prosperetti and L. Van Wijngaarden, "On the Characteristics of the Equations of Motion for Bubbly Flow and the Related Problem of Critical Flow", Journal of Engineering Mathematics Volume 10, 1976, pp. 153 - 162.
- 1.17 Y. Hsu and R. W. Graham, "Transport Processes in Boiling and Two-Phase Systems" 1976, Hemisphere Publishing Corporation, Chapter 11.
- 1.18 J. M. Gonzales, R. T. Lahey, Jr., "An Exact Solution for Flow Transients in Two-Phase Systems by the Method of Characteristics", Journal of Heat Transfer, Trans. ASME Volume 95, 1973, pp. 470 - 476.
- 1.19 G. B. Wallis, One-Dimensional Two-Phase Flow, 1969, McGraw-Hill Book Company, New York, Chapter 4.
- 1.20 N. Zuber and F. W. Staub, "An Analytical Investigation of the Transient Response of the Volumetric Concentration in a Boiling Forced Flow System", Nuc. Sci. and Eng. Volume 30, 1967, pp. 268 - 278.
- 1.21 M. J. Lighthill and G. B. Whitham, "On Kinematic Waves I Flood Movement in Long Rivers", Proceedings of the Royal Society Volume 229, 1955, pp. 281 - 316.
- 1.22 M. J. Lighthill and G. B. Whitham, "On Kinematic Waves II A Theory of Traffic Flow on Long Crowded Roads", Proceedings of the Royal Society Volume 229, 1955, pp. 317 - 345.
- 1.23 N. Zuber and F. W. Staub, "The Propagation and the Wave Form of the Vapor Volumetric Concentration in Boiling Forced Convection System under Oscillatory Conditions", Int. Journal of Heat and Mass Transfer Volume 9, 1966, pp. 871 - 895.

- 1.24 F. W. Staub, N. Zuber and G. Bijwaard, "Experimental Investigation of the Transient Response of the Volumetric Concentration in a Boiling Forced Flow System", Nuc. Sci. and Eng. Volume 30, 1967, pp. 279 - 295.
- 1.25 M. Ishii, Thermo-Fluid Dynamics Theory of Two-Phase Flow , 1975, Eyrolles, Chapter 5.
- 1.26 I. M. Chernyy, "Concerning the Dynamics of Bubble-Type Flows in a Gas-Liquid Nozzle", Fluid Mechanics - Soviet Research Volume 2, Number 6, Nov. - Dec. 1973, pp. 92 - 99.

CHAPTER 2

The Equations Governing Bubbly Two-Phase Flow

The description of the flow of a liquid-bubble mixture as a continuous medium is not completely agreed upon, largely because of the "constitutive relations" which describe interactions between bubbles and liquid.

Many aspects of the flow of liquid-bubble mixtures can be described using simple formulations which ignore relative motion between the bubbles and liquid. Such a model was successfully used by van Wijngaarden (2.1), 1968, to study pressure waves of small and moderate amplitude propagating in a bubbly mixture. Of course, such a formulation will be of little help if prediction of the extent to which the bubbles will migrate through the liquid is the desired result.

A formulation accounting for relative motion in a general (not necessarily bubbly) two-phase flow has been presented by Ishii (2.2), 1975. He shows that mathematically rigorous continuum equations may be obtained by time-averaging the governing equations for each individual phase. In this manner he obtains mass, momentum and energy conservation equations for each phase. These equations involve unspecified interfacial transfer terms, which would depend on flow regime. Ishii shows that these equations may be used directly in a two-fluid model, or combined to form mixture equations for use as a diffusion model. A diffusion model uses conservation equations for the mixture, and supplements them with a diffusion equation which prescribes changes in concentration. The model we will present here resembles a diffusion model in that we will use a mixture equation of

motion, and specify the relative velocity through use of an equation arrived at by considering the forces on individual bubbles. The equations we use to enforce mass conservation of each phase, and our mixture equation of motion may be obtained from Ishii's through the neglect of viscous stress and phase change terms.

In order to make clear the assumptions that underlie the formulation to be employed here, we develop in detail the equations with which we shall examine the flow of bubbly gas-liquid mixtures. We will consider only the circumstances where the bubble size is sufficiently small in comparison with other characteristic lengths that the mixture may be described as a continuum.

To develop these equations we will invoke the following four physical laws:

- 1) That the liquid is conserved.
- 2) That the gas comprising the bubbles is conserved.
- 3) That the mixture as a whole obeys Newton's second law.
- 4) That the individual bubbles obey Newton's second law.

If the bubbles are far enough apart to be non-interacting, as we will assume, then (2) implies also that the number of bubbles is conserved.

To permit description of the mixture as a continuum, we must require that the bubble sizes and the distances between adjacent bubbles be small in comparison with any characteristic length of the flow. This permits us to define some volume which is small compared to the flow dimensions and yet is large enough to contain many bubbles. The existence of such a volume enables

us to compute average properties of the mixture unambiguously and without appealing to the time-averaging procedures described by Ishii. For example, the void fraction is simply defined as the fraction of such a volume which is occupied by gas. Also, we can easily define average velocity fields for the gas and liquid by averaging over this same volume. We will assume that within this volume the density of the gas and the density of the liquid do not vary. This means the mass flux of gas will be $\rho_g \alpha \vec{u}_g$, where \vec{u}_g is the averaged gas velocity, and that of the liquid will be $\rho_L (1 - \alpha) \vec{u}_L$ where \vec{u}_L is the averaged liquid velocity. Strictly speaking, to compute the flux of momentum we need to compute averaged values of the velocities squared. Assuming, though, that locally (in the volume over which we average) all of the bubbles are the same size, they will all have the same velocity. In this case we will not incur too great an error by taking the average squared velocity as the square of the average velocity. This does involve the neglect of some momentum flux terms similar to Reynolds stresses in turbulent flow, but these should be small compared with those accounted for. The average properties we calculate vary continuously in space since the volume over which we perform the averaging contains many bubbles.

We may now consider a stationary volume, V , arbitrary except that it is taken to be larger than the volume over which we average. We choose to work with a stationary control volume to avoid the ambiguity of having the control surface follow either the liquid or the gas. At every point within V we may calculate

average properties for the mixture. The mass of liquid within the volume V is:

$$\iiint_V \rho_L (1 - \alpha) dV$$

This mass changes only because of the flux of liquid out of the volume V , which is:

$$\iint_S \rho_L (1 - \alpha) \vec{u}_L \cdot \hat{n} dS$$

in which \hat{n} is the outward pointing normal unit vector of the surface, S , of V .

So, for liquid to be conserved:

$$\iint_S \rho_L (1 - \alpha) \vec{u}_L \cdot \hat{n} dS + \frac{d}{dt} \iiint_V \rho_L (1 - \alpha) dV = 0 \quad (2.1)$$

The first integral in (2.1) may be transformed into a volume integral and combined with the second integral:

$$\iiint_V \left\{ \frac{\partial \rho_L (1 - \alpha)}{\partial t} + \nabla \cdot (\rho_L (1 - \alpha) \vec{u}_L) \right\} dV = 0 \quad (2.2)$$

Since the volume V is arbitrary it must be that:

$$\frac{\partial \rho_L (1 - \alpha)}{\partial t} + \nabla \cdot (\rho_L (1 - \alpha) \vec{u}_L) = 0 \quad (2.3)$$

An exactly analogous argument for the gas yields:

$$\frac{\partial \rho_g \alpha}{\partial t} + \nabla \cdot (\rho_g \alpha \vec{u}_g) = 0 \quad (2.4)$$

Equations 2.3 and 2.4 express mathematically the conservation

of liquid and gas for a bubbly mixture in which there is no exchange of mass between the two phases (by condensation, for example). Had we included the possibility of mass exchange, Equations 2.3 and 2.4 would have source terms on the right hand side.

The x-component of the momentum of the mixture within our arbitrary volume, V , is:

$$\iiint_V \{ \rho_g \alpha u_{g_x} + \rho_L (1 - \alpha) u_{L_x} \} dV$$

This quantity changes for two reasons. First, because the mixture entering and leaving the volume, V , possesses a certain amount of momentum, and second, since there are forces acting on the mixture inside V . The x-component of the momentum leaving V per unit time is:

$$\iint_S \{ \rho_g \alpha u_{g_x} (\vec{u}_g \cdot \hat{n}) + \rho_L (1 - \alpha) u_{L_x} (\vec{u}_L \cdot \hat{n}) \} dS$$

The forces on the mixture in V fall into two classes:

1) surface stresses, and 2) body forces. If viscous stresses are unimportant then the surface stresses reduce to pressure forces given by:

$$\iint_S - p \hat{n}_x dS$$

The body forces which will here be taken to be due to a gravitational force are given by:

$$\iiint_V \{ \rho_g \alpha + \rho_L (1 - \alpha) \} g_x dV$$

Combining these, the equation expressing conservation of momentum

in the x-direction for the mixture is:

$$\begin{aligned}
 & \frac{d}{dt} \iiint_V \{ \rho_g \alpha u_{g_x} + \rho_L (1 - \alpha) u_{L_x} \} dV + \iint_S \{ \rho_g \alpha u_{g_x} (\vec{u}_g \cdot \hat{n}) \\
 & + \rho_L (1 - \alpha) u_{L_x} (\vec{u}_L \cdot \hat{n}) \} dS = \iint_S - p \hat{n}_x dS \\
 & + \iiint_V \{ \rho_g \alpha + \rho_L (1 - \alpha) \} g_x dV
 \end{aligned} \tag{2.5}$$

The surface integrals in (2.5) may be transformed into volume integrals and thus all the integrals combined:

$$\begin{aligned}
 & \iiint_V \left\{ \frac{\partial \rho_g \alpha u_{g_x}}{\partial t} + \nabla \cdot \rho_g \alpha u_{g_x} \vec{u}_g + \frac{\partial \rho_L (1 - \alpha) u_{L_x}}{\partial t} \right. \\
 & \left. + \nabla \cdot \rho_L (1 - \alpha) u_{L_x} \vec{u}_L + \frac{\partial p}{\partial x} - (\rho_g \alpha + \rho_L (1 - \alpha)) g_x \right\} dV = 0
 \end{aligned} \tag{2.6}$$

Again, because the volume V is arbitrary the quantity in brackets must be zero:

$$\begin{aligned}
 & \left[\frac{\partial \rho_g \alpha u_{g_x}}{\partial t} + \nabla \cdot \rho_g \alpha u_{g_x} \vec{u}_g \right] + \left[\frac{\partial \rho_L (1 - \alpha) u_{L_x}}{\partial t} + \nabla \cdot \rho_L (1 - \alpha) u_{L_x} \vec{u}_L \right] \\
 & = - \frac{\partial p}{\partial x} + [\rho_g \alpha + \rho_L (1 - \alpha)] g_x
 \end{aligned} \tag{2.7}$$

With the aid of Equations 2.3 and 2.4 this may be written:

$$\rho_g \alpha \frac{D}{Dt} (u_{g_x}) + \rho_L (1 - \alpha) \frac{d}{dt} (u_{L_x}) = - \frac{\partial p}{\partial x} + [\rho_g \alpha + \rho_L (1 - \alpha)] g \tag{2.8}$$

where $\frac{D}{Dt}$ is the convective derivative following the gas and $\frac{d}{dt}$ is that following the liquid. Equation 2.8 expresses conservation of the x-component of momentum for the mixture. Similar equations

for the y and z components of momentum can be derived in the same manner. The three equations can be combined into the single vector equation:

$$\rho_g \alpha \frac{D\vec{u}_g}{Dt} + \rho_L (1 - \alpha) \frac{d\vec{u}_L}{dt} = -\nabla p + \{\rho_g \alpha + \rho_L (1 - \alpha)\} \vec{g} \quad (2.9)$$

This equation is quite similar to the equation of motion for an ordinary fluid except that we have two contributions to time rate of change of the momentum of the mixture.

Equations 2.3, 2.4 and 2.9 have appeared in the literature on two-phase flow before and are well accepted. They actually do not rely on the flow being bubbly, only on both phases being capable of description as continua and our ability to perform the averaging previously described.

In contrast to the manner in which we developed the previous three equations, we now consider the forces on a single bubble, whose nearest neighboring bubbles are far enough away that they do not interact with our bubble. To do this we must analyze the flow of the liquid in the immediate neighborhood of our bubble.

The bubble is taken to be spherical and may be expanding or contracting as it moves through the liquid. The liquid around the bubble is itself moving and in general will have a velocity and acceleration different from that of the bubble.

Because of the absence of a no-slip boundary condition on the surface of a bubble, we can closely approximate the flow of the liquid around the bubble by a potential flow. This assumes that the Reynolds number based on the bubble size, relative velocity and

liquid kinematic viscosity is reasonably large. This is not a very restrictive assumption and will be met in many practical flow situations. We may divide the potential describing the flow of the liquid near the bubble into two portions:

$$\phi = \phi_o + \phi_b$$

The first portion ϕ_o describes the motion the liquid would execute in the absence of the bubble. The second portion ϕ_b describes the motion caused entirely by the presence and motion of the bubble.

We place at the center of our bubble both a cartesian coordinate system and a spherical coordinate system. This is shown in Figure 2.1. The relations between the two coordinate systems are:

$$x = r \cos \theta \quad ; \quad y = r \sin \theta \cos \omega \quad ; \quad z = r \sin \theta \sin \omega$$

Both ϕ_o and ϕ_b must satisfy Laplace's Equation. We take the attitude that ϕ_o is known, and we wish to find ϕ_b , the potential due to the presence of the bubble. The potential, ϕ_b , is the solution of the following mathematical problem:

$$\nabla^2 \phi_b = 0 \tag{2.10}$$

$$\begin{aligned} \left. \frac{\partial \phi_b}{\partial r} \right|_{r=a} = & - \left. \frac{\partial \phi_o}{\partial r} \right|_{r=a} + \dot{a} + \dot{\xi} \cos \theta \\ & + \dot{\eta} \sin \theta \cos \omega + \dot{\zeta} \sin \theta \sin \omega \end{aligned} \tag{2.11}$$

$$\phi_b \rightarrow 0 \quad \text{as} \quad r \rightarrow \infty \tag{2.12}$$

The boundary condition (2.11) states that the liquid does not flow through the surface of the bubble. The other boundary condition (2.12) is a statement that the neighboring bubbles are far enough away so as not to interact with our bubble.

In order to solve this mathematical problem we expand the potential, ϕ_0 , in Taylor's Series about the center of the bubble:

$$\phi_0(x, y, z) = \phi_0 \Big|_0 + \frac{\partial \phi_0}{\partial x} \Big|_0 x + \frac{\partial \phi_0}{\partial y} \Big|_0 y + \frac{\partial \phi_0}{\partial z} \Big|_0 z + \dots \quad (2.13)$$

With the aid of (2.13) we can now solve our problem for ϕ_b . Adding this to ϕ_0 we have the complete potential, ϕ .

$$\begin{aligned} \phi = & \phi_0 - \frac{a^2 \ddot{a}}{r} + \frac{a^3}{2r^2} \left\{ \left(\frac{\partial \phi_0}{\partial x} \Big|_0 - \dot{\xi} \right) P_1^0(\cos \theta) \right. \\ & + \left(\frac{\partial \phi_0}{\partial y} \Big|_0 - \dot{\eta} \right) \cos \omega P_1^1(\cos \theta) + \left(\frac{\partial \phi_0}{\partial z} \Big|_0 - \dot{\zeta} \right) \sin \omega P_1^1(\cos \theta) \Big\} \\ & + \frac{a^5}{r^3} \left\{ \frac{1}{3} \frac{\partial^2 \phi_0}{\partial x^2} \Big|_0 P_2^0(\cos \theta) + \frac{2}{9} \frac{\partial^2 \phi_0}{\partial x \partial y} \Big|_0 \cos \omega P_2^1(\cos \theta) \right. \\ & + \frac{2}{9} \frac{\partial^2 \phi_0}{\partial x \partial z} \Big|_0 \sin \omega P_2^1(\cos \theta) + \frac{1}{18} \left(\frac{\partial^2 \phi_0}{\partial z^2} \Big|_0 \right) \cos 2\omega P_2^2(\cos \theta) \\ & \left. + \frac{1}{9} \frac{\partial^2 \phi_0}{\partial y \partial x} \Big|_0 \sin 2\omega P_2^2(\cos \theta) \right\} + 0 \left(\frac{\partial^3 \phi_0}{\partial x^3} \frac{a^7}{r^4} \right) \end{aligned} \quad (2.14)$$

Knowing this potential we may use the Bernoulli Integral to calculate the pressure on the surface of the bubble. We must use care, though, since we have calculated the potential in an accelerating reference frame. If we integrate the pressure over the surface of the bubble to find the force on it we find, for the x-component of this force:

$$\begin{aligned}
F_x^H &= -\rho_L \frac{1}{2} \sigma \dot{\xi} - \frac{1}{2} \rho_L (\dot{\xi} - U_0) \dot{\sigma} \\
&+ \frac{3}{2} \rho_L \sigma \left\{ \frac{\partial U_0}{\partial t} + U_0 \frac{\partial U_0}{\partial x} + V_0 \frac{\partial U_0}{\partial y} + W_0 \frac{\partial U_0}{\partial z} \right\} \\
&- \rho_L \sigma g_x
\end{aligned} \tag{2.15}$$

in which we have recognized that $\left. \frac{\partial \phi_0}{\partial x} \right|_0$ is U_0 the x-component of the liquid velocity in the absence of the bubble and so on. This is also the average velocity of the liquid in the neighborhood of the bubble.

The first term in Equation 2.15 is the familiar virtual mass term. The second term corresponds to a change in the virtual mass as the bubble changes size. The third term is the acceleration of the liquid times the mass of a volume of liquid equivalent to the bubble volume plus the volume of its virtual mass. The final term is a buoyancy force.

There is also a viscous force on the bubble. Still believing that the potential flow solution closely resembles the actual flow, we calculate the dissipation that occurs when a viscous fluid executes the potential flow past a sphere. Although this is slightly inconsistent, we can get a reasonable approximation to the true dissipation in this manner. Equating this to the rate at which the viscous force on the bubble does work on the surrounding liquid, we find, as does Batchelor (2.3) that the x-component of the viscous force on the bubble is:

$$F_x^V = -12\pi\mu a (\dot{\xi} - U_0) \tag{2.16}$$

Finally, there is a gravitational force on the bubble:

$$\mathbf{F}_x^g = \rho_g \sigma g_x \quad (2.17)$$

The sum of the forces on the bubble equals its mass times its acceleration. Enforcing this, and describing the bubble and liquid velocities as field variables, we arrive at the equation of motion for the bubbles:

$$\begin{aligned} (\rho_g + \frac{1}{2}\rho_L) \frac{D\vec{u}_g}{Dt} + \frac{1}{2} \rho_L (\vec{u}_g - \vec{u}_L) \frac{1}{\sigma} \frac{D\sigma}{Dt} \\ - \frac{3}{2} \rho_L \frac{d\vec{u}_L}{dt} + \frac{\rho_L}{2\tau_v} (\vec{u}_g - \vec{u}_L) = (\rho_g - \rho_L) \vec{g} \end{aligned} \quad (2.18)$$

$$\tau_v = \frac{18a^2}{\nu}$$

in which τ_v is the viscous relaxation time of the bubble. If we set a massless bubble in motion through a stagnant liquid this is the time it will take to decay to $1/e$ of its initial velocity. A less general form of Equation 2.18 was derived by Chernyy (2.4), 1973, in a one-dimensional situation.

In the following chapters we will apply our four governing equations (2.3, 2.4, 2.9 and 2.18) to several interesting physical problems. In all of these problems we will find it sufficient to assume that the liquid is incompressible and that the gas expands and contracts isothermally. This means, in effect, that each of the phases is a barotropic fluid. Because of this we will not find it necessary to use mathematical equations expressing the conservation of energy. So at this point we have developed all of the

equipment necessary to analyze physical problems in the flow of bubbly mixtures.

REFERENCES

- 2.1 L. van Wijngaarden, "On the Equations of Motion for Mixtures of Liquid and Gas Bubbles", Journal of Fluid Mechanics Volume 33, Part 3, 1968, pp. 465 - 474.
- 2.2 M. Ishii, "Thermo-Fluid Dynamic Theory of Two-Phase Flow", (1975) (Pub. Eyrolles), Chapter 5.
- 2.3 G.K. Batchelor, "An Introduction to Fluid Dynamics", Cambridge University Press , 1967, Chapter 5.
- 2.4 I.M. Chernyy, "Concerning the Dynamics of Bubble-Type Flows in a Gas-Liquid Nozzle", Fluid Mechanics - Soviet Research Volume 2, Number 6, Nov. - Dec. 1973, pp. 92 - 99.

Notation for Chapter 2

a	Radius of bubble
F	Force on bubble
g	Acceleration of gravity
\hat{n}	Outward pointing normal unit vector
p	Pressure
P_l^m	Associated Legendre function
\vec{u}	Velocity
U_0, V_0, W_0	Velocity components of liquid
α	Void fraction
μ	Liquid viscosity
ν	Liquid kinematic viscosity
$\dot{\xi}, \dot{\eta}, \dot{\zeta}$	Velocity components of bubble
ρ	Density
σ	Volume of bubble
τ_v	Viscous relaxation time
ϕ	Velocity potential

Subscripts

g	Gas
l	Liquid

Superscripts

g	Gravitational
H	Hydrodynamic
v	Viscous

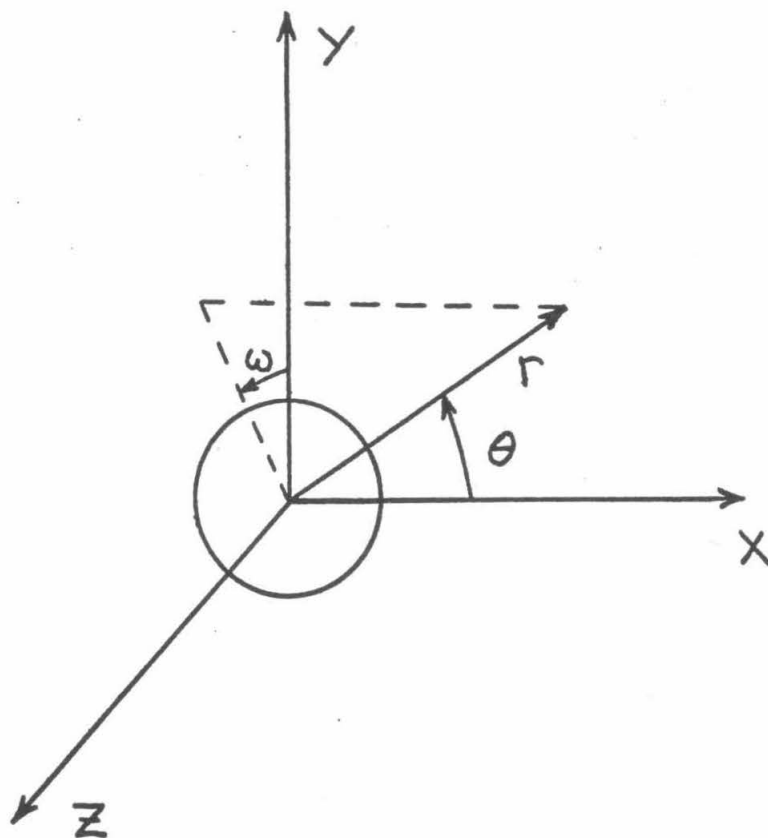


Figure 2.1 Geometry and Notation for Calculation of Forces on a Single Bubble

CHAPTER 3

One-Dimensional Flow in a Duct

Consider the flow of a bubbly mixture in a one-dimensional duct of varying cross-sectional area . The problem of choked bubbly flow was apparently first treated by Tangren, Dodge and Seifert (3.1), 1949 using a homogeneous flow model and assuming that the gas bubbles flowed with the liquid, and at the liquid temperature, which was allowed to vary through the channel. Under these assumptions the mixture is equivalent to a single barotropic fluid with a peculiar equation of state. This made it possible to obtain exact integrals of the equations of motion. These solutions were compared to a limited number of experiments they performed on a choked two-phase nozzle and the comparison was not completely satisfactory.

A more complete experimental investigation was presented by Muir and Eichhorn (3.2) in 1963. Their experiments were performed on a two-phase nozzle with an air-water mixture flowing through it. They determined that the homogeneous flow theory of Tangren, Dodge and Seifert predicted pressure ratios between the throat and upstream sections that were in all instances lower than those measured. They attributed these discrepancies directly to the fact that the homogeneous flow model excludes the possibility of having a relative velocity between the phases. One of the aims of the present analysis is to account for the relative velocity.

The assumptions made in the present analysis are:

- (I) That the flow is everywhere one-dimensional
- (II) That the liquid and gas behave isothermally as they

flow through the contraction

- (III) That the liquid is incompressible
- (IV) That the gas has negligible inertia compared with that of the liquid
- (V) That the pressure inside the gas bubbles is essentially the same as that in the surrounding liquid
- (VI) That the gas bubbles do not interact with each other and that their viscous interaction with the surrounding liquid may be described by a linear drag law
- (VII) That the frictional forces on the walls of the duct are negligible

The governing equations are considerably simplified by the preceding assumptions and the justification of assumptions (II) and (V) will be examined later.

Under these assumptions the conservation equations take the form:

Gas Conservation

$$\frac{1}{\alpha} \left[\frac{\partial \alpha}{\partial t} + V_g \frac{\partial \alpha}{\partial x} \right] + \frac{1}{p} \left[\frac{\partial p}{\partial t} + V_g \frac{\partial p}{\partial x} \right] + \frac{\partial V_g}{\partial x} = \frac{-V_g}{A} \frac{dA}{dx} \quad (3.1)$$

Liquid Conservation

$$- \frac{1}{1-\alpha} \left[\frac{\partial \alpha}{\partial t} + V_L \frac{\partial \alpha}{\partial x} \right] + \frac{\partial V_L}{\partial x} = \frac{-V_L}{A} \frac{dA}{dx} \quad (3.2)$$

Mixture Motion

$$\rho_L (1-\alpha) \left[\frac{\partial V_L}{\partial t} + V_L \frac{\partial V_L}{\partial x} \right] + \frac{\partial p}{\partial x} = 0 \quad (3.3)$$

Bubble Motion

$$\begin{aligned}
 & \left[\frac{\partial V_g}{\partial t} + V_g \frac{\partial V_g}{\partial x} \right] - \left(\frac{V_g - V_L}{p} \right) \left[\frac{\partial p}{\partial t} + V_g \frac{\partial p}{\partial x} \right] \\
 & - 3 \left[\frac{\partial V_L}{\partial t} + V_L \frac{\partial V_L}{\partial x} \right] + \frac{1}{\tau_v} (V_g - V_L) = 0
 \end{aligned} \tag{3.4}$$

Formally Equations 3.1 - 3.3 follow from Equations 2.3, 2.4 and 2.9 by integration across the channel, satisfying appropriate boundary conditions on the duct walls and taking the remaining variables as averages across the channel. One consequence of this is the appearance of terms to account for the area change of the duct. Equation 3.4 is derived from first principles as was (2.18) and ignoring gradients normal to the channel axis. The material derivative of the gas density in the gas conservation equation has been replaced by a derivative of the pressure as a result of our assuming isothermal behavior for the bubbles. For the same reason, the term accounting for changes of the virtual mass of the bubbles, in the bubble motion equation, has also become a material derivative of the pressure. In the mixture motion equation, the momentum of the gas has been ignored in favor of the much greater momentum of the liquid. Finally, in the bubble motion equation, the actual mass of the bubbles has been ignored compared with their virtual mass.

When we examine the characteristics of this set of equations, we find that four characteristic speeds are determined by the equation:

$$\begin{aligned}
 & \frac{\rho_L}{p} (V_L - \dot{x})^2 (V_g - \dot{x}) \{ (V_g - \dot{x}) + (V_g - V_L) \} \\
 & - \frac{1}{\alpha} (V_g - \dot{x})^2 - \frac{3}{1-\alpha} (V_L - \dot{x})^2 = 0
 \end{aligned} \tag{3.5}$$

In the circumstance that the gas and liquid velocities are equal we find that the four roots of this equation are:

$$\dot{x} = V, \text{ a double root}$$

$$\text{and } \dot{x} = V \pm \left(\frac{p(1+2\alpha)}{\rho_L \alpha(1-\alpha)} \right)^{\frac{1}{2}}$$

The second of these pairs of roots corresponds to a pair of acoustic waves that may travel up and down the duct. The speed of these waves, $\sqrt{\frac{p(1+2\alpha)}{\rho_L \alpha(1-\alpha)}}$, is the acoustic speed one would calculate

for an isothermal mixture of bubbles and liquid if there were no viscous forces between the liquid and bubbles. The significance of the double root $\dot{x} = V$ is not as clear. If the liquid and gas velocities are not equal the double root $\dot{x} = V$ splits into a complex conjugate pair of roots. If we have a small relative velocity between the phases, that is $(V_g - V_L) \ll \bar{V}$, we can easily determine that the two roots are approximately:

$$\dot{x} \approx \frac{(1-\alpha)V_g + 3\alpha V_L}{(1+2\alpha)} \pm \frac{i\sqrt{3\alpha(1-\alpha)}}{(1+2\alpha)}(V_g - V_L) \quad (3.6)$$

where the imaginary part of each root is proportional to the relative velocity. Similarly, for small relative velocity, the two acoustic roots are approximately:

$$\dot{x} \approx \frac{1}{2} \left\{ \frac{(1+8\alpha)V_g + (1-4\alpha)V_L}{(1+2\alpha)} \right\} \pm \left(\frac{p(1+2\alpha)}{\rho_L \alpha(1-\alpha)} \right)^{\frac{1}{2}} \quad (3.7)$$

which remain real and keep their significance as acoustic waves.

The fact that two of the characteristics become complex when there is a relative velocity, causes mathematical problems when we attempt to solve an initial value problem, because these characteristics are the curves in the $x - t$ plane, along which disturbances may propagate. It is clear therefore that these complex characteristics will be of considerable interest and this will be dealt with in Chapter 5.

For steady flow, however, the partial derivatives with respect to time vanish and leave the following regular set:

Gas Conservation

$$\frac{1}{\alpha} \frac{d\alpha}{dx} + \frac{1}{p} \frac{dp}{dx} + \frac{1}{V_g} \frac{dV_g}{dx} = -\frac{1}{A} \frac{dA}{dx} \quad (3.8)$$

Liquid Conservation

$$\frac{-1}{1-\alpha} \frac{d\alpha}{dx} + \frac{1}{V_L} \frac{dV_L}{dx} = -\frac{1}{A} \frac{dA}{dx} \quad (3.9)$$

Mixture Motion

$$\rho_L (1-\alpha) V_L \frac{dV_L}{dx} + \frac{dp}{dx} = 0 \quad (3.10)$$

Bubble Motion

$$\begin{aligned} V_g \frac{dV_g}{dx} - \frac{V_g (V_g - V_L)}{p} \frac{dp}{dx} - 3 V_L \frac{dV_L}{dx} \\ + \frac{1}{\tau_v} (V_g - V_L) = 0 \end{aligned} \quad (3.11)$$

The relaxation time, in the bubble motion equation, is not a constant, but varies as the bubbles expand. Because of the isothermal behavior assumed for the bubbles, τ_v can be expressed in terms of the pressure and the conditions upstream of the contraction. That relationship is:

$$\tau_v = \tau_{v_0} \left(\frac{p}{p_0} \right)^{-2/3}$$

To make these equations dimensionless, we use: 1) the length scale, L_0 , the length of the contraction; 2) the pressure scale p_0 , the upstream pressure; and 3) the velocity scale, U_0 , formed by taking the square root of the upstream pressure divided by the liquid density. They then take the form:

Gas Conservation

$$\frac{1}{\alpha} \frac{d\alpha}{dx} + \frac{1}{p} \frac{dp}{dx} + \frac{1}{u_g} \frac{du_g}{dx} = \frac{-1}{A} \frac{dA}{dx} \quad (3.12)$$

Liquid Conservation

$$-\frac{1}{1-\alpha} \frac{d\alpha}{dx} + \frac{1}{u_L} \frac{du_L}{dx} = \frac{-1}{A} \frac{dA}{dx} \quad (3.13)$$

Mixture Motion

$$(1-\alpha) u_L \frac{du_L}{dx} + \frac{dp}{dx} = 0 \quad (3.14)$$

Bubble Motion

$$u_g \frac{du_g}{dx} - \frac{u_g(u_g - u_L)}{p} \frac{dp}{dx} - 3u_L \frac{du_L}{dx} + \left(\frac{L_0}{U_0 \tau_{v_0}} \right) p^{2/3} (u_g - u_L) = 0 \quad (3.15)$$

Of particular significance in the transformed equations is the appearance of the dimensionless number, $\left(\frac{L_0}{U_0 \tau_{v_0}} \right)$, which has an interesting physical significance. It is a ratio between the time we may expect a bubble to reside in the contraction, L_0 / U_0 , and the viscous relaxation time. It is therefore a measure of how effective viscosity is in reducing the relative velocity between the phases. If this number were very large we would expect viscosity to be very effective and hence expect the flow to be nearly homogeneous. If, however, this number were instead very small, we would expect viscosity to be rather ineffective, and that the relative motion would be determined almost wholly by the dynamic terms in the bubble equation of motion. In many cases of interest this number is small. For instance if we consider 1/8" dia. bubbles in room temperature water, with a 1 foot contraction and upstream pressure 80 psia, it turns out that:

$$\frac{L_0}{U_0 \tau_{v_0}} = .0938$$

In this case we would expect the dynamic forces on the bubbles to determine their motion. This is, of course, exactly the opposite of the case considered by Tangren and Dodge, with their homogeneous flow model.

The dimensionless equations may now be written in a convenient

matrix form,

$$\begin{bmatrix} \frac{1}{u_g} & 0 & \frac{1}{p} & \frac{1}{\alpha} \\ 0 & \frac{1}{u_L} & 0 & -\frac{1}{1-\alpha} \\ 0 & (1-\alpha)u_L & 1 & 0 \\ u_g & -3u_L & \frac{-u_g(u_g - u_L)}{p} & 0 \end{bmatrix} \times \begin{bmatrix} \frac{du_g}{dx} \\ \frac{du_L}{dx} \\ \frac{dp}{dx} \\ \frac{d\alpha}{dx} \end{bmatrix} = \begin{bmatrix} -\frac{1}{A} \frac{dA}{dx} \\ -\frac{1}{A} \frac{dA}{dx} \\ 0 \\ -\left(\frac{L_0}{U_0 \tau_{v_0}}\right) p^{2/3} (u_g - u_L) \end{bmatrix} \quad (3.16)$$

a form similar to that in which the equations of one-dimensional gas dynamics are often written. In gas dynamics we find a choking condition on the flow by setting the determinant of the matrix of coefficients equal to zero. When this is done in the present case we find

$$\frac{u_L}{p} (2u_g - u_L) - \frac{3u_L}{(1-\alpha)u_g} - \frac{u_g}{\alpha u_L} = 0 \quad (3.17)$$

We could have arrived at this relation utilizing Equation 3.5. When the characteristic speed, \dot{x} , is set equal to zero and the gas and liquid velocities are non-dimensionalized, 3.5 becomes identical to 3.17.

We can conclude from this that 3.17 is the choking condition for our flow. The condition that any of $\frac{du_g}{dx}$, $\frac{du_L}{dx}$, $\frac{dp}{dx}$ and $\frac{d\alpha}{dx}$ must be finite at the location where the flow chokes, leads to the conclusion that the flow chokes at the location where:

$$\frac{1}{A} \frac{dA}{dx} = \left(\frac{L_0}{U_0 \tau_{v_0}} \right) \alpha p^{2/3} \frac{u_g - u_L}{u_g^2} \quad (3.18)$$

Since we realize that $u_g > u_L$, it is clear that one effect of the finite inter-phase friction is to move the location of the sonic point downstream of the geometric throat of the contraction. To proceed further we must actually solve the equations. To do this it is convenient to interchange the roles of the variables x and p , as was done by Rannie (3.3), 1962, and Marble (3.4), 1963, making p our independent variable. This can be accomplished by simply multiplying our equations through by $\frac{dx}{dp}$. This leaves only the drag term in the equation for bubble motion involving x . That term is also the one term involving our dimensionless number, $\frac{L_0}{U_0 \tau_{v_0}}$, which in many cases we expect will be small. One convenient method for approximate solution of these equations is a perturbation expansion in the small parameter

$\frac{L_0}{U_0 \tau_{v_0}}$. If we denote $\frac{L_0}{U_0 \tau_{v_0}}$ by ϵ , and form the following

expansion:

$$\begin{aligned}
 u_L(p) &= u_L^{(0)}(p) + \epsilon u_L^{(1)}(p) + \epsilon^2 u_L^{(2)}(p) \dots \\
 u_g(p) &= u_g^{(0)}(p) + \epsilon u_g^{(1)}(p) + \epsilon^2 u_g^{(2)}(p) \dots \\
 \alpha(p) &= \alpha^{(0)}(p) + \epsilon \alpha^{(1)}(p) + \epsilon^2 \alpha^{(2)}(p) \dots \\
 A(p) &= A^{(0)}(p) + \epsilon A^{(1)}(p) + \epsilon^2 A^{(2)}(p) \dots \\
 x(p) &= x^{(0)}(p) + \epsilon x^{(1)}(p) + \epsilon^2 x^{(2)}(p) \dots
 \end{aligned} \tag{3.19}$$

we may derive sets of equations for the successive terms in the expansion. This is done by simply substituting each of the above series into Equations 3.12, 3.13, 3.14, and 3.15 and equating like powers of ϵ . Of course we presume that the area distribution

$$A = A(x)$$

is known from the geometry of our particular nozzle or contraction.

The sets of equations for the zeroth and first orders of the expansion are:

Zeroth Order

$$\begin{aligned}
 & \frac{-1}{1-\alpha^{(0)}} \frac{d\alpha^{(0)}}{dp} + \frac{1}{u_L^{(0)}} \frac{du_L^{(0)}}{dp} + \frac{1}{A^{(0)}} \frac{dA^{(0)}}{dp} = 0 \\
 & \frac{1}{\alpha^{(0)}(1-\alpha^{(0)})} \frac{d\alpha^{(0)}}{dp} + \frac{1}{u_g^{(0)}} \frac{du_g^{(0)}}{dp} - \frac{1}{u_L^{(0)}} \frac{du_L^{(0)}}{dp} + \frac{1}{p} = 0 \\
 & (1-\alpha^{(0)}) u_L^{(0)} \frac{du_L^{(0)}}{dp} + 1 = 0 \\
 & u_g^{(0)} \frac{du_g^{(0)}}{dp} - \frac{u_g^{(0)}}{p} (u_g^{(0)} - u_L^{(0)}) - 3 u_L^{(0)} \frac{du_L^{(0)}}{dp} = 0 \\
 & A^{(0)}(p) = A(x^{(0)}(p))
 \end{aligned} \tag{3.20}$$

First Order

$$\begin{aligned}
 & \frac{d}{dp} \left\{ -\frac{\alpha^{(1)}}{1-\alpha^{(0)}} + \frac{u_L^{(1)}}{u_L^{(0)}} + \frac{A^{(1)}}{A^{(0)}} \right\} = 0 \\
 & \frac{d}{dp} \left\{ \frac{\alpha^{(1)}}{\alpha^{(0)}(1-\alpha^{(0)})} + \frac{u_g^{(1)}}{u_g^{(0)}} - \frac{u_L^{(1)}}{u_L^{(0)}} \right\} = 0 \\
 & \frac{du_L^{(0)}}{dp} = \frac{1}{u_L^{(0)}(1-\alpha^{(0)})} \left\{ \frac{u_L^{(1)}}{u_L^{(0)}} - \frac{\alpha^{(1)}}{1-\alpha^{(0)}} \right\}
 \end{aligned} \tag{3.21}$$

$$\begin{aligned}
& u_g^{(0)} \frac{du_g^{(1)}}{dp} + u_g^{(1)} \frac{du_g^{(0)}}{dp} - \frac{u_g^{(1)}}{p} (u_g^{(0)} - u_L^{(0)}) \\
& - \frac{u_g^{(0)}}{p} (u_g^{(1)} - u_L^{(1)}) + \frac{3\alpha^{(1)}}{[1 - \alpha^{(0)}]^2} \\
& + \frac{dx^{(0)}}{dp} p^{2/3} (u_g^{(0)} - u_L^{(0)}) = 0
\end{aligned}$$

$$A^{(1)}(p) = \left. \frac{dA}{dx} \right|_{x=x^{(0)}(p)} \cdot x^{(1)}(p)$$

These ten equations, upon integration, will yield the zeroth and first order terms in our perturbation expansions. The boundary conditions that we should apply depend strongly on the flow situation upstream of the contraction. In the most unambiguous situation, which we will consider first, consider fluid flowing in a long pipe before entering the contraction. By a long pipe we imply that the liquid and gas entering the contraction will be flowing at the same velocity. The boundary conditions for this situation are:

- (I) That upstream of the contraction the dimensionless pressure equals one.
- (II) That upstream of the contraction the velocities of gas and liquid are equal, but unknown for the choked flow until the entire problem is solved.
- (III) That the area of the channel upstream, where $p = 1$, is given.
- (IV) That the area of the contraction at its minimum,

where $\frac{dA}{dp} = 0$, is given.

(V) That the void fraction upstream of the contraction is given.

Expressing these conditions mathematically, from (II) we have:

$$u_g^{(0)}(1) + \epsilon u_g^{(0)}(1) + \epsilon^2 u_g^{(2)}(1) \dots = u_L^{(0)}(1) + \epsilon u_L^{(1)}(1) \dots$$

which means that

$$u_g^{(n)}(1) = u_L^{(n)}(1) \quad n = 0, 1, 2 \dots \quad (3.22)$$

From (III) we get

$$A(1) = A^{(0)}(1) + \epsilon A^{(1)}(1) + \epsilon^2 A^{(2)}(1) \dots = A_{\text{upstream}}$$

so

$$A^{(0)}(1) = A_{\text{upstream}}$$

$$A^{(n)}(1) = 0 \quad n = 1, 2, 3 \dots$$

Mathematical expression of (IV) is not quite as simple as the previous conditions. For this reason we will only work out the condition to $O(\epsilon^2)$. The condition is to be enforced at the throat pressure, p_{th} , given by:

$$p_{th} = p_{th}^{(0)} + \epsilon p_{th}^{(1)} + \epsilon^2 p_{th}^{(2)} \dots$$

This throat pressure is defined by:

$$\left. \frac{dA}{dp} \right|_{p_{th}} = \left. \frac{dA^{(0)}}{dp} \right|_{p_{th}} + \epsilon \left. \frac{dA^{(1)}}{dp} \right|_{p_{th}} + \dots = 0$$

If we expand each term in this equation we get:

$$\left. \frac{dA^{(0)}}{dp} \right|_{p_{th}^{(0)}} + \epsilon \left\{ \left. \frac{dA^{(1)}}{dp} \right|_{p_{th}^{(0)}} + \left. \frac{d^2 A^{(0)}}{dp^2} \right|_{p_{th}^{(0)}} p_{th}^{(1)} \right\} + \dots = 0$$

So

$$\left. \frac{dA^{(0)}}{dp} \right|_{p_{th}^{(0)}} = 0$$

which defines $p_{th}^{(0)}$, and

$$p_{th}^{(1)} = - \left(\left. \frac{dA^{(1)}}{dp} / \frac{d^2 A^{(0)}}{dp^2} \right) \right|_{p_{th}^{(0)}}$$

so

$$p_{th} = p_{th}^{(0)} - \epsilon \left(\left. \frac{dA^{(1)}}{dp} / \frac{d^2 A^{(0)}}{dp^2} \right) \right|_{p_{th}^{(0)}} + \dots \quad (3.24)$$

Now, our boundary condition says:

$$A(p_{th}) = A^{(0)}(p_{th}) + \epsilon A^{(1)}(p_{th}) + \epsilon^2 A^{(2)}(p_{th}) + \dots = A_{th}$$

Again, we must expand each term in the equation, to get;

$$\begin{aligned} & A^{(0)}(p_{th}^{(0)}) + \epsilon \left\{ A^{(1)}(p_{th}^{(0)}) + \left. \frac{dA^{(0)}}{dp} \right|_{p_{th}^{(0)}} p_{th}^{(1)} \right\} \\ & + \epsilon^2 \left\{ A^{(2)}(p_{th}^{(0)}) + \left. \frac{dA^{(1)}}{dp} \right|_{p_{th}^{(0)}} p_{th}^{(1)} + \left. \frac{dA^{(0)}}{dp} \right|_{p_{th}^{(0)}} p_{th}^{(2)} \right. \\ & \left. + \frac{1}{2} \frac{d^2 A^{(0)}}{dp^2} (p_{th}^{(1)})^2 \right\} + \dots = A_{th} \end{aligned}$$

Realizing that $\left. \frac{dA^{(0)}}{dp} \right|_{p_{th}^{(0)}} = 0$ and knowing $p_{th}^{(1)}$ we can now state

the boundary condition on the zeroth, first, and second orders:

$$\begin{aligned} A^{(0)}(p_{th}^{(0)}) &= A_{th} \\ A^{(1)}(p_{th}^{(0)}) &= 0 \\ A^{(2)}(p_{th}^{(0)}) &= \frac{1}{2} \left[\left(\frac{dA^{(1)}}{dp} \right)^2 / \frac{d^2 A^{(0)}}{dp^2} \right] \Big|_{p_{th}^{(0)}} \end{aligned} \quad (3.25)$$

Our final boundary condition is on the upstream void fraction:

$$\alpha(1) = \alpha^{(0)}(1) + \epsilon \alpha^{(1)}(1) + \epsilon^2 \alpha^{(2)}(1) \dots = \alpha_0$$

So

$$\begin{aligned} \alpha^{(0)}(1) &= \alpha_0 \\ \alpha^{(m)}(1) &= 0 \quad m = 1, 2, 3, \dots \end{aligned} \quad (3.26)$$

With these boundary conditions we have enough information to integrate Equations 3.20 and 3.21 and obtain solutions for the zeroth and first order terms of our perturbation expansion.

Because of the choking condition we have a two-point boundary value problem and the numerical integration requires some care. We are unable to specify the gas and liquid velocities upstream. This is because the flow is choked and we do not have the ability to specify the mass flow rate a priori. To surmount this difficulty we make an initial guess as to the upstream velocity. Then the equations are integrated as an initial value problem. The solution obtained is then checked to see if it obeys the condition to be enforced at $p_{th}^{(0)}$, (3.25).

If the condition is not met, the initial guess of the upstream velocity is improved and the process repeated. This is continued until a solution that obeys (3.25) is obtained.

Next, we consider the case of a nozzle being supplied from a stagnation chamber. The situation is described by the same equations but with different boundary conditions. A stagnation chamber upstream is effectively a section with infinite area. Hence the gas and liquid velocities upstream will be zero. This condition replaces condition (III) in the contraction problem. This enables us to integrate the governing equations, without use of the shooting procedure described previously. But this change in boundary conditions has more important consequences than enabling easy integration. Examining the bubble motion equation near the upstream condition we find:

$$\frac{1}{2} \frac{du_g^{(0)^2}}{dp} - \frac{3}{2} \frac{du_L^{(0)^2}}{dp} - \frac{u_g^{(0)}}{p} (u_g^{(0)} - u_L^{(0)}) = 0$$

At the upstream condition $u_g^{(0)} = u_L^{(0)} = 0$, so we conclude that near $p = 1$;

$$u_g^{(0)} \approx \sqrt{3} u_L^{(0)} \quad (3.27)$$

From the mixture motion equation we find that in particular:

$$\begin{aligned} u_L^{(0)} &\approx \sqrt{\frac{2(1-p)}{(1-\alpha)}} \\ u_g^{(0)} &\approx \sqrt{\frac{6(1-p)}{(1-\alpha_0)}} \quad (\text{near } p = 1) \end{aligned} \quad (3.28)$$

From (3.27) we may calculate the volume flow ratio, β , at the entrance to the nozzle:

$$\beta = \frac{\alpha u_g}{(1 - \alpha) u_L} = \sqrt{3} \frac{\alpha_0}{(1 - \alpha_0)}$$

This is $\sqrt{3}$ times as great as the volume ratio in the stagnation chamber. This means that the gas in the chamber will be depleted faster than the liquid. If we are considering a stagnation chamber of finite size, which is being idealized as infinite, then our problem is inherently time-dependent. We also see now that the important characteristic of a given flow is not its upstream void fraction, but the volume flow fraction of gas upstream. In the contraction problem these two quantities are equal, so there is no confusion. In a general situation, we have no guarantee the two will be equal so it is important to realize which quantity more completely characterizes the flow situation.

With this in mind we can examine the computed solutions for both the contraction in a duct and the nozzle. Tables 3.1 through 3.3 are computed zeroth order solutions for a contraction in a duct with an upstream to throat area ratio of four to one. These three solutions are for upstream void fractions of 0.05, 0.10, and 0.20. The most noticeable feature of these solutions is the magnitude of slip between the phases. When the upstream void fraction is 0.20 the gas travels a full 50% faster than the liquid at the throat of the contraction. Another feature of the solution is that the void fraction goes down just as the mixture is entering the contraction. On the basis of the gas expanding we expect the void fraction to go up, as it ultimately does. Near the entrance to the contraction though, the dominant effect is

that of the gas accelerating much faster than the liquid. The gas thus requires less area to flow through and the void fraction decreases initially. When the gas has accelerated to about $\sqrt{3}$ times the liquid speed, the expansion of the gas begins to dominate and the void fraction increases from then on.

Tables 3.4 - 3.6 are steady-state solutions to the nozzle problem. Both the zeroth and first order solution solutions have been calculated for a special nozzle whose geometry (the function $A(x)$) was just such that:

$$x^{(0)}(p) = (1 - p)^2$$

This choice of the geometry simplifies calculation of the first order solution considerably and yields a reasonable looking nozzle. The calculations were made for stagnation void fractions of 0.05, 0.10, and 0.20. Unlike the case of a contraction, the void fraction in the nozzle increases monotonically as the pressure decreases. This is because the volume flow fraction upstream is not constrained to equal the upstream void fraction.

From the first order nozzle solution we can see that the largest correction to the zeroth order solution will occur in the gas velocity. This is reasonable since one would expect that the effect of inter-phase friction would be to slow the gas down. To assess how good an approximation the zeroth order solution is alone, we compute the value of ϵ for which the first order correction in the gas velocity is about 10%. This occurs for ϵ about equal to 5. This indicates that the zeroth order solution is quite a bit better approximation than we

had any right to expect. The reasons for this are two-fold. Firstly, we have estimated the time of residence in the nozzle of a bubble based on the assumption that it travels at speed $\sqrt{p_0/\rho_L}$, as we can see from the zeroth order solution the bubbles can go considerably faster than this. Secondly, to estimate the relaxation time of the bubbles we have used their relaxation time upstream. The bubbles expand to quite low pressures as they go through the nozzle, their size increases, and so does their relaxation time. We therefore underestimate the relaxation time by quite a bit. The combination of these two errors makes our estimate for the ratio of residence time to relaxation time, $\frac{L_0}{U_0 \tau_{v_0}}$, considerably high. This explains why the zeroth order solution is a reasonable approximation even for ϵ quite a bit greater than one. We can also compute the effect of interphase friction on the pressure at the throat. We have already seen that:

$$p_{th} = p_{th}^{(0)} - \epsilon \left(\frac{dA^{(1)}}{dp} \bigg/ \frac{d^2 A^{(0)}}{dp^2} \right) \bigg|_{p_{th}^{(0)}}$$

For the nozzle solution with $\alpha_0 = 0.05$:

$$\frac{dA^{(1)}}{dp} = -A^{(0)} \times (0.010)$$

Which means that:

$$p_{th} = p_{th}^{(0)} + \epsilon \left(\frac{0.010}{\frac{1}{A^{(0)}} \frac{d^2 A^{(0)}}{dp^2}} \right) \bigg|_{p_{th}^{(0)}}$$

Since $\frac{d^2 A^{(0)}}{dp^2}$ is a positive quantity, interphase friction will have the effect of increasing the pressure at the throat of the nozzle. We may not have guessed this at the outset. The interphase friction not only slows down the bubbles but also speeds up the liquid. Hence the greater the friction between gas and liquid the greater the amount of kinetic energy associated with bulk motion of the liquid. On this basis we would expect that the throat pressure would decrease as ϵ increases. But, there is also a certain amount of kinetic energy associated with the relative motion between bubbles and liquid (virtual mass effect). This kinetic energy decreases with increasing ϵ and thus the throat pressure would increase if this were the dominant effect. Since the throat pressure does increase with increasing ϵ this must be the dominant effect.

We can now better justify assumptions (II) and (V) made in arriving at our simplified equations.

Assumption (V) states that the pressure inside the bubbles is essentially that in the surrounding liquid. This would be untrue only if the bubbles could not expand as fast as the pressure around them decreased. The rate of expansion of the bubbles is governed by the Rayleigh Equation:

$$R \ddot{R} + \frac{3}{2} \dot{R}^2 = \frac{(p_b - p_s)}{\rho_L}$$

Here, R is the radius of the bubble and $(p_b - p_s)$ is the pressure difference between inside the bubble and in the surrounding liquid. From this equation we find that the characteristic time for bubble

expansion is:

$$\tau_{\text{ex}} = R / \sqrt{\frac{\Delta p}{\rho_L}}$$

where Δp is a measure of the change in the surrounding pressure.

Replacing Δp by the upstream pressure p_0 :

$$\tau_{\text{ex}} = R / \sqrt{\frac{p_0}{\rho_L}} = R / U_0 = \frac{R}{L_0} t_{\text{res}}$$

So the ratio between the characteristic time for bubble expansion and bubble residence time is:

$$\frac{\tau_{\text{ex}}}{t_{\text{res}}} = R / L_0$$

Since the bubble radius is much smaller than the length of the nozzle the bubbles will have no trouble expanding quickly enough to keep the pressure inside the bubbles essentially equal to that outside.

Justification of (II) by analytical means is difficult. This is because the major impedance to heat transfer between the gas and liquid is the low thermal conductivity of the gas. To compute the heat transferred between the gas and liquid we need to know the flow field inside the bubbles. Not wishing to compute the flow field inside the bubbles we will rely on indirect experimental verification of (II). In 1966 R. B. Eddington (3.5) presented an extensive experimental investigation of shock phenomena in bubbly two-phase mixtures. He concluded that shock angles and pressure rises could be accurately predicted by a simple isothermal theory. Since Eddington studied shocks with pressure ratios as high as 40 to 1, and still found an

isothermal equation of state to be applicable, we can conclude that in a nozzle, in which pressure gradients will be much less drastic, isothermal expansion of the gas will be a justified assumption.

With our initial assumptions now justified, we have a consistent model for the choked flow of a bubbly mixture in a one-dimensional duct, and can apply it with confidence in the results.

REFERENCES

- 3.1 R.F. Tangren, C.H. Dodge, and H. S. Seifert, "Compressibility Effects in Two-Phase Flow", Journal of Applied Physics Volume 20, Number 7, July 1949, pp. 637 - 645.
- 3.2 T.F. Muir and R. Eichhorn, "Compressible Flow of an Air-Water Mixture Through a Vertical, Two-Dimensional, Converging-Diverging Nozzle", (1963), Proceedings of the 1963 Heat Transfer and Fluid Mechanics Inst., Stanford University, Stanford University Press, pp. 183 - 204.
- 3.3 W.D. Rannie, "A perturbation analysis of one-dimensional heterogeneous flow in rocket nozzles", Progress in Astronautics and Rocketry: Detonation and Two-Phase Flow (Academic Press, New York, 1962), Volume 6.
- 3.4 F.E. Marble, "Dynamics of a gas containing small solid particles", Proceedings of the Fifth AGARD Combustion and Propulsion Colloquium (Pergamon Press, New York, 1963).
- 3.5 R.B. Eddington, "Investigation of Shock Phenomena in a Super Sonic Two-Phase Tunnel", AIAA 3rd Aerospace Sciences Meeting, Paper No. 66-87, 1966.

Notation for Chapter 3

A	Area of duct
L_o	Length of contraction or nozzle
p	Pressure
p_o	Upstream pressure
R	Radius of bubble
u	Dimensionless velocity
U_o	Velocity scale based on upstream pressure and liquid velocity
V	Velocity
\dot{x}	Characteristic velocity
α	Void fraction
β	Volume flow fraction of gas upstream
ϵ	Ratio of nozzle residence time and viscous relaxation time
ρ	Density
τ_v	Viscous relaxation time

Subscripts

g	Gas
L	Liquid
th	Throat of contraction or nozzle

TABLE 3.1 Computed Solution for a Choked Contraction - Zeroth Order
(Pressure Normalized by p_0 ; Velocities by $\sqrt{p_0/\rho_L}$).

UPSTREAM VOID FRACTION=0.050

CONTRACTION RATIO= 4.00

PRESS*	U-LIQ(0)	U-GAS(0)	ALPHA(0)	A(0)/A(TH)
1.00000	0.29842	0.29842	0.05000	4.00004
0.97500	0.37591	0.49244	0.03958	3.14098
0.95000	0.43965	0.62491	0.03752	2.67980
0.92500	0.49521	0.73145	0.03709	2.37814
0.90000	0.54513	0.82261	0.03731	2.16086
0.87500	0.59086	0.90327	0.03786	1.99475
0.85000	0.63333	0.97614	0.03862	1.86248
0.82500	0.67315	1.04290	0.03955	1.75397
0.80000	0.71079	1.10472	0.04061	1.66294
0.77500	0.74657	1.16238	0.04180	1.58519
0.75000	0.78076	1.21648	0.04310	1.51785
0.72500	0.81356	1.26749	0.04452	1.45882
0.70000	0.84513	1.31575	0.04607	1.40660
0.67500	0.87562	1.36153	0.04775	1.36002
0.65000	0.90513	1.40507	0.04958	1.31820
0.62500	0.93377	1.44654	0.05156	1.28044
0.60000	0.96162	1.48609	0.05371	1.24620
0.57500	0.98874	1.52383	0.05606	1.21503
0.55000	1.01521	1.55986	0.05863	1.18658
0.52500	1.04108	1.59426	0.06144	1.16056
0.50000	1.06640	1.62708	0.06454	1.13676
0.47500	1.09121	1.65836	0.06795	1.11498
0.45000	1.11557	1.68813	0.07174	1.09509
0.42500	1.13951	1.71640	0.07597	1.07698
0.40000	1.16307	1.74316	0.08071	1.06060
0.37500	1.18629	1.76840	0.08605	1.04592
0.35000	1.20920	1.79207	0.09212	1.03297
0.32500	1.23185	1.81411	0.09907	1.02180
0.30000	1.25427	1.83443	0.10711	1.01256
0.27500	1.27651	1.85293	0.11649	1.00549
0.25000	1.29862	1.86944	0.12758	1.00094
0.22500	1.32066	1.88375	0.14089	0.99947
0.20000	1.34272	1.89559	0.15712	1.00198
0.17500	1.36438	1.90457	0.17731	1.00991
0.15000	1.38730	1.91015	0.20308	1.02572
0.12500	1.41020	1.91155	0.23700	1.05392
0.10000	1.43393	1.90759	0.28348	1.10371
0.07500	1.45917	1.89630	0.35064	1.19680
0.05000	1.48746	1.87409	0.45518	1.39930
0.02500	1.52376	1.83290	0.63638	2.04669

THROAT PRESSURE= 0.240753
 THROAT U-LIQUID= 1.306776
 THROAT U-GAS= 1.875000
 THROAT VOID FRACTION= 0.132216

TABLE 3.2 Computed Solution for a Choked Contraction - Zeroth Order
(Pressure Normalized by P_0 ; Velocities by $\sqrt{P_0 \rho_L}$).

UPSTREAM VOID FRACTION=0.100
CONTRACTION RATIO= 4.00

PRESS*	U-LIQ(0)	U-GAS(0)	ALPHA(0)	A(0)/A(TH)
1.00000	0.28554	0.28554	0.10000	4.00001
0.97500	0.36909	0.49201	0.07876	3.02315
0.95000	0.43631	0.62941	0.07500	2.54700
0.92500	0.49436	0.73925	0.07436	2.24636
0.90000	0.54628	0.83305	0.07489	2.03405
0.87500	0.59372	0.91598	0.07605	1.87386
0.85000	0.63770	0.99091	0.07760	1.74755
0.82500	0.67891	1.05960	0.07944	1.64476
0.80000	0.71784	1.12324	0.08152	1.55909
0.77500	0.75485	1.18267	0.08384	1.48639
0.75000	0.79022	1.23851	0.08636	1.42378
0.72500	0.82417	1.29124	0.08910	1.36924
0.70000	0.85688	1.34121	0.09207	1.32129
0.67500	0.88848	1.38871	0.09528	1.27880
0.65000	0.91912	1.43393	0.09875	1.24093
0.62500	0.94888	1.47721	0.10249	1.20703
0.60000	0.97785	1.51856	0.10654	1.17657
0.57500	1.00613	1.55814	0.11094	1.14916
0.55000	1.03377	1.59606	0.11571	1.12446
0.52500	1.06085	1.63241	0.12091	1.10225
0.50000	1.08741	1.66726	0.12659	1.08232
0.47500	1.11351	1.70066	0.13282	1.06454
0.45000	1.13920	1.73264	0.13967	1.04882
0.42500	1.16454	1.76323	0.14724	1.03511
0.40000	1.18957	1.79245	0.15565	1.02343
0.37500	1.21434	1.82030	0.16504	1.01382
0.35000	1.23890	1.84675	0.17558	1.00642
0.32500	1.26331	1.87179	0.18748	1.00144
0.30000	1.28763	1.89535	0.20103	0.99918
0.27500	1.31194	1.91737	0.21658	1.00014
0.25000	1.33631	1.93776	0.23459	1.00500
0.22500	1.36086	1.95638	0.25568	1.01433
0.20000	1.38573	1.97306	0.28067	1.03124
0.17500	1.41109	1.98756	0.31071	1.05684
0.15000	1.43724	1.99955	0.34744	1.09601
0.12500	1.46458	2.00860	0.39325	1.15677
0.10000	1.49381	2.01404	0.45179	1.25522
0.07500	1.52623	2.01491	0.52878	1.42931
0.05000	1.56480	2.00975	0.63373	1.79351
0.02500	1.61897	1.99689	0.78276	2.92276

THROAT PRESSURE= 0.313107
 THROAT U-LIQUID= 1.274887
 THROAT U-GAS= 1.883183
 THROAT VOID FRACTION= 0.193703

TABLE 3.3 Computed Solution for a Choked Contraction - Zeroth Order
(Pressure Normalized by p_0 ; Velocities by $\sqrt{p_0 \rho_L}$).

UPSTREAM VOID FRACTION=0.200
CONTRACTION RATIO= 4.00

PRESS*	U-LIQ(0)	U-GAS(0)	ALPHA(0)	A(0)/A(TH)
1.00000	0.27793	0.27793	0.20000	3.99995
0.97500	0.37099	0.50449	0.15864	2.84931
0.95000	0.44359	0.65036	0.15218	2.36476
0.92500	0.50567	0.76631	0.15135	2.07244
0.90000	0.56094	0.86520	0.15261	1.87101
0.87500	0.61134	0.95268	0.15494	1.72149
0.85000	0.65803	1.03182	0.15794	1.60505
0.82500	0.70179	1.10451	0.16145	1.51128
0.80000	0.74315	1.17202	0.16538	1.43388
0.77500	0.78252	1.23524	0.16963	1.36879
0.75000	0.82019	1.29482	0.17434	1.31328
0.72500	0.85642	1.35126	0.17935	1.26542
0.70000	0.89139	1.40495	0.18474	1.22380
0.67500	0.92527	1.45620	0.19050	1.18739
0.65000	0.95819	1.50526	0.19668	1.15541
0.62500	0.99027	1.55235	0.20329	1.12727
0.60000	1.02160	1.59763	0.21038	1.10251
0.57500	1.05228	1.64125	0.21799	1.08078
0.55000	1.08239	1.68334	0.22617	1.06182
0.52500	1.11200	1.72398	0.23498	1.04544
0.50000	1.14118	1.76329	0.24448	1.03152
0.47500	1.17001	1.80132	0.25476	1.01999
0.45000	1.19855	1.83815	0.26592	1.01083
0.42500	1.22686	1.87384	0.27805	1.00409
0.40000	1.25502	1.90843	0.29120	0.99990
0.37500	1.28310	1.94196	0.30579	0.99845
0.35000	1.31118	1.97447	0.32173	1.00002
0.32500	1.33936	2.00598	0.33932	1.00506
0.30000	1.36773	2.03653	0.35884	1.01416
0.27500	1.39642	2.06613	0.38058	1.02820
0.25000	1.42559	2.09481	0.40495	1.04841
0.22500	1.45544	2.12258	0.43242	1.07661
0.20000	1.48622	2.14949	0.46350	1.11560
0.17500	1.51830	2.17556	0.49924	1.16976
0.15000	1.55219	2.20089	0.54032	1.24645
0.12500	1.58871	2.22566	0.58808	1.35899
0.10000	1.62917	2.25021	0.64413	1.53398
0.07500	1.67609	2.27541	0.71059	1.83347
0.05000	1.73502	2.30371	0.79017	2.44286
0.02500	1.82365	2.34495	0.88606	4.23031

THROAT PRESSURE= 0.400837
 THROAT U-LIQUID= 1.254083
 THROAT U-GAS= 1.907290
 THROAT VOID FRACTION= 0.290828

TABLE 3.4 Computed Solution for a Choked Nozzle - Zeroth and First Orders

(Pressure Normalized by p_0 ; Velocities by $\sqrt{p_0/\rho_L}$)STAGNATION VOID FRACTION= 0.050
X(0)=(1.0-P)**2

PRESS*	U-LIQ(0)	U-GAS(0)	ALPHA(0)	A(0)/A(TH)
1.00000	0.0	0.0	0.05000	
0.97500	0.22956	0.39061	0.05207	4.74188
0.95000	0.32479	0.54850	0.05375	3.35741
0.92500	0.39797	0.66805	0.05544	2.74497
0.90000	0.45974	0.75779	0.05717	2.38051
0.87500	0.51424	0.85459	0.05898	2.13228
0.85000	0.56359	0.93237	0.06086	1.94950
0.82500	0.60904	1.00320	0.06285	1.80782
0.80000	0.65141	1.06840	0.06494	1.69400
0.77500	0.69128	1.12921	0.06715	1.60009
0.75000	0.72907	1.18607	0.06950	1.52098
0.72500	0.76508	1.23959	0.07200	1.45331
0.70000	0.79956	1.29018	0.07466	1.39461
0.67500	0.83272	1.33816	0.07750	1.34322
0.65000	0.86470	1.38379	0.08055	1.29782
0.62500	0.89565	1.42726	0.08383	1.25747
0.60000	0.92567	1.46875	0.08736	1.22139
0.57500	0.95486	1.50839	0.09118	1.18902
0.55000	0.98331	1.54630	0.09532	1.15991
0.52500	1.01109	1.58255	0.09983	1.13359
0.50000	1.03827	1.61722	0.10476	1.11009
0.47500	1.06490	1.65037	0.11016	1.08990
0.45000	1.09105	1.68203	0.11611	1.06995
0.42500	1.11677	1.71223	0.12270	1.05317
0.40000	1.14210	1.74097	0.13003	1.03848
0.37500	1.16710	1.76826	0.13823	1.02590
0.35000	1.19183	1.79407	0.14747	1.01550
0.32500	1.21633	1.81836	0.15794	1.00743
0.30000	1.24067	1.84108	0.16992	1.00193
0.27500	1.26491	1.86213	0.18374	0.99936
0.25000	1.28913	1.88141	0.19985	1.00033
0.22500	1.31342	1.89875	0.21886	1.00571
0.20000	1.33791	1.91395	0.24157	1.01638
0.17500	1.36276	1.92673	0.26918	1.03605
0.15000	1.38821	1.93670	0.30337	1.06698
0.12500	1.41461	1.94329	0.34671	1.11652
0.10000	1.44257	1.94570	0.40322	1.19356
0.07500	1.47320	1.94265	0.47956	1.34579
0.05000	1.50904	1.93207	0.58739	1.65716
0.02500	1.55825	1.91045	0.74332	2.63095

TABLE 3.4 (Cont'd.)

STAGNATION VOID FRACTION= 0.050
 $X(0)=(1.0-P)^{**2}$

PRESS*	U-LIQ(1)	U-GAS(1)	ALPHA(1)	A(1)/A(T4)
1.00000	0.0	0.0	0.0	
0.97500	0.0	-0.00020	0.00003	-0.00355
0.95000	0.0	-0.00078	0.00007	-0.00351
0.92500	0.00001	-0.00170	0.00013	-0.00347
0.90000	0.00002	-0.00293	0.00021	-0.00341
0.87500	0.00003	-0.00445	0.00029	-0.00333
0.85000	0.00005	-0.00621	0.00039	-0.00326
0.82500	0.00006	-0.00819	0.00049	-0.00316
0.80000	0.00008	-0.01036	0.00060	-0.00307
0.77500	0.00010	-0.01269	0.00071	-0.00297
0.75000	0.00013	-0.01514	0.00084	-0.00286
0.72500	0.00016	-0.01769	0.00097	-0.00275
0.70000	0.00019	-0.02031	0.00110	-0.00263
0.67500	0.00022	-0.02296	0.00125	-0.00249
0.65000	0.00026	-0.02562	0.00139	-0.00237
0.62500	0.00030	-0.02825	0.00155	-0.00223
0.60000	0.00034	-0.03082	0.00170	-0.00209
0.57500	0.00039	-0.03330	0.00186	-0.00195
0.55000	0.00044	-0.03555	0.00203	-0.00179
0.52500	0.00049	-0.03783	0.00219	-0.00164
0.50000	0.00054	-0.03991	0.00236	-0.00147
0.47500	0.00060	-0.04172	0.00253	-0.00130
0.45000	0.00066	-0.04329	0.00270	-0.00113
0.42500	0.00073	-0.04458	0.00287	-0.00097
0.40000	0.00080	-0.04557	0.00304	-0.00079
0.37500	0.00087	-0.04621	0.00320	-0.00062
0.35000	0.00095	-0.04648	0.00336	-0.00044
0.32500	0.00102	-0.04635	0.00350	-0.00027
0.30000	0.00111	-0.04578	0.00363	-0.00011
0.27500	0.00119	-0.04475	0.00375	0.00007
0.25000	0.00128	-0.04322	0.00383	0.00021
0.22500	0.00138	-0.04117	0.00389	0.00034
0.20000	0.00148	-0.03856	0.00389	0.00044
0.17500	0.00158	-0.03538	0.00384	0.00051
0.15000	0.00168	-0.03161	0.00371	0.00053
0.12500	0.00179	-0.02723	0.00346	0.00045
0.10000	0.00190	-0.02224	0.00307	0.00024
0.07500	0.00201	-0.01665	0.00248	-0.00018
0.05000	0.00212	-0.01052	0.00166	-0.00097
0.02500	0.00221	-0.00402	0.00066	-0.00233

TABLE 3.5 Computed Solution for a Choked Nozzle - Zeroth and First Orders

(Pressure Normalized by p_0 ; Velocities by $\sqrt{p_0/\rho_L}$)STAGNATION VOID FRACTION= 0.100
X(0)=(1.0-P)**2

PRESS*	U-LIQ(0)	U-GAS(0)	ALPHA(0)	A(0)/A(TH)
1.00000	0.0	0.0	0.10000	
0.97500	0.23599	0.40175	0.10387	4.32056
0.95000	0.33404	0.56452	0.10701	3.06302
0.92500	0.40948	0.63798	0.11016	2.50753
0.90000	0.47325	0.79109	0.11338	2.17753
0.87500	0.52959	0.88115	0.11672	1.95324
0.85000	0.58067	0.96194	0.12021	1.78846
0.82500	0.62780	1.03566	0.12385	1.66109
0.80000	0.67181	1.10377	0.12769	1.55908
0.77500	0.71323	1.15727	0.13172	1.47525
0.75000	0.75266	1.22689	0.13597	1.40495
0.72500	0.79026	1.28316	0.14047	1.34511
0.70000	0.82635	1.33652	0.14525	1.29356
0.67500	0.86111	1.38730	0.15032	1.24874
0.65000	0.89474	1.43576	0.15573	1.20952
0.62500	0.92735	1.48212	0.16150	1.17502
0.60000	0.95907	1.52657	0.16767	1.14458
0.57500	0.99002	1.56924	0.17430	1.11769
0.55000	1.02027	1.61028	0.18142	1.09399
0.52500	1.04991	1.64976	0.18911	1.07319
0.50000	1.07902	1.68780	0.19743	1.05506
0.47500	1.10767	1.72445	0.20645	1.03945
0.45000	1.13593	1.75973	0.21628	1.02631
0.42500	1.16386	1.79384	0.22703	1.01560
0.40000	1.19153	1.82666	0.23882	1.00739
0.37500	1.21901	1.85827	0.25131	1.00176
0.35000	1.24638	1.88868	0.26610	0.99898
0.32500	1.27371	1.91791	0.28220	0.99934
0.30000	1.30110	1.94596	0.30010	1.00334
0.27500	1.32866	1.97281	0.32027	1.01167
0.25000	1.35651	1.99844	0.34313	1.02538
0.22500	1.38483	2.02282	0.36924	1.04599
0.20000	1.41383	2.04590	0.39932	1.07583
0.17500	1.44382	2.06762	0.43429	1.11862
0.15000	1.47522	2.08792	0.47540	1.18060
0.12500	1.50870	2.10674	0.52431	1.27310
0.10000	1.54537	2.12407	0.58329	1.41881
0.07500	1.58729	2.14012	0.65543	1.67078
0.05000	1.63911	2.15594	0.74525	2.18811
0.02500	1.71559	2.17732	0.85843	3.76181

TABLE 3.5 (Cont'd.)

STAGNATION VOID FRACTION= 0.100
 $X(0)=(1.0-P)**2$

PRESS*	U-LIQ(1)	U-GAS(1)	ALPHA(1)	A(1)/A(T4)
1.00000	0.0	0.0	0.0	
0.97500	0.0	-0.00020	0.00005	-0.00511
0.95000	0.00001	-0.00077	0.00013	-0.00505
0.92500	0.00002	-0.00163	0.00025	-0.00494
0.90000	0.00004	-0.00290	0.00038	-0.00483
0.87500	0.00006	-0.00440	0.00053	-0.00468
0.85000	0.00009	-0.00614	0.00069	-0.00454
0.82500	0.00012	-0.00809	0.00087	-0.00437
0.80000	0.00016	-0.01023	0.00105	-0.00419
0.77500	0.00021	-0.01252	0.00126	-0.00401
0.75000	0.00026	-0.01493	0.00147	-0.00381
0.72500	0.00031	-0.01744	0.00169	-0.00360
0.70000	0.00037	-0.02001	0.00191	-0.00338
0.67500	0.00044	-0.02250	0.00215	-0.00315
0.65000	0.00051	-0.02520	0.00238	-0.00292
0.62500	0.00059	-0.02777	0.00262	-0.00268
0.60000	0.00067	-0.03027	0.00287	-0.00242
0.57500	0.00076	-0.03269	0.00311	-0.00217
0.55000	0.00085	-0.03498	0.00335	-0.00191
0.52500	0.00095	-0.03711	0.00359	-0.00165
0.50000	0.00106	-0.03906	0.00382	-0.00139
0.47500	0.00117	-0.04078	0.00405	-0.00112
0.45000	0.00129	-0.04226	0.00426	-0.00087
0.42500	0.00141	-0.04346	0.00446	-0.00061
0.40000	0.00154	-0.04435	0.00465	-0.00035
0.37500	0.00163	-0.04489	0.00481	-0.00012
0.35000	0.00182	-0.04506	0.00495	0.00012
0.32500	0.00197	-0.04482	0.00505	0.00032
0.30000	0.00212	-0.04415	0.00511	0.00050
0.27500	0.00228	-0.04301	0.00512	0.00065
0.25000	0.00244	-0.04137	0.00507	0.00075
0.22500	0.00261	-0.03922	0.00495	0.00079
0.20000	0.00278	-0.03652	0.00475	0.00077
0.17500	0.00296	-0.03325	0.00446	0.00066
0.15000	0.00314	-0.02940	0.00404	0.00040
0.12500	0.00332	-0.02496	0.00350	-0.00001
0.10000	0.00350	-0.01994	0.00283	-0.00064
0.07500	0.00367	-0.01436	0.00204	-0.00156
0.05000	0.00382	-0.00832	0.00118	-0.00287
0.02500	0.00393	-0.00205	0.00039	-0.00471

TABLE 3.6 Computed Solution for a Choked Nozzle - Zeroth and First Orders
(Pressure Normalized by p_0 ; Velocities by $\sqrt{p_0/\rho_L}$)

STAGNATION VOID FRACTION= 0.200
X(0)=(1.0-P)**2

PRESS*	U-LIQ(0)	U-GAS(0)	ALPHA(0)	A(0)/A(T)
1.00000	0.0	0.0	0.20000	
0.97500	0.25059	0.42703	0.20669	3.84748
0.95000	0.35502	0.60083	0.21213	2.73440
0.92500	0.43557	0.73314	0.21755	2.24418
0.90000	0.50383	0.84402	0.22307	1.95391
0.87500	0.56430	0.94123	0.22876	1.75740
0.85000	0.61929	1.02875	0.23464	1.61365
0.82500	0.67015	1.10394	0.24075	1.50319
0.80000	0.71730	1.18334	0.24712	1.41527
0.77500	0.76285	1.25302	0.25376	1.34354
0.75000	0.80576	1.31875	0.26072	1.28396
0.72500	0.84689	1.38111	0.26801	1.23377
0.70000	0.88650	1.44053	0.27566	1.19110
0.67500	0.92482	1.49750	0.28370	1.15456
0.65000	0.96203	1.55218	0.29217	1.12319
0.62500	0.99830	1.60485	0.30111	1.09623
0.60000	1.03374	1.65574	0.31056	1.07316
0.57500	1.06849	1.70501	0.32056	1.05353
0.55000	1.10265	1.75281	0.33116	1.03708
0.52500	1.13632	1.79928	0.34242	1.02359
0.50000	1.16959	1.84453	0.35441	1.01294
0.47500	1.20257	1.88868	0.36720	1.00506
0.45000	1.23533	1.93183	0.38086	1.00000
0.42500	1.26797	1.97406	0.39549	0.99783
0.40000	1.30059	2.01548	0.41120	0.99376
0.37500	1.33330	2.05616	0.42810	1.00304
0.35000	1.36621	2.09619	0.44632	1.01110
0.32500	1.39945	2.13568	0.46604	1.02354
0.30000	1.43318	2.17473	0.48742	1.04115
0.27500	1.46758	2.21346	0.51069	1.06509
0.25000	1.50289	2.25201	0.53603	1.09693
0.22500	1.53941	2.29058	0.56389	1.13926
0.20000	1.57752	2.32939	0.59445	1.19551
0.17500	1.61777	2.36880	0.62817	1.27147
0.15000	1.66096	2.40931	0.66550	1.37663
0.12500	1.70827	2.45173	0.70700	1.52809
0.10000	1.76171	2.49744	0.75331	1.75987
0.07500	1.82501	2.54916	0.80515	2.15084
0.05000	1.90641	2.61328	0.86331	2.93514
0.02500	2.03184	2.71123	0.92845	5.26097

TABLE 3.6 (Cont'd.)

STAGNATION VOID FRACTION= 0.200
 $X(0)=(1.0-P)**2$

PRESS*	U-LIQ(1)	U-GAS(1)	ALPHA(1)	A(1)/A(TH)
1.00000	0.0	0.0	0.0	
0.97500	0.0	-0.00019	0.00008	-0.00665
0.95000	0.00002	-0.00075	0.00022	-0.00652
0.92500	0.00004	-0.00164	0.00040	-0.00633
0.90000	0.00008	-0.00284	0.00061	-0.00612
0.87500	0.00012	-0.00429	0.00084	-0.00587
0.85000	0.00019	-0.00590	0.00110	-0.00560
0.82500	0.00025	-0.00730	0.00137	-0.00532
0.80000	0.00032	-0.00907	0.00165	-0.00500
0.77500	0.00041	-0.01219	0.00194	-0.00468
0.75000	0.00050	-0.01453	0.00224	-0.00434
0.72500	0.00061	-0.01695	0.00255	-0.00398
0.70000	0.00073	-0.01943	0.00286	-0.00362
0.67500	0.00085	-0.02193	0.00316	-0.00325
0.65000	0.00099	-0.02443	0.00347	-0.00287
0.62500	0.00114	-0.02638	0.00376	-0.00251
0.60000	0.00129	-0.02927	0.00405	-0.00212
0.57500	0.00146	-0.03155	0.00433	-0.00174
0.55000	0.00164	-0.03371	0.00459	-0.00137
0.52500	0.00183	-0.03571	0.00483	-0.00101
0.50000	0.00202	-0.03751	0.00505	-0.00065
0.47500	0.00223	-0.03910	0.00524	-0.00032
0.45000	0.00244	-0.04042	0.00540	0.00000
0.42500	0.00267	-0.04147	0.00553	0.00030
0.40000	0.00290	-0.04220	0.00561	0.00055
0.37500	0.00315	-0.04258	0.00565	0.00077
0.35000	0.00340	-0.04259	0.00564	0.00095
0.32500	0.00365	-0.04219	0.00557	0.00108
0.30000	0.00392	-0.04137	0.00544	0.00113
0.27500	0.00419	-0.04009	0.00524	0.00111
0.25000	0.00447	-0.03830	0.00497	0.00099
0.22500	0.00474	-0.03602	0.00463	0.00079
0.20000	0.00502	-0.03321	0.00420	0.00043
0.17500	0.00530	-0.02985	0.00371	-0.00005
0.15000	0.00553	-0.02594	0.00314	-0.00072
0.12500	0.00585	-0.02148	0.00252	-0.00157
0.10000	0.00610	-0.01548	0.00187	-0.00263
0.07500	0.00631	-0.01102	0.00122	-0.00394
0.05000	0.00643	-0.00520	0.00064	-0.00546
0.02500	0.00652	0.00057	0.00020	-0.00716

CHAPTER 4

Experiments on One-Dimensional Duct Flow

Some rudimentary experiments on choked bubbly flow were performed utilizing a contraction in a rectangular duct. The duct was designed so that the upstream boundary conditions used in chapter three for the analysis of flow through a contraction would be realistic, and the variations in area were made particularly gentle to increase the accuracy of the one-dimensional analysis. This is in contrast to the experiment described in reference 4.2.

Figure 4.1 is a photograph of the contraction. It was made of two $3/4$ " Plexiglass sheets spaced by $1/2$ " Plexiglass. Figure 4.2 shows the countour of the contraction. The cross section up and downstream of the contraction is $2" \times 1/2"$. That at the throat is $1/2" \times 1/2"$. The length of the contraction is six inches. The bubble injection system is situated upstream of the contraction and consists of 20 tubes running across the channel, each with 36 holes of $1/64$ " diameter. Figure 4.3 is a photograph of these tubes taken from the rear of the channel. The axial extent of this injection system was six inches.

The contraction and bubble injection system was placed in the flow system shown in Figure 4.4. The system operated in a blow down manner. The sixty gallon tank on the right provided enough water for the choked contraction to operate in a steady-state for about a minute. High pressure nitrogen forced the water up the pipe extending down into the tank. It then flowed through the venturi where its flow rate was measured using a mercury manometer. Next the water flowed into the bubble injection system and was joined by nitrogen gas bubbles. The flow rate of the bubble gas was measured with a rotameter before it

entered the injection system. From this point the mixture flowed directly into the contraction. The pressure of the mixture was measured at five stations in the contraction. The pressure taps at these locations consisted of $1/32$ " dia. holes in the wall of the channel. Each of the taps was connected to a solenoid valve. These valves may be seen in Figure 4.1. This allowed any of the five pressures to be measured alternatively using the same bourdon tube pressure gauge. After leaving the contraction the mixture flowed through a gate valve, and into a fifty-five gallon drum, to be drained later.

The procedure for running each test was as follows: First, the high pressure tank was filled with water. Next the gate valve downstream and the bubble injection tubes were closed off. The system was then pressurized to about 110 psig. The bubble gas pressure was then adjusted so that bubbles would flow into the liquid when the injection tubes were opened. The final step before operation was to bleed any air out of the pressure tap lines, and out of the lines from the venturi to the manometer. To begin operation the bubble injection tubes and the downstream gate valve were opened. As the gate valve was opened the throat pressure in the contraction was monitored. At some point, opening the gate valve further no longer decreased the throat pressure, indicating the flow was choked. Before taking data the gate valve was opened fully so that the mixture expanded throughout the contraction. At this point the following measurements were recorded.

- 1) The rotameter reading and the pressure of the gas in the rotameter

- 2) The pressure difference across the venturi
- 3) The pressure in the upstream tank
- 4) The pressure at each of five locations in the contraction

This procedure was carried out eighteen separate times. For each test the pressure in the bubble injection tubes was set at a different level to achieve different upstream void fractions. In this manner we were able to vary the upstream void fraction between 0.04 and 0.45. Table 4.1 contains all the data recorded in the eighteen tests.

Several photographs were taken of the flow in and upstream of the contraction to verify that the bubble injectors were producing a uniform stream of bubbles. Two of these are shown in Figure 4.5. They were taken with speed 3600 black and white Polaroid film using a spark discharge which gave an exposure time of less than 10 μ sec. This was sufficiently fast to stop the motion of the bubbles. The contraction was illuminated from the rear. Both the photos in Figure 4.5 were taken just a bit upstream of the throat. It appears that the distribution of the gas, which appears black in the photographs, is reasonably uniform. We can even make out an occasional single bubble in the photographs. These appear to be round so modeling them as spheres should be a reasonable approximation.

Local measurements of the void fraction were attempted using a resistivity probe similar to that of Nassos and Bankoff (4.1). This probe consisted of a needle pointed directly into the oncoming flow. The sides of the needle were insulated so that current could pass only through the very tip. The probe was placed in a bridge circuit powered

by a 1.5 volt battery and the signal from the bridge was monitored on an oscilloscope. It was concluded that the signal associated with the arrival of a bubble at the probe tip was not sharp enough to determine the void fraction with confidence. The probe was located just upstream of the contraction where the flow velocity was about 20 ft/sec in most cases. This is quite a bit higher than the velocities at which these probes have been used previously, and it seems that they are not well suited for use at high speeds.

Figures 4.6 through 4.11 are direct comparisons of the pressure data taken in six of the eighteen tests to the zeroth order analytical solution described in Chapter 3. Each is a plot of the area of the channel, normalized by the throat area, versus the pressure normalized by the upstream pressure. The measured quantity is the pressure, plotted on the abscissa. Agreement between the measurements and the theory is quite reasonable until we reach the divergent section of the contraction where it is doubtful that bubbly flow persists. Because the flow is choked, whether or not the flow is bubbly in the divergent section will have no influence on the flow upstream of the throat. We can be reasonably certain that the flow will remain bubbly up to the throat. The reason is, that even though the mixture has expanded to quite a low pressure at the throat, the void fraction does not increase proportionately since the gas accelerates faster than the liquid. For example, when the upstream void fraction is 0.20 we can expect the throat void fraction to be less than 0.30 even though the pressure decreases by a factor of 2.5. This indicates that we can expect bubbly flow, at least up to the throat, for upstream void

fractions considerably higher than we might originally estimate.

The pressure gauge used to measure the pressures in the contraction was graduated in units of $1/2$ psi. Assuming we could read it to $\pm 1/4$ psi the accuracy of our pressure ratio measurements should be better than $\pm 2\%$. Measurements of the gas flow rate were made with either of two rotameters used in the experiment, both of which were graduated in one-percent divisions of full scale. So the accuracy of our gas flow rate measurements is $\pm 1\%$. The manometer connected to the venturi was graduated in tenths of an inch. This made for an accuracy of $\pm 1\%$ in our water flow rate. We can therefore estimate that the accuracy of the upstream void fraction, calculated on the basis of equal velocities upstream is $\pm 2\%$.

This brings us to an interesting point. In reducing our data we calculate the upstream void fraction assuming that the velocities of both phases are equal. This is also the boundary condition we used in our analytical work. Since the gas shoots ahead of the liquid as soon as it enters the contraction (accompanied by a decrease in void fraction) the analytical solution is very sensitive to this condition being met. If instead of $u_g = u_L$ we enforced the condition $u_g = 1.1 \times u_L$ the solution we would calculate would be considerably different. With this in mind, reasonable care was taken to be sure the experimental situation was one in which $u_g = u_L$ upstream. Tests 10 through 13 were made with only the four bubble injectors farthest from the contraction operating. If a difference between the results of these tests and the others was noticed it would indicate that bubbles being injected from those tubes close to the contraction did not have sufficient time to

accelerate to the liquid speed. No such difference could be discerned. This is shown in Figure 4.12 which gives the throat pressure normalized by the upstream pressure vs. the upstream void fraction. The line on the graph is the zeroth order analytical solution. The points denoted by boxes represent data taken with all the bubble injectors operating. The points denoted by asterisks represent data taken with only the four farthest upstream injectors operating. We can see that the experiment and theory agree well until the upstream void fraction reaches about .3. Above this value the predicted pressure ratios are slightly higher than those observed. This may be due to the increasing importance of interactions between bubbles at higher void fractions.

Figure 4.13 is a comparison of the data taken by Muir and Eichhorn (4.2) 1963, to the zeroth order analytical solution for a nozzle. Muir and Eichhorn used a contraction ratio of 14 in their experiments so in the upstream section the fluid was essentially at rest. The throat pressure ratio is plotted against the upstream volume flow fraction of gas.

The agreement is only slightly better than that obtained using the homogeneous flow theory of Tangren, Dodge and Seifert (4.3). Muir and Eichhorn explained the difference between their data and the homogeneous theory as a consequence of the failure of the homogeneous theory to account for slip between the phases. Our calculation accounts for the slip and yet still does not agree with their data. Inclusion of the next order term in our theoretical calculation will bring our prediction into closer agreement with Muir and

Eichhorn's data, but it seems unlikely that this will account for all of the difference. A more plausible explanation is that two-dimensional effects are important in the Muir and Eichhorn experiment. The radius of curvature at the throat region of their nozzle was $1/2''$. This indicates that bubbles passing through the nozzle may experience considerable accelerations normal to the nozzle axis. Our model assumes these accelerations are unimportant and is therefore not exactly applicable to this experimental situation. The radius of curvature at the throat of our contraction was $3\ 3/16''$ so these two-dimensional effects will be much less important. It seems possible that the two-dimensional effects in the Muir and Eichhorn nozzle could be accounted for in the manner used by Henry and Fauske (4.4) in studying one-component critical flow through orifices and short tubes.

The preliminary experiments described herein show quite good agreement with the zeroth order analytical solution for flow through a contraction which was described in Chapter 3. This indicates that the model described in Chapter 3 is accurate and may be used in other similar situations with a high degree of confidence.

It also shows that the flow in our contraction is bubbly even at void fractions as high as .3 or .4, where bubbly flow is usually not thought to persist. This is probably because we create the mixture not very far upstream as a bubbly one, and there is not enough time for a change of flow regime to take place. This idea may have implications for the analysis of a

blow-down from a pressure vessel which has undergone a sudden depressurization. If bubbles are generated homogeneously in the fluid it is likely that the flow out of the vessel will remain bubbly to higher void fractions than previously expected.

REFERENCES

- 4.1 G. P. Nassos and S. G. Bankoff, "Local Resistivity Probe for Study of Point Properties in Gas-Liquid Flows", The Canadian Journal of Chemical Engineering Volume 45, Oct. 1967, pp. 271-274.
- 4.2 T.F. Muir and R. Eichhorn, "Compressible Flow of an Air-Water Mixture Through a Vertical, Two-Dimensional, Converging-Diverging Nozzle", (1963), Proceedings of the 1963 Heat Transfer and Fluid Mechanics Inst., Stanford University, Stanford University Press, pp. 183-204.
- 4.3 R.F. Tangren, C.H. Dodge, and H.S. Seifert, "Compressibility Effects in Two-Phase Flow", Journal of Applied Physics Volume 20, Number 7, July 1949, pp. 637 - 645.
- 4.4 R.E. Henry and H.K. Fauske, "The Two-Phase Critical Flow of One Component Mixtures in Nozzles, Orifices and Short Tubes", Journal of Heat Transfer - Transactions of the ASME, May, 1971, pp. 179 - 187.

TABLE 4.1 Summary of Experimental Data

Test No.	Gas Flow Rate (lbm / sec)	Water Flow Rate (lbm/sec)	1st Station	Pressures in the Contraction (psia)				5th Station	Upstream Void Fraction(calc.)
				2nd Station	3rd Station	4th Station			
1	0.0141	7.61	92½	88½	37	—	—	0.203	
2	0.0217	6.99	93½	90½	41	14	12½	0.420	
3	0.0117	7.80	89¾	85	34½	12½	10½	0.175	
4	0.00787	8.42	87½	82	29	11	10	0.120	
5	0.0137	7.49	88	84	35	12½	10½	0.211	
6	0.0220	6.86	93	89½	40½	15	12½	0.307	
7	0.0152	7.68	92	87½	36	11	9	0.216	
8	0.00987	8.24	88	83	30½	10	8½	0.149	
9	0.0265	6.80	97	93	43	11½	10½	0.340	
10*	0.00905	8.30	89½	84	31	10	9	0.135	
11*	0.0214	7.86	90½	86	34	10	9	0.183	
12*	0.0194	7.18	91	87¼	38¼	11	10	0.276	
13*	0.0236	6.74	92	89	41	12	11	0.328	
14	0.0373	5.99	97½	95	48	12½	12	0.450	
15	0.0104	8.36	92	87	32½	15	12½	0.148	
16	0.00244	9.80	83½	77	20	12½	10½	0.0366	
17	0.00635	8.74	87	81½	27	10	9	0.0960	
18	0.00755	8.61	89	83½	28½	11	10	0.112	

*Test run with only four farthest upstream bubble injectors operating

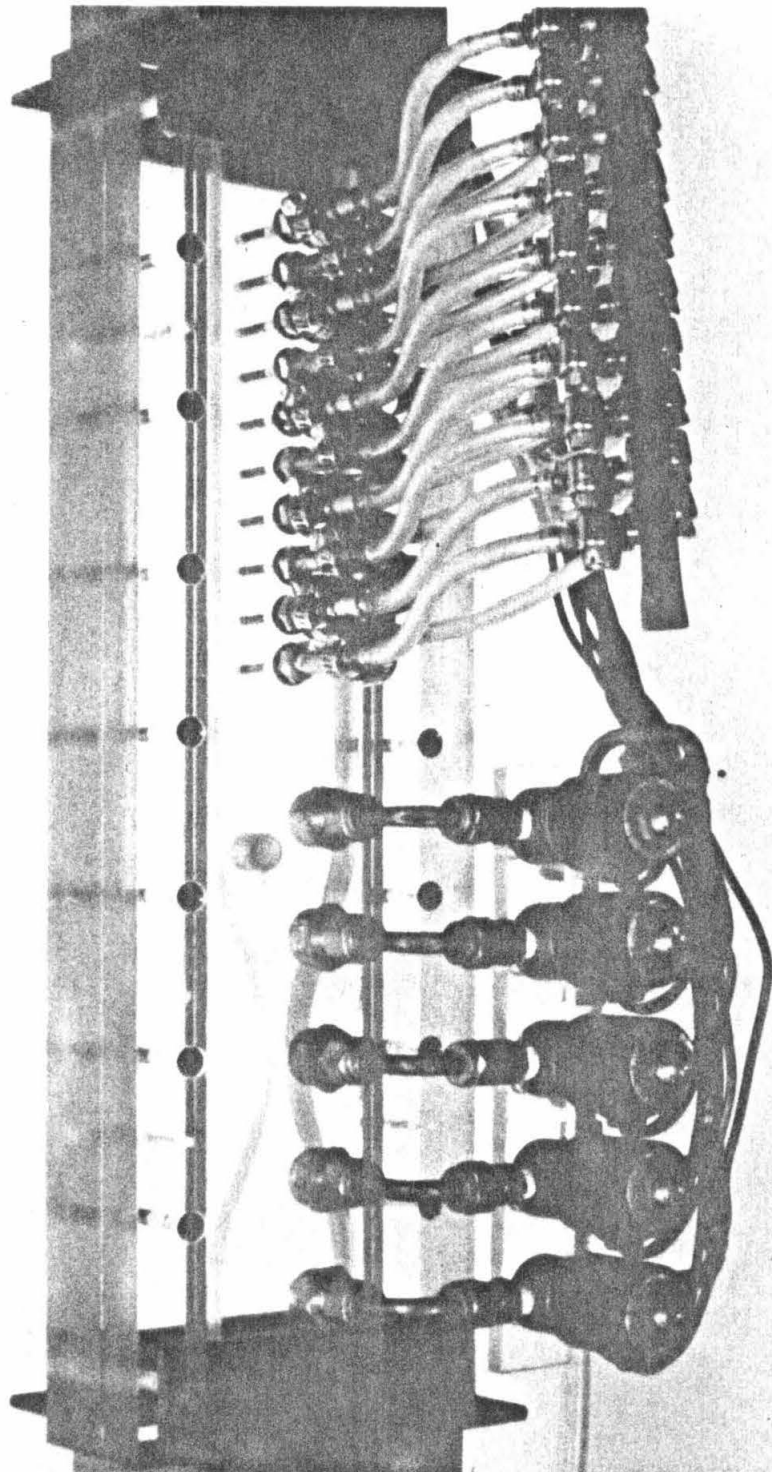


FIGURE 4.1 Photograph of the Contraction

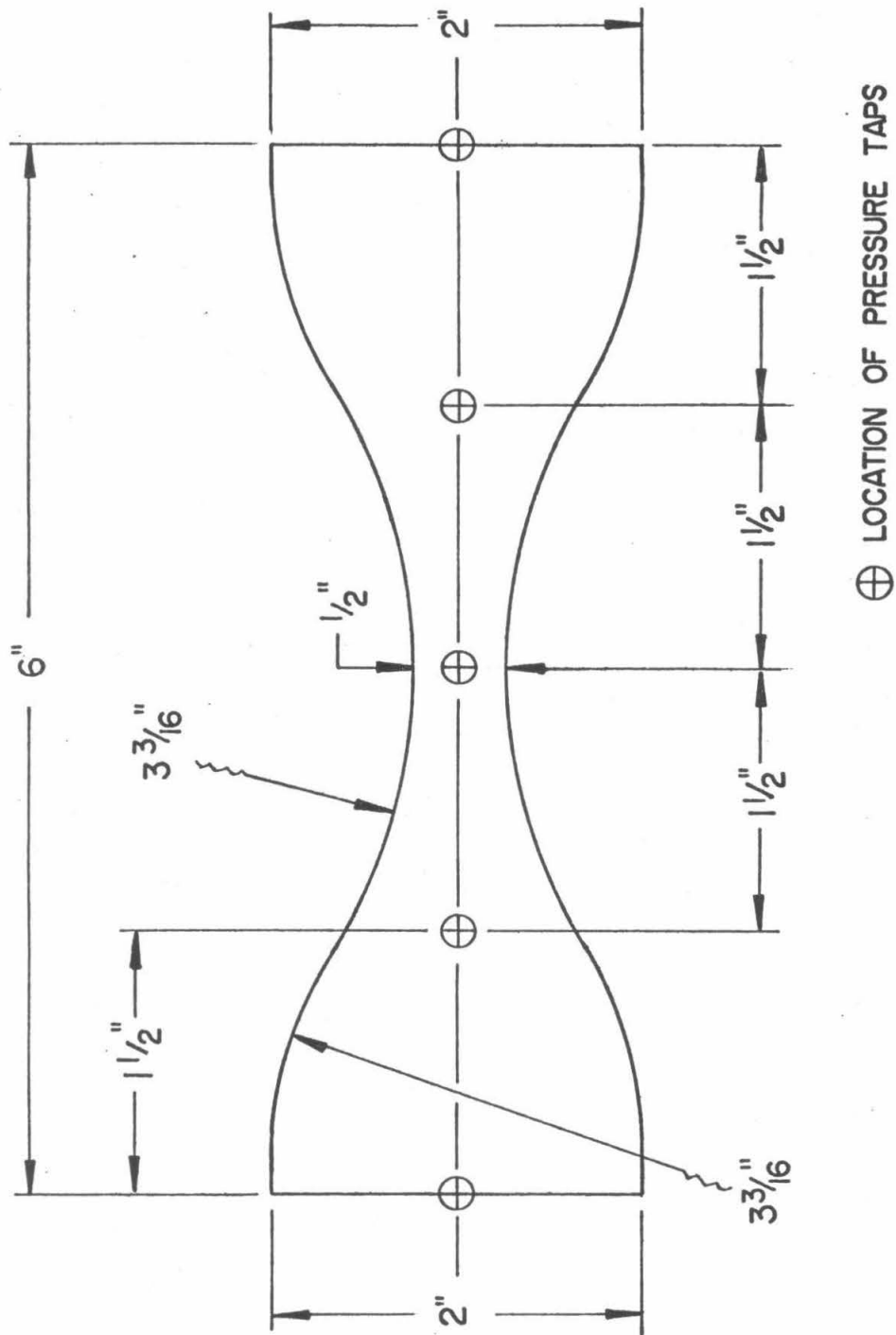


FIG. 4.2 DIMENSIONS OF THE CONTRACTION

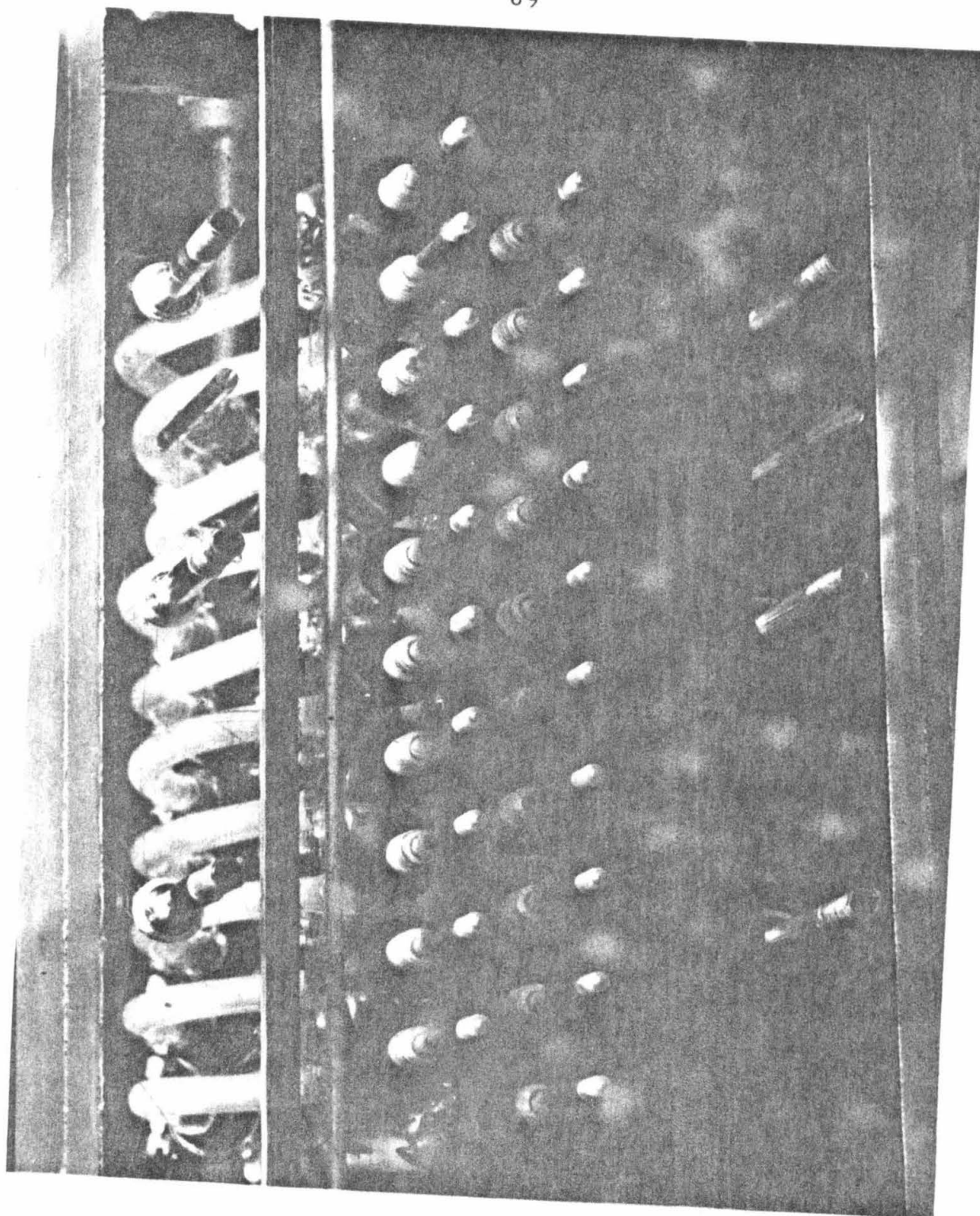


FIGURE 4.3 Photograph of the Bubble Injection Tubes

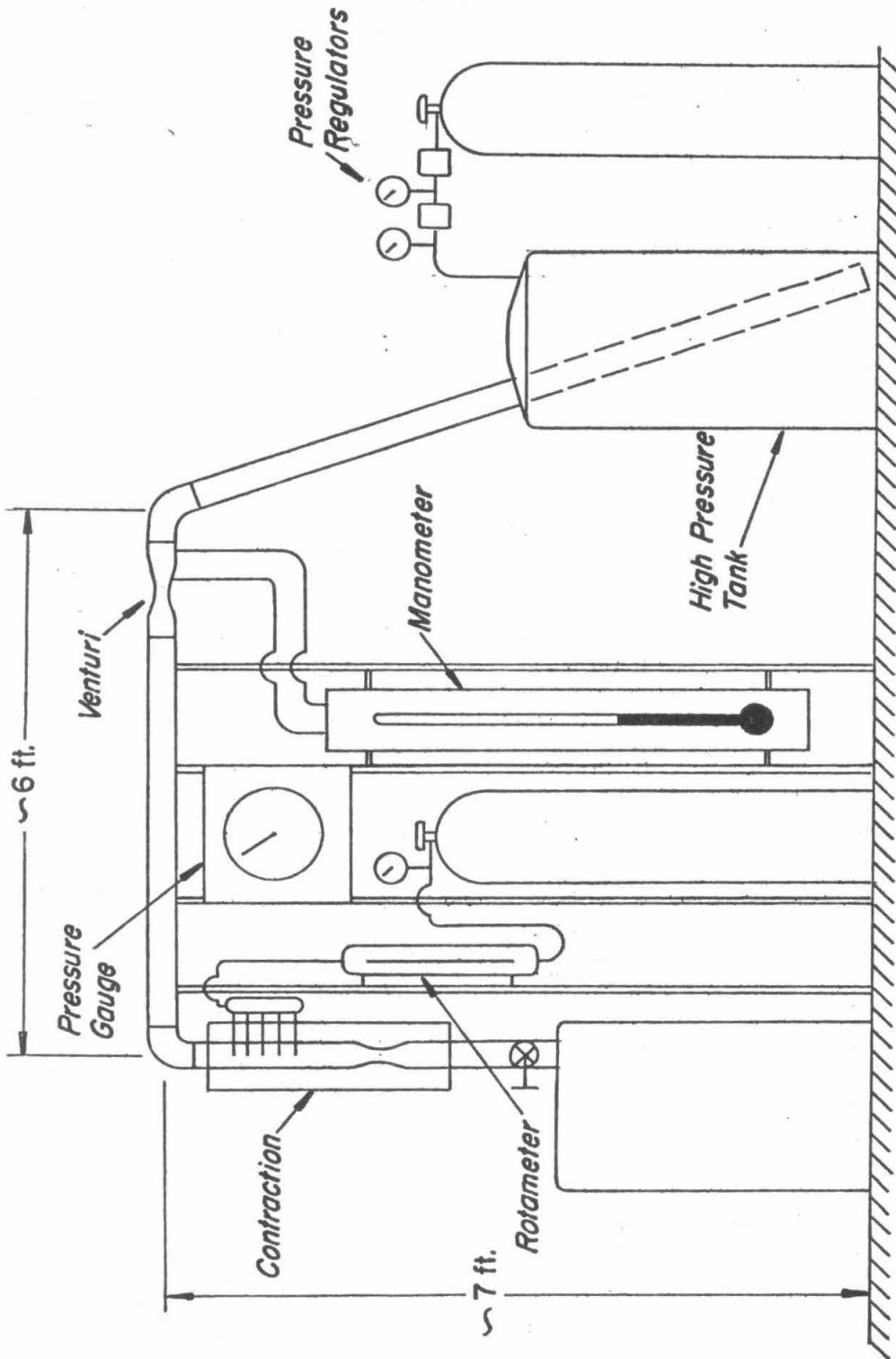


FIG. 4.4 SCHEMATIC OF FLOW SYSTEM

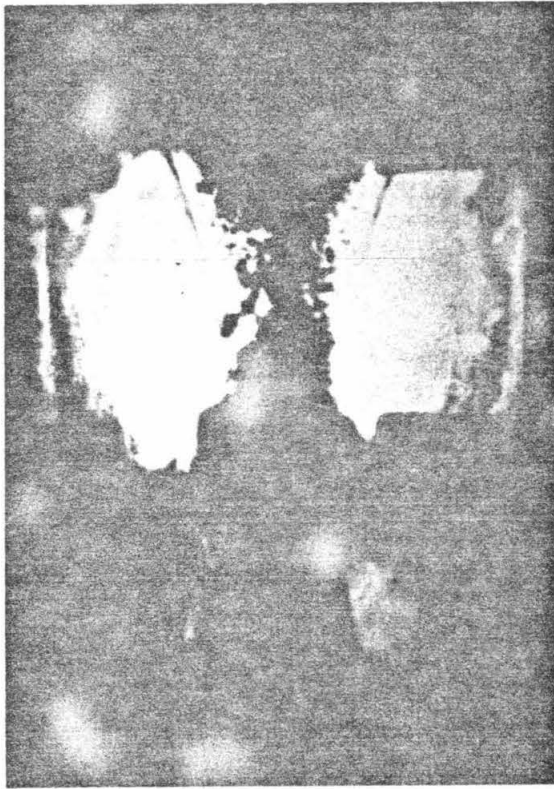


FIGURE 4.5 Photographs of the Flow in the Contraction;
Upstream Void Fraction Approximately 0.1

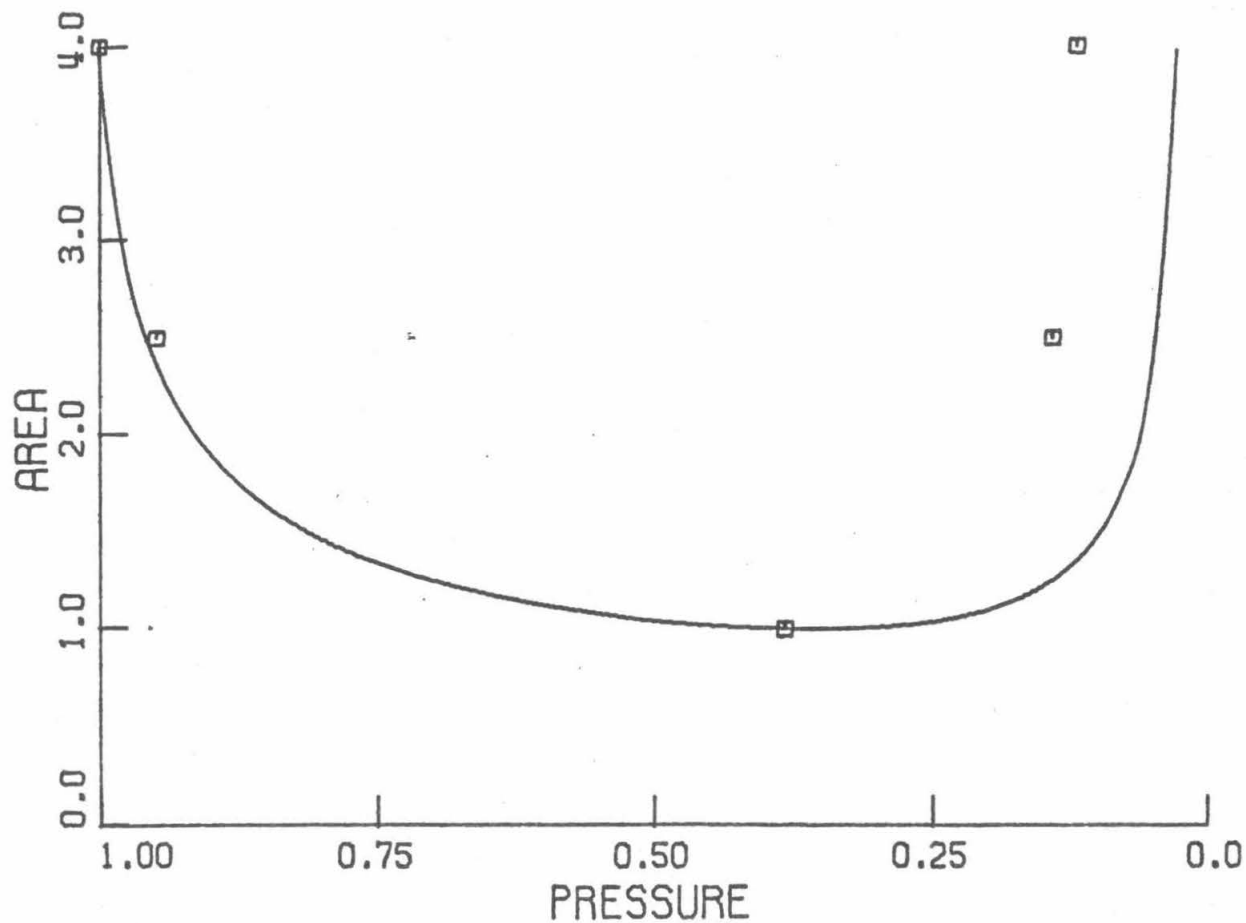


FIG. 4.6 AREA(NORMALIZED BY THROAT AREA) vs PRESSURE(NORMALIZED BY UPSTREAM PRESSURE); EXPERIMENT AND THEORY - RUN 3; UPSTREAM VOID FRACTION = 0.175

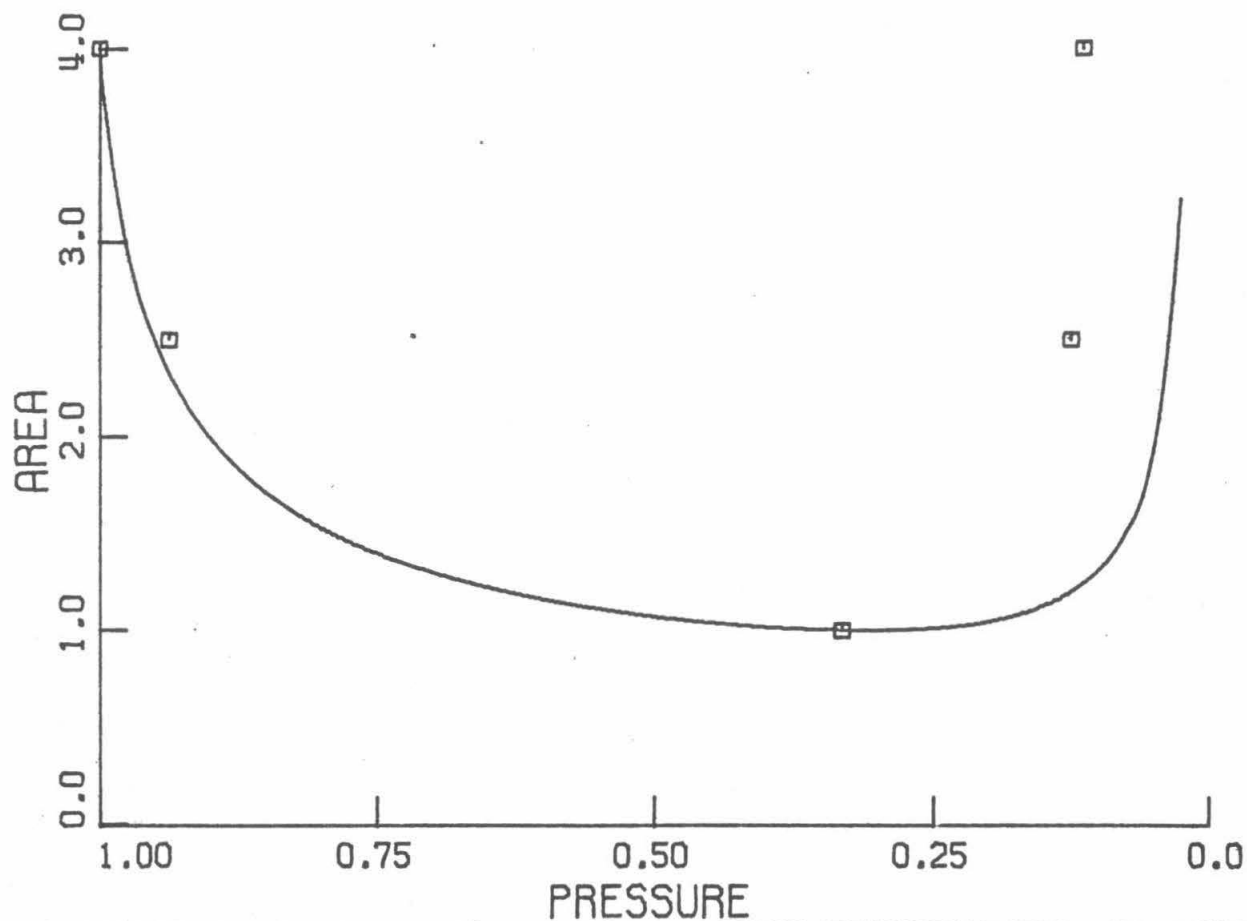


FIG. 4.7 AREA(NORMALIZED BY THROAT AREA) vs PRESSURE(NORMALIZED BY UPSTREAM PRESSURE); EXPERIMENT AND THEORY - RUN 4; UPSTREAM VOID FRACTION = 0.120

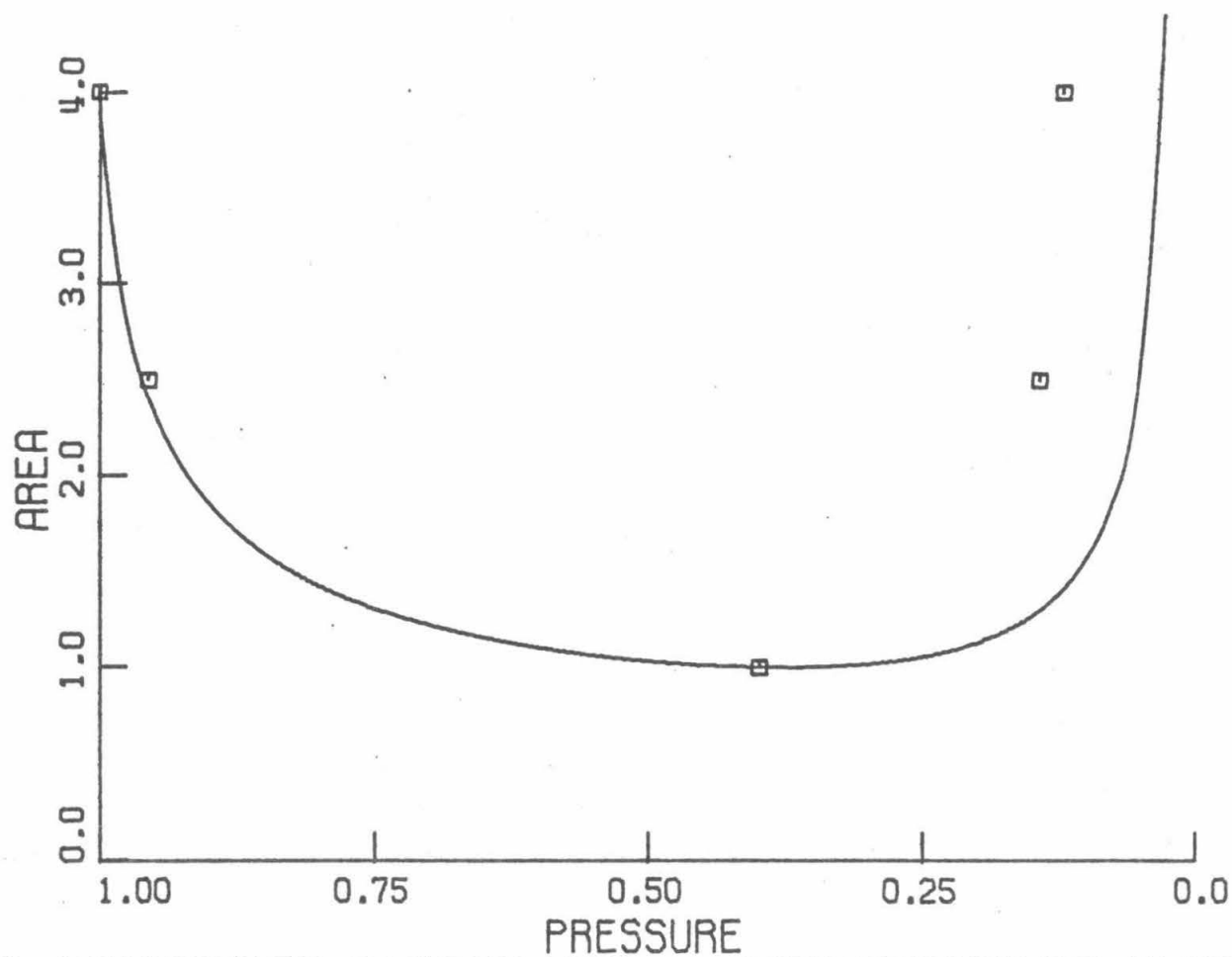


FIG. 4.8 AREA(NORMALIZED BY THROAT AREA) vs PRESSURE(NORMALIZED BY UPSTREAM PRESSURE); EXPERIMENT AND THEORY - RUN 5; UPSTREAM VOID FRACTION = 0.211

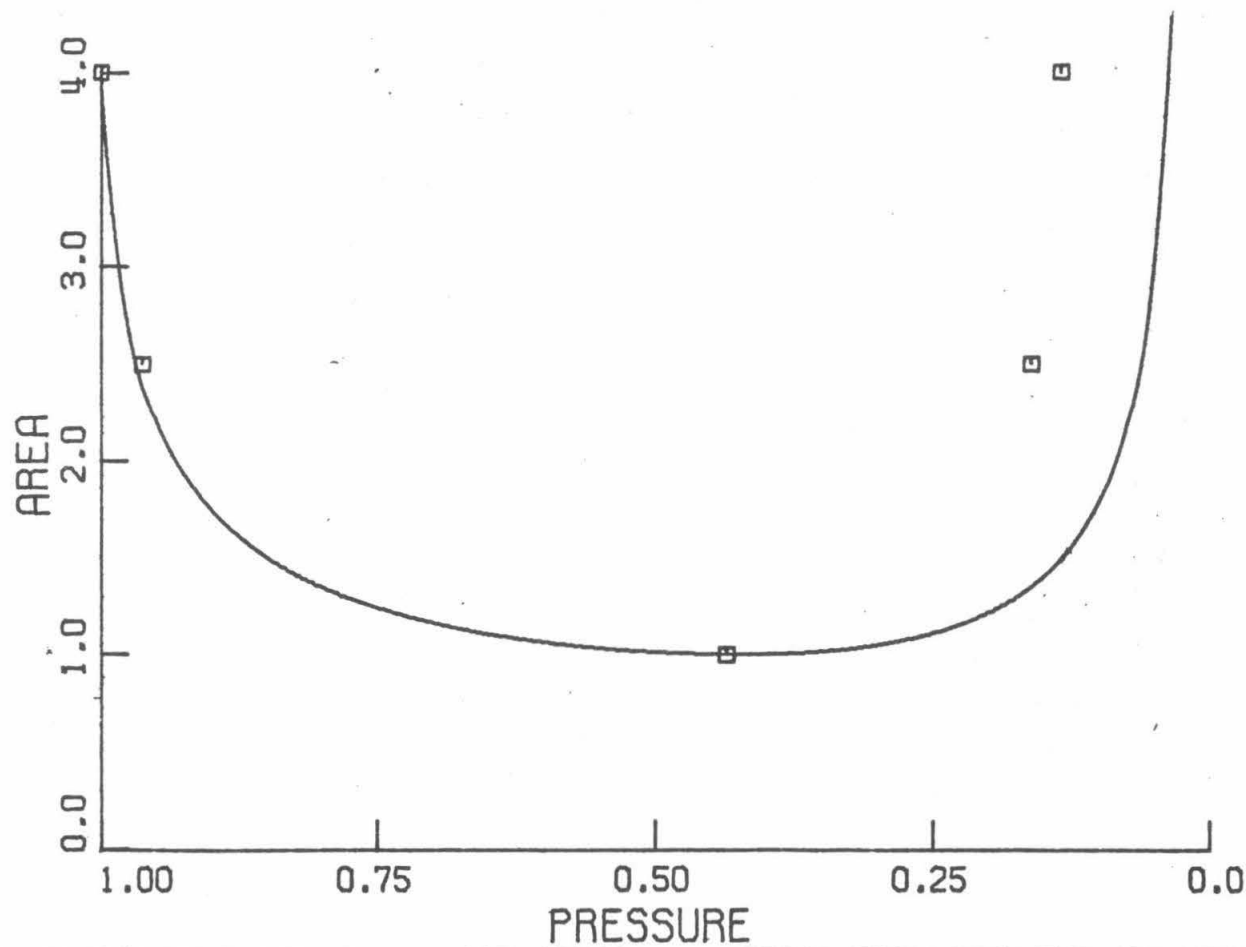


FIG. 4.9 AREA(NORMALIZED BY THROAT AREA) vs PRESSURE(NORMALIZED BY UPSTREAM PRESSURE); EXPERIMENT AND THEORY - RUN 6; UPSTREAM VOID FRACTION = 0.307

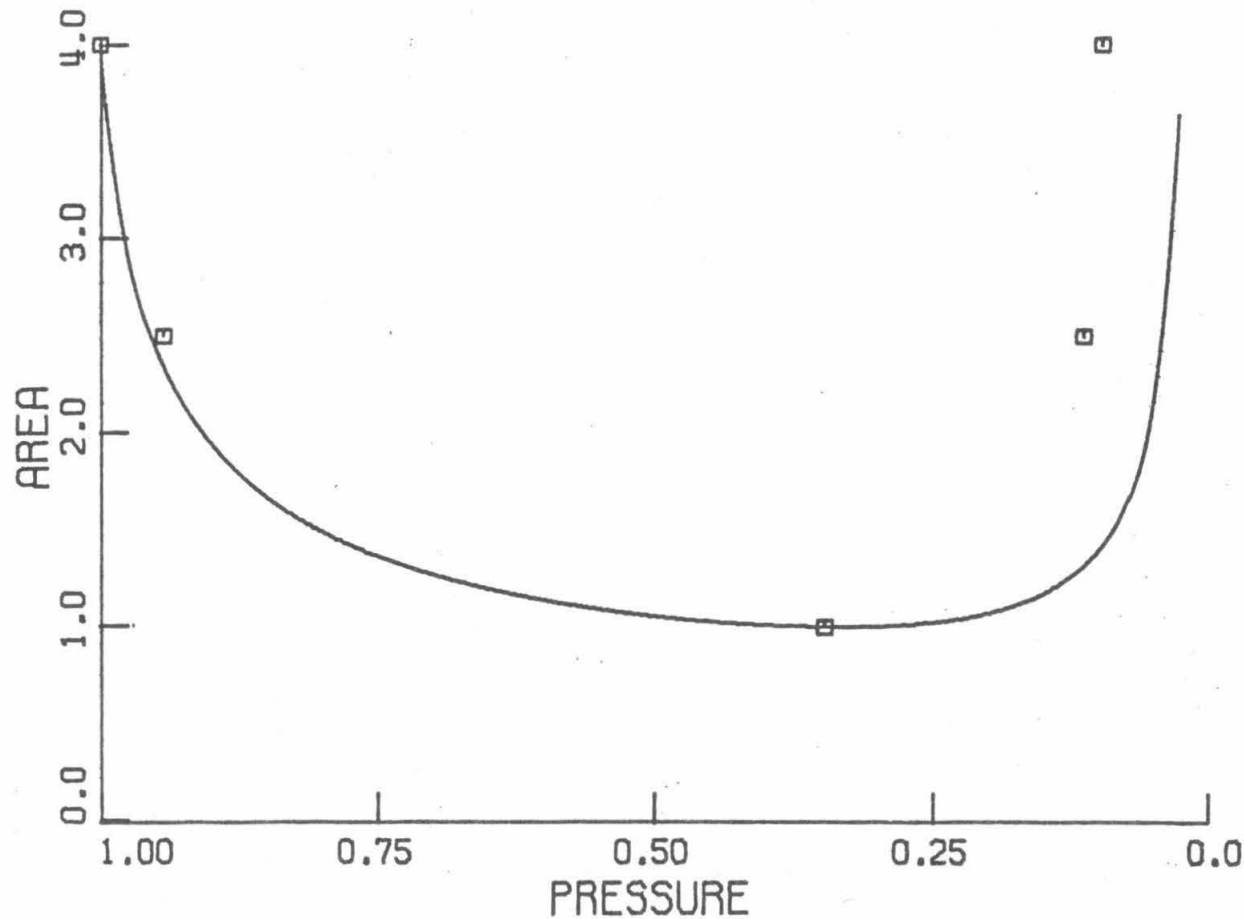


FIG. 4.10 AREA(NORMALIZED BY THROAT AREA) vs PRESSURE(NORMALIZED BY UPSTREAM PRESSURE); EXPERIMENT AND THEORY - RUN 8; UPSTREAM VOID FRACTION = 0.149

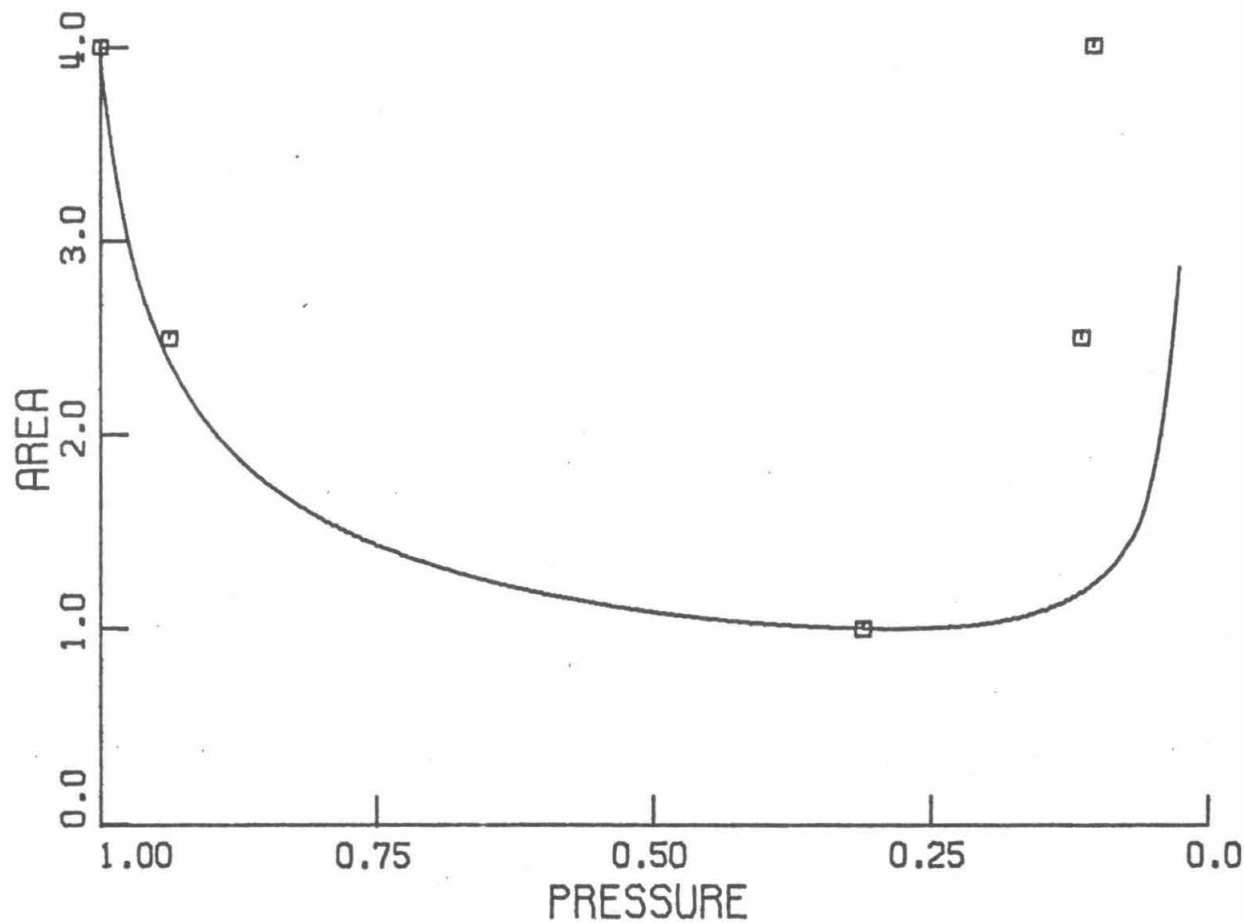


FIG. 4.11 AREA(NORMALIZED BY THROAT AREA) vs PRESSURE(NORMALIZED BY UPSTREAM PRESSURE); EXPERIMENT AND THEORY - RUN 17; UPSTREAM VOID FRACTION = 0.096

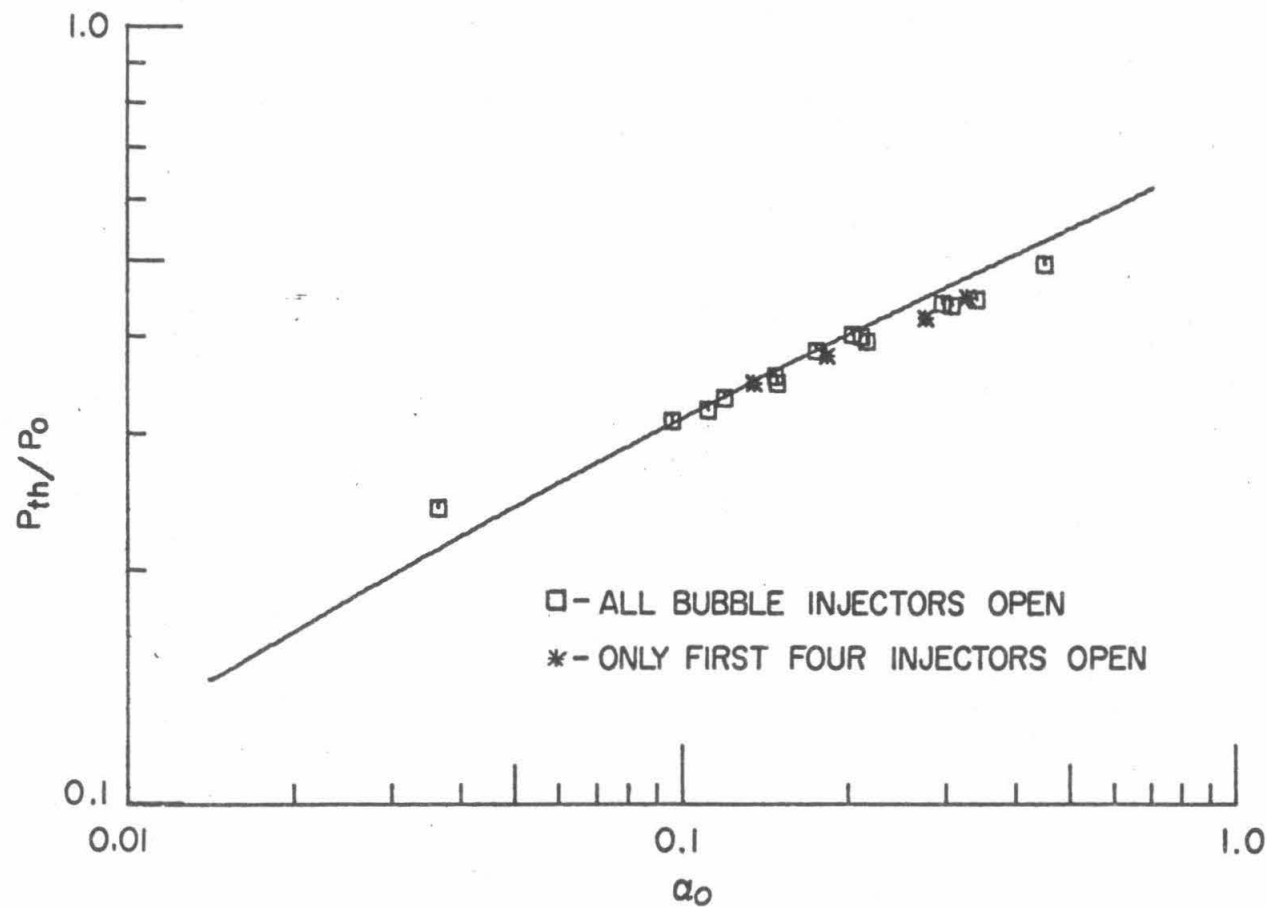


FIG. 4.12 DIMENSIONLESS THROAT PRESSURE, P_{th}/P_0 , vs UPSTREAM VOID FRACTION, α_0 , FOR A CHOKED CONTRACTION; EXPERIMENT AND THEORY.

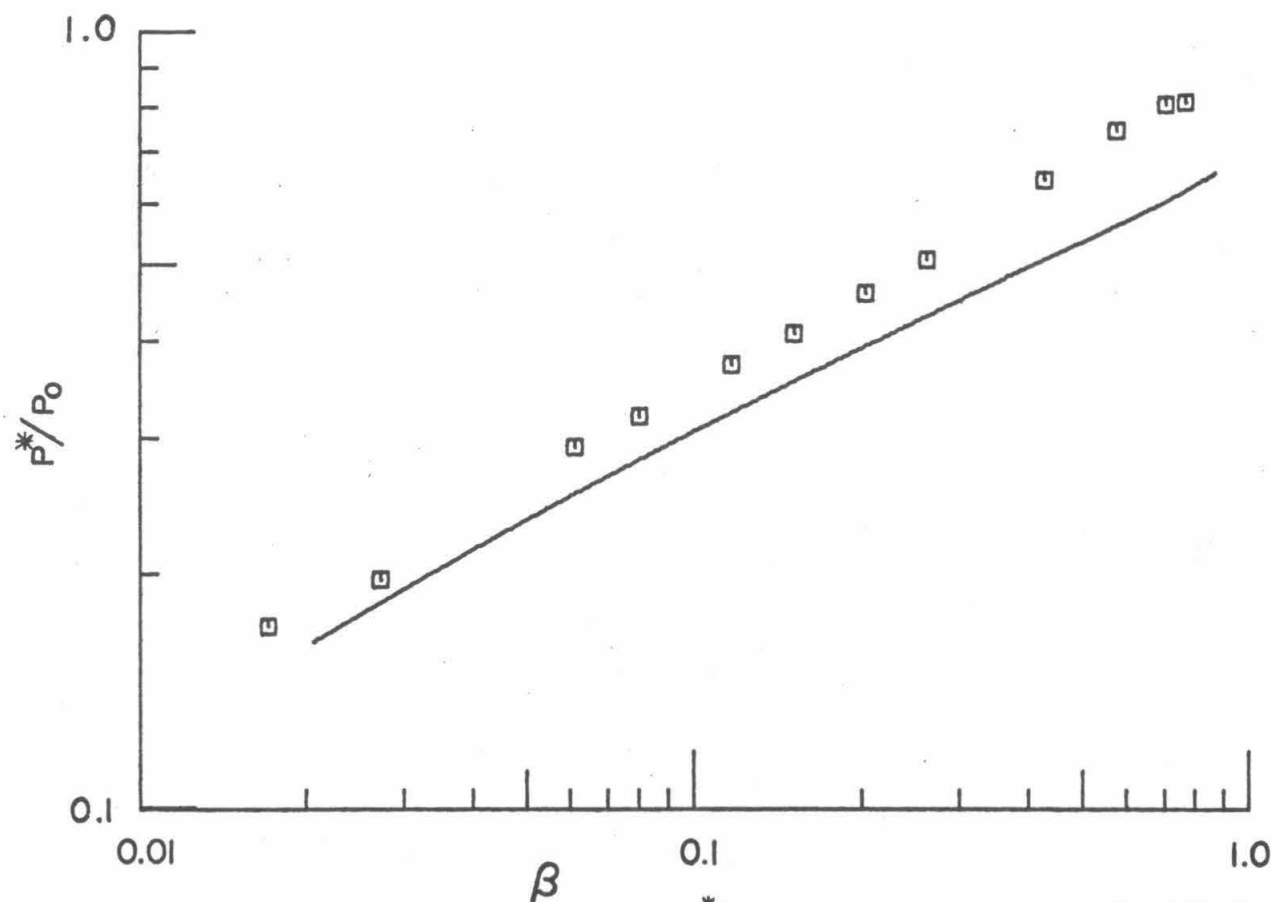


FIG. 4.13 CRITICAL PRESSURE RATIO, P^*/P_0 , vs UPSTREAM VOLUME FLOW FRACTION, β ; COMPARISON OF THEORY TO DATA OF REFERENCE 4.2

CHAPTER 5

The Rise of a Cloud of Bubbles Through a Liquid5.1 Statement of the Problem

In this chapter we address an interesting stability problem which appears to have some bearing on the question of whether a bubbly flow will maintain its bubbly structure or will eventually develop into some other sort of flow, perhaps a slug-type flow. The problem concerns disturbances to a uniform state which grow on a time scale related to the viscous relaxation time of the bubbles. The results will thus be important for the analysis of devices in which a bubbly liquid resides for at least a few relaxation times.

The possible mechanism for this change of flow regime is related to the fact that the characteristics of the equations for one-dimensional flow are not always real. We recall from our discussion in Chapter 3 that two of the four characteristics are complex whenever a relative velocity between the gas and liquid exists. The other two characteristics are altered only slightly by the relative velocity, and retain their significance as acoustic speeds. This suggests that compressibility is not an essential feature of the physical phenomena related to the two complex characteristics. Therefore, to gain an understanding of these phenomena, we should analyze a problem in which the relative velocity between the phases is the sole essential feature.

We consider the one-dimensional situation depicted in Figure 5.1. Liquid is flowing down, through a cloud of small gas bubbles. The liquid velocity is equal to the terminal rise

velocity of the bubbles which are at rest. The void fraction of the mixture is uniform at value α_0 . Our analysis will examine the development of a small disturbance to this uniform state.

A somewhat similar situation was treated by Likht and Shteinbert (5.1) 1974, who found that a horizontal layer of liquid with bubbles rising through it is unstable. Our work will show that even the one-dimensional situation is unstable and we shall further attempt to discover the final form this disturbance reaches.

Table 5.1 gives pertinent information about 1/32" dia. air bubbles rising through water. It is worthwhile to note that the Reynolds number of such a bubble is 133, which is high enough to be well within the range described by our bubble equation of motion. It is also important that even with such a large Reynolds number, the Weber number, a comparison between pressure and surface tension forces, is only .16. This indicates that the bubbles will indeed be spherical, as we have assumed in deriving their equation of motion. A final item to be noted from Table 5.1 is that $\frac{\rho_L V_o^2}{\rho_g c_g^2}$, the scale on which we expect fractional bubble size changes to occur, is only .0002. Therefore, any effects associated with the bubbles changing size will be unimportant, and we can assume them to be incompressible without incurring significant error. With this in mind we can write down our governing equations for the situation. They are, referring to (2.3, 2.4, 2.9, 2.18)

Gas Conservation

$$\frac{\partial \alpha}{\partial t} + \frac{\partial}{\partial y} (\alpha v_g) = 0 \quad (5.1)$$

Liquid Conservation

$$\frac{\partial(1-\alpha)}{\partial t} + \frac{\partial}{\partial y} ((1-\alpha)v_L) = 0 \quad (5.2)$$

Mixture Motion

$$\rho_L(1-\alpha) \left\{ \frac{\partial v_L}{\partial t} + v_L \frac{\partial v_L}{\partial y} \right\} + \frac{\partial p}{\partial y} = -\rho_L(1-\alpha)g \quad (5.3)$$

Bubble Motion

$$\left\{ \frac{\partial v_g}{\partial t} + v_g \frac{\partial v_g}{\partial y} \right\} - 3 \left\{ \frac{\partial v}{\partial t} + v_L \frac{\partial v_L}{\partial y} \right\} + \frac{1}{\tau_v} (v_g - v_L) = 2g \quad (5.4)$$

The approximations we have made to this point are:

- 1) One-dimensional flow
- 2) Mass of the gas bubbles is negligible
- 3) Both liquid and gas are incompressible

Seeking the characteristics of the above set of equations we discover that there are only two, instead of the previous four. This follows from the assumption that the gas is incompressible and as such will no longer carry acoustic disturbances. Therefore, the characteristics corresponding to these disturbances no longer appear. The two remaining characteristic speeds are given by the expression:

$$\dot{Y} = \frac{(1-\alpha)v_g + 3\alpha v_L \pm i\sqrt{3\alpha(1-\alpha)}(v_g - v_L)}{(1+2\alpha)} \quad (5.5)$$

This expression, which gives the characteristics of the approximate equations we are now dealing with, is identical to Equation 3.5.

That equation gives approximate values of the characteristic speeds

of our more exact set of one-dimensional equations. This confirms our belief that compressibility is not an important feature of the phenomena associated with these complex characteristic speeds.

5.2 Linear Analysis of the Growth of a Disturbance

In problems such as this, where one wishes to follow the development of a small disturbance about a uniform state, the first procedure to try is linearization. If the linearized equations predict that the magnitude of the disturbance will decay with the passage of time, then the linearization technique will be valid for all time. If, on the other hand, the linearized equations predict amplification of the disturbance, they will only be accurate while the disturbance is still small enough to make linearization valid. In either case the linearized equations will provide an accurate description of the situation initially.

Using the linearized versions of (5.1 - 5.4) we can easily find an equation for the void fraction perturbation by differentiating the bubble motion equation with respect to y and utilizing the two continuity equations. The equation thus obtained is:

$$\begin{aligned} \frac{\partial}{\partial t} \left\{ \frac{\partial}{\partial t} + \frac{1}{\tau_v} \right\} \alpha' + \left(\frac{\alpha_0}{1 - \alpha_0} \right) \left\{ 3 \left(\frac{\partial}{\partial t} - V_0 \frac{\partial}{\partial y} \right) \right. \\ \left. + \frac{1}{\tau_v} \right\} \left\{ \frac{\partial}{\partial t} - V_0 \frac{\partial}{\partial y} \right\} \alpha' = 0 \end{aligned} \quad (5.6)$$

Because this equation is of second order in α' , we need two initial values. For instance, we could specify $\alpha'(0, y)$ and $\frac{\partial \alpha'}{\partial t}(0, y)$.

Assuming that we have solved for α' we can then go ahead and

use the other three linearized equations to find the gas and liquid velocity and pressure perturbations. These equations are:

$$\begin{aligned}\frac{\partial v_g'}{\partial y} &= -\frac{1}{\alpha_0} \frac{\partial \alpha'}{\partial t} \\ \frac{\partial v_L'}{\partial y} &= -\frac{1}{1-\alpha_0} \left[\frac{\partial \alpha'}{\partial t} - V_0 \frac{\partial \alpha'}{\partial y} \right] \\ \frac{\partial p'}{\partial y} &= -\rho_L(1-\alpha_0) \left[\frac{\partial v_L'}{\partial t} - V_0 \frac{\partial v_L'}{\partial y} \right] + \rho_L g \alpha'\end{aligned}\tag{5.7}$$

If $\alpha'(y, t)$ is known it becomes a simple matter to calculate $v_g'(y, t)$, $v_L'(y, t)$ and $p'(y, t)$. For this reason we will concentrate our efforts on calculating $\alpha'(y, t)$.

Equation 5.6, from which we expect to find $\alpha'(y, t)$, is of course a linear elliptic partial differential equation. The initial value problem for this equation is therefore an ill-posed one, as discussed by Garabedian (5.2). We realize that, except for certain special initial conditions, solutions of Equation 5.6 will in general diverge as time passes. As we mentioned before, this is not particularly alarming because we know that at some time nonlinear terms will become important and Equation 5.6 will cease to be accurate. We can still use Equation 5.6 though, to calculate the solution initially. If we measure time in units of τ_v , the relaxation time, and length in units of $V_0 \tau_v$, the relaxation length, then Equation 5.6 becomes:

$$\frac{\partial}{\partial t} \left\{ \frac{\partial}{\partial t} + 1 \right\} \alpha' + \frac{\alpha_0}{1-\alpha_0} \left\{ 3 \left(\frac{\partial}{\partial t} - \frac{\partial}{\partial y} \right) + 1 \right\} \left\{ \frac{\partial}{\partial t} - \frac{\partial}{\partial y} \right\} \alpha' = 0\tag{5.8}$$

If we let $\frac{\alpha_0}{1 - \alpha_0}$ equal γ and multiply this equation out we then have the mathematical problem:

$$\alpha'_{tt} + \left(\frac{1+\gamma}{1+3\gamma}\right)\alpha'_t - \left(\frac{6\gamma}{1+3\gamma}\right)\alpha'_{yt} + \left(\frac{3\gamma}{1+3\gamma}\right)\alpha'_{yy} - \left(\frac{\gamma}{1+3\gamma}\right)\alpha'_y = 0 \quad (5.9)$$

$$\alpha'(y, 0) = g(y) \quad ; \quad \alpha'_t(y, 0) = h(y)$$

We can solve this problem by using the Fourier transform in the y-direction. The resulting solution is:

$$\alpha'(y, t) = \frac{1}{\sqrt{2\pi}} \int_{-\infty}^{\infty} F(k, t) e^{-iky} dk \quad (5.10)$$

where

$$\begin{aligned} F(k, t) = & \frac{s_-(k)G(k) - H(k)}{s_-(k) - s_+(k)} e^{s_+(k)t} \\ & + \frac{H(k) - s_+(k)G(k)}{s_-(k) - s_+(k)} e^{s_-(k)t} \end{aligned} \quad (5.11)$$

in which

$$s_{\pm}(k) = \frac{-\{(1+\gamma) + 6\gamma ik\} \pm \sqrt{(1+\gamma)^2 + 12\gamma k^2 + 8\gamma ik}}{2(1+3\gamma)} \quad (5.12)$$

and

$$\begin{aligned} G(k) &= \frac{1}{\sqrt{2\pi}} \int_{-\infty}^{\infty} g(y) e^{iky} dy \\ H(k) &= \frac{1}{\sqrt{2\pi}} \int_{-\infty}^{\infty} h(y) e^{iky} dy \end{aligned} \quad (5.13)$$

Examining $s_{\pm}(k)$ we realize that:

$$s_{\pm}(-k) = s_{\pm}^*(k) \quad (5.14)$$

and for all real k :

$$\operatorname{Re}\{s_+(k)\} > 0 \quad ; \quad \operatorname{Re}\{s_-(k)\} \leq 0 \quad (5.15)$$

As we expected, most solutions of Equation 5.6 will be divergent. The only solutions which will not diverge are those special ones corresponding to initial conditions for which:

$$s_-(k) G(k) - H(k) = 0 \quad (\text{for all } k)$$

For these special initial conditions none of the divergent solutions involving the $e^{s_+(k)t}$ term in $F(kt)$ are excited. As we have stated, though, a general set of initial data leads to a divergent solution. Also, under certain initial conditions, no solution may be calculated at all. To see this, we write our solution in the form of two integrals:

$$\begin{aligned} \alpha'(yt) = \frac{1}{\sqrt{2\pi}} \left\{ \int_{-\infty}^{\infty} q_+(k) e^{s_+(k)t} e^{-iky} dk \right. \\ \left. + \int_{-\infty}^{\infty} q_-(k) e^{s_-(k)t} e^{-iky} dk \right\} \end{aligned} \quad (5.16)$$

The first integral contains the term $e^{s_+(k)t}$ where $t \geq 0$ and $\operatorname{Re}\{s_+(k)\} > 0$. In fact

$$\operatorname{Re}\{s_+(k)\} \sim \frac{\sqrt{3}\gamma}{1+3\gamma} |k| \text{ as } |k| \rightarrow \infty \quad (5.17)$$

So, if $q_{\pm}(k)$ does not go to zero fast enough, for large $|k|$, the first integral will not converge and no solution exists. The two functions $q_{\pm}(k)$, are formed from the Fourier transforms of the initial data. For a solution of the problem to exist we must put a limit on their high wave number content. This is equivalent to a restriction on the high wave number content of the initial data. Luckily, this is a restriction which will be met by any sensible initial data. The reason is that we are, of course, describing a collection of discrete bubbles as a continuum. There is, then, a natural limit on the high wave number content of the initial data. This is because we need a volume of at least a few bubble spacings cubed, just to define quantities like the void fraction. It would therefore make very little sense to impose initial data on our problem, which varied on a length scale shorter than a few bubble spacings. We can expect then that for sensible initial data the functions $q_{\pm}(k)$ will have the property:

$$q_{\pm}(k) \equiv 0 \quad \text{for } |k| > k_{\max}$$

So we see that the restriction of the high wave number content of the initial data is a physical one as well as a mathematical one.

Having established that we can calculate solutions for all reasonable initial data, we can now investigate the properties of the solutions we calculate. Actually, all of the important information about the solutions is contained within the two functions $s_{\pm}(k)$. Of course, $s_{\pm}(k)$ are two quite complicated functions of k .

For this reason analysis of $s_{\pm}(k)$ is most conveniently done with the aid of a computer. If we set:

$$s_{\pm}(k) = a_{\pm}(k) + ib_{\pm}(k)$$

our basic solutions become:

$$e^{s_{\pm}(k)t} e^{-iky} = e^{a_{\pm}(k)t} e^{-i(ky - b_{\pm}(k)t)}$$

This exhibits their wavelike nature and shows that $b_{\pm}(k)/k$ is the phase speed of the wave. Tables 5.2 and 5.3 give values of $a_{\pm}(k)$ and $b_{\pm}(k)$ as a function of wave number for $\gamma = .10$ and $.25$. From these tables we can learn several things. First:

$$b_{\pm}(k) \leq 0$$

which indicates that the wave motion will be in the downward direction. Second, by plotting $\frac{b_{\pm}(k)}{k}$ in a normalized form, $-\frac{(1 + 3\gamma)b_{\pm}(k)}{3\gamma k}$, as we have done in Figure 5.2, we can see that we can expect considerable dispersion in our solutions. This is because the phase speed of our waves is not constant but is dependent on wave number. We can therefore expect our solutions to exhibit three properties:

- 1) The disturbance as a whole will move in the downward direction
- 2) The disturbance will be amplified as it moves
- 3) The disturbance will spread out due to the dispersive nature of the waves.

These three properties can be seen readily in the calculated solution, shown in Figures 5.3 through 5.6. These give the solution for the initial conditions:

$$\alpha'(y, 0) = -\frac{4}{\pi} \frac{\sin \pi y}{(y+2)(y-2)y}$$

$$\frac{\partial \alpha'}{\partial t}(y, 0) = 0$$

The specific functional form of $\alpha'(y, 0)$ was chosen with considerable care so that the condition that $q_{\pm}(k) \equiv 0$ for $k > k_{\max}$ would be met. This function is part of the more general set of functions:

$$f(y) = -\frac{4\pi^2}{(k_{\max})^3} \frac{\sin(k_{\max} y)}{y(y - \frac{2\pi}{k_{\max}})(y + \frac{2\pi}{k_{\max}})}$$

whose Fourier transforms are:

$$F(k) = \begin{cases} \frac{\sqrt{8\pi}}{k_{\max}} \left\{ 1 - \cos 2\pi \left(\frac{k}{k_{\max}} \right) \right\} & |k| < k_{\max} \\ 0 & |k| > k_{\max} \end{cases}$$

Our specific initial value corresponds to $k_{\max} = \pi$. Since

$\int_{-\infty}^{\infty} \alpha'(y, 0) dy = 0$ this solution corresponds to a disturbance which does not involve any addition of bubbles to the system, just a rearrangement of them. The graphs in Figures 5.3 through 5.6 are to be read in the following manner:

- 1) In each case the abscissa is the y -axis ; it is in units of

$V_0 \tau_v$ and up is to the right

- 2) All the quantities plotted are dimensionless. Figure 5.3 gives the void fraction perturbation, α' , Figure 5.4 gives the dimensionless gas velocity perturbation, $\frac{v_g'}{V_0}$, Figure 5.5 gives the dimensionless liquid velocity perturbation, $\frac{v_L'}{V_0}$ and Figure 5.6 the dimensionless pressure perturbation, $\frac{p'}{\rho_L V_0^2}$.
- 3) All of the graphs are normalized by the maximum of the absolute value of the quantity plotted. This value is written in the lower right hand corner of each graph.
- 4) The time is written in the lower right hand corner of each graph in units of τ_v .

The solution shown was calculated for a value of γ equal to 0.1. As the reader can verify all three of the properties expected are exhibited by this solution. Of course, the gas velocity for time equals zero is not plotted because it is identically zero.

Before leaving our linear analysis entirely, it is interesting to consider what happens to a disturbance which has a length scale that is long compared to the relaxation length. In such a case the two functions $q_{\pm}(k)$ are non-zero only for very small k . This means it will be sufficient to approximate $s_{\pm}(k)$ for very small k . These approximations are:

$$\begin{aligned} s_+(k) &\approx -i\alpha_0 k \\ s_-(k) &\approx -\left(\frac{1+\gamma}{1+3\gamma}\right) \end{aligned}$$

So, the second integral in Equation 5.16 will become very un-

important after only a few τ_v . The solution will then be approximately:

$$\alpha'(y, t) \approx \frac{1}{\sqrt{2\pi}} \int_{-\infty}^{\infty} q_+(k) e^{-i k(y + \alpha_0 t)} dk \quad (5.18)$$

This is just a wave that maintains its form and moves downward at speed $\alpha_0 V_0$. Using Equation 5.18 and the Equations 5.7, we can also discover that when Equation 5.18 applies:

$$\frac{v_L'}{V_0} = \frac{v_g'}{V_0} = -\alpha'$$

So, long length scale disturbances quickly relax to a situation in which the gas and liquid velocity perturbations are equal to the negative of the void fraction perturbation. This implies that after this quick relaxation our description of the system can in some way be simplified. We will see later that this is actually the case.

5.3 Non-Linear Analysis of the Growth of a Disturbance

We now return to our full non-linear equations with the hope that somehow the non-linear terms which have been omitted in our linear analysis will act to stop the growth of a disturbance.

The simplest thing we can do with a set of non-linear equations such as (5.1) to (5.4) is to look for wave solutions of permanent form. That is, we look for solutions such that:

$$\begin{aligned} \alpha &= \alpha(y + u_0 t) \\ v_g &= v_g(y + u_0 t) \\ v_L &= v_L(y + u_0 t) \\ p &= p(y + u_0 t) \end{aligned} \quad (5.19)$$

Since the pressure only appears in the mixture motion equation, we really only need to work with the other three equations and the quantities α , v_g and v_L . If we substitute the assumed solution from Equation 5.19 into our equations, we find that (5.19) is a possible solution form and that the solution is:

$$v_g = -u_0 + \left(\frac{\alpha_0}{\alpha}\right) u_0$$

$$v_L = -u_0 + \left(\frac{1-\alpha_0}{1-\alpha}\right)(u_0 - V_0)$$

$$\eta = \int_{\alpha(0)}^{\alpha(\eta)} \frac{\left[\frac{\alpha_0^2 a^2}{\alpha^3} + 3 \frac{(1-\alpha_0)^2 (a-1)^2}{(1-\alpha)^3} \right] \alpha (1-\alpha)}{(\alpha - \alpha_0)(\alpha - a)} d\alpha \quad (5.20)$$

$$u_0 = aV_0 \quad ; \quad \eta = \frac{y + u_0 t}{V_0 \tau_v}$$

The solution comes out in an implicit form; we can calculate η as a function of α . What we do is pick $\alpha(0)$ somewhere between α_0 and a . Then, as $\alpha(\eta)$ goes to α_0 or a , η will go to plus or minus infinity. Thus the void fraction profile will look like that in Figure 5.7, and the solution we have found is a sort of transition between regions of undisturbed void fractions α_0 and a . It turns out that the greater of α_0 and a will always be the void fraction below the transition, and that to interchange the two amounts only to a Galilean transformation. This is evident from the symmetry in the integral in (5.20) between α_0 and a .

Figure 5.7 is actually a solution calculated from Equation 5.20 for a transition between $\alpha = .2$ and $\alpha = .1$. The void fraction is plotted as a function of $\frac{y + u_0 t}{V_0 \tau_v}$, and up is to the right on the graph. We can see that what this solution resembles most is a region of high void fraction below the transition, from which bubbles are escaping into a region of lower void fraction above. This interpretation is useful in dealing with a more general disturbance, and seems physically reasonable.

In the case of a very weak wave, in which a is very close to α_0 , we can compute the integral in Equation 5.20 approximately to find:

$$\alpha \approx \left(\frac{a + \alpha_0}{2}\right) + \left(\frac{a - \alpha_0}{2}\right) \tanh \frac{a - \alpha_0}{\nu} \eta \quad (5.21)$$

$$\nu = \alpha_0 (1 - \alpha_0) (3 - 2\alpha_0)$$

In addition, we note that for a weak wave there is a simple relationship between the strength of the wave, $(a - \alpha_0)$, and the maximum slope thickness in units of $V_0 \tau_v$. That relationship is:

$$\text{Strength} \times \text{Thickness} = 2\nu \quad (5.22)$$

Now, the existence of wave-like solutions such as the ones we have found poses a question for us: Just what role do they play in the solution of a general initial value problem, and under what circumstances are they created? In an effort to answer this question we consider disturbances which have length scales that are much greater than the relaxation length of the bubbles. In many

cases this is not a severe limitation and it greatly simplifies our task. If we call this long length scale L_0 and the time scale associated with it t_0 ($L_0 = V_0 t_0$), then a logical approach to the solution of our problem is to form the perturbation series:

$$\begin{aligned}
 \alpha &= \alpha_0 + \epsilon \alpha^{(1)} \left(\frac{y}{L_0}, \frac{t}{t_0} \right) + \dots \\
 \frac{v_g}{V_0} &= \epsilon v_g^{(1)} \left(\frac{y}{L_0}, \frac{t}{t_0} \right) + \dots \\
 \frac{v_L}{V_0} &= -1 + \epsilon v_L^{(1)} \left(\frac{y}{L_0}, \frac{t}{t_0} \right) + \dots \\
 \epsilon &= \frac{\tau_v}{t_0}
 \end{aligned} \tag{5.23}$$

Upon substitution of these series into our equations we find that:

$$\begin{aligned}
 \frac{\partial \alpha^{(1)}}{\partial (t/t_0)} - \alpha_0 \frac{\partial \alpha^{(1)}}{\partial (y/L_0)} &= 0 \\
 v_g^{(1)} &= v_L^{(1)} = -\alpha^{(1)}
 \end{aligned} \tag{5.24}$$

This equation describes waves that maintain their form and move downward with speed $\alpha_0 V_0$. This is exactly the same result we arrived at in our linear analysis by considering long length scale disturbances. Of course, the waves described by Equation 5.24 actually do change form slowly as they propagate. After all, one of our reasons for setting up the perturbation scheme in Equation 5.23 was to describe this slow modulation of the waves

formed by a long disturbance. Although (5.23) is too crude an approximation to do this, it does point us in the right direction. What we should have done is to set up the following type of perturbation scheme:

$$\begin{aligned}
 \alpha &= \alpha_0 + \epsilon \alpha^{(1)}(\eta, \sigma) + \dots \\
 \frac{v_g}{V_0} &= \epsilon v_g^{(1)}(\eta, \sigma) + \dots \\
 \frac{v_L}{V_0} &= -1 + \epsilon v_L^{(1)}(\eta, \sigma) + \dots
 \end{aligned} \tag{5.25}$$

where:

$$\eta = \frac{y + \alpha_0 V_0 t}{V_0 t_0} \quad ; \quad \sigma = \epsilon \frac{t}{t_0}$$

In this manner the motion of the waveform is described by the dependence on η , and the slow change in shape of the waveform is described by the σ dependence. On substituting these series into our equations we discover that to first order in ϵ they are satisfied identically if:

$$v_g^{(1)}(\eta, \sigma) = v_L^{(1)}(\eta, \sigma) = -\alpha^{(1)}(\eta, \sigma) \tag{5.26}$$

which, by this time, comes as no surprise. On examining the equations of the second order in ϵ , we find that if they are not to contradict one another it must be that:

$$\begin{aligned}
 \frac{\partial \alpha^{(1)}}{\partial \sigma} - 2\alpha^{(1)} \frac{\partial \alpha^{(1)}}{\partial \eta} &= -v \frac{\partial^2 \alpha^{(1)}}{\partial \eta^2} \\
 v &= \alpha_0 (1 - \alpha_0) (3 - 2\alpha_0)
 \end{aligned} \tag{5.27}$$

This will be recognized as Burger's equation with a negative diffusion coefficient. Using the Cole - Hopf transformation:

$$\alpha^{(1)} = -\nu \frac{\partial \phi}{\partial \eta} / \phi \quad (5.28)$$

This equation may be transformed into a linear diffusion equation.

$$\frac{\partial \phi}{\partial \sigma} = -\nu \frac{\partial^2 \phi}{\partial \eta^2} \quad (5.29)$$

We can therefore solve Equation 5.27 by offering one initial condition on the disturbance. This is somewhat surprising since originally we had a second order problem and required two initial conditions. The reason is, that the perturbation we have performed is a singular one. We could have guessed that this would be the case from our linearized analysis of long length scale disturbances. From that discussion we recall, no matter what combination of initial data we gave, the disturbance quickly decayed into one for which; $\frac{v_g'}{V_0} = \frac{v_L'}{V_0} = -\alpha'$. This type of behavior is characteristic of systems described by singular perturbations. In our case we can expect that the quick decay will take place on the time scale, τ_v . Therefore, to analyze the behavior in this initial layer, we can assume that:

$$\begin{aligned} \alpha &= \alpha_0 + \epsilon \alpha^{(1)} \left(\frac{y}{L_0}, \frac{t}{\tau_v} \right) + \dots \\ \frac{v_g}{V_0} &= \epsilon v_g^{(1)} \left(\frac{y}{L_0}, \frac{t}{\tau_v} \right) + \dots \\ \frac{v_L}{V_0} &= -1 + \epsilon v_L^{(1)} \left(\frac{y}{L_0}, \frac{t}{\tau_v} \right) + \dots \end{aligned} \quad (5.30)$$

Substitution of these into our equations yields:

$$\begin{aligned}
 \alpha^{(1)}\left(\frac{y}{L_0}, \frac{t}{\tau_v}\right) &= \alpha^{(1)}\left(\frac{y}{L_0}, 0\right) \\
 (1 + 2\alpha_0) \frac{dv_g^{(1)}}{d\left(\frac{t}{\tau_v}\right)} + v_g^{(1)} &= -\alpha^{(1)} \\
 v_L^{(1)} &= -\frac{\alpha_0}{1 - \alpha_0} v_g^{(1)} - \frac{\alpha^{(1)}}{1 - \alpha_0}
 \end{aligned} \tag{5.31}$$

From these it is evident that whatever initial conditions we offer on $v_g^{(1)}$ and $v_L^{(1)}$, they will quickly (after a few τ_v) decay to $-\alpha^{(1)}$. Meanwhile $\alpha^{(1)}$ will remain constant through the initial layer.

This indicates that the proper condition to be enforced on Equation 5.27 is the value of the void fraction initially.

Knowing the proper initial condition we can now solve Equation 5.27 for $\alpha^{(1)}(\eta, \sigma)$. This is done by using (5.28) and (5.29). When $\sigma = 0$, whatever reasonable initial value $\alpha^{(1)}(\eta, 0)$ we give yields a transformed variable $\phi(\eta, 0)$ that is either always positive or always negative, but never zero. We can see from Equation 5.28 that if $\phi(\eta, \sigma)$ were ever to go to zero, it would signify the breakdown of our perturbation scheme. Of course, since we have a negative diffusion coefficient, we can expect that at some time ϕ will go to zero. What occurs when this happens can be seen in the computed solution shown in Figure 5.8.

In Figure 5.8 we see plots of $\frac{\alpha^{(1)}(\eta, \sigma)}{v}$ versus η for three different values of $v\sigma$. The value of $v\sigma$, and the scale of the

ordinate are read from the lower left hand corner of each graph. The initial data for this solution are shown in the first graph. Again we have chosen initial data which correspond to no net addition or removal of bubbles, only a rearrangement of them. We can not see any net wave motion of the disturbance because our coordinate η is already following this motion. We can see that the disturbance grows with passing time, and there is still evidence of the dispersion found in the linearized solution. A new feature, which is of a strictly non-linear nature, can be seen in the third of these graphs. At two points on the graph there are regions of particularly steep gradients of $\alpha^{(1)}$. Both of these regions appear to be transitions of some sort between regions of high void fraction below and lower void fraction above. What is happening here is that our transformed variable ϕ is approaching zero. Since ϕ obeys the linear diffusion equation, as it approaches zero it must be described approximately by:

$$\phi(\eta, \sigma) \approx (\eta - \eta_0)^2 - 2\nu(\sigma - \sigma_0) \quad (5.32)$$

so that at $\eta = \eta_0$; $\sigma = \sigma_0$, ϕ will become zero. Based on this approximate equation we can compute the approximate profile $\alpha^{(1)}(\eta, \sigma)$ for the transition. If we find from this the relation between the strength and maximum slope thickness for these transition regions, we discover it is identical to Equation 5.22. That relation was found to hold for weak, finite-amplitude waves of permanent form. So, it seems that the breakdown of our perturbation scheme is associated with the formation of one of the finite

amplitude waves we discovered earlier.

This knowledge enables us to paint a reasonably clear picture of what will happen to a long length scale disturbance. This is illustrated in Figure 5.9. Figure 5.9a is a $y - t$ diagram. It shows that if we prescribe a smooth long-length scale disturbance as shown in Figure 5.9b, the disturbance will quickly relax to a condition in which $v_g^{(1)} = v_L^{(1)} = -\alpha^{(1)}$. This will take place in an initial layer which is several relaxation times long. For a time period of approximately (τ_v/ϵ^2) the disturbance will be described accurately by Equation 5.24. The end of this period is marked by the formation of one or more of the finite-amplitude permanent waves we found earlier. At this time we can expect the disturbance to look somewhat like Figure 5.9c. This shows a series of finite-amplitude waves separated by regions of only gentle variations in void fraction. Just below each of the finite-amplitude waves the void fraction may become quite high. This suggests that the formation of these waves could be a mechanism for a change in flow regime. The clump of bubbles just below the finite wave may coalesce into a slug of gas, thus forming slug flow.

5.4 Speculation on the Effect of Bubble-Bubble Interactions

We have still not discovered exactly what it is that limits the growth of these disturbances if the flow remains bubbly. This is an important question in determining whether a disturbance will grow to great enough strength to cause a change in flow regime. It seems likely that the physical mechanism that limits this growth is not included in our model.

The most obvious shortcoming of our equations is that the bubble motion equation does not include the effects of bubble-bubble hydrodynamic interactions. Previous work on the interaction between bubbles (5.3, 5.4) has concentrated on calculating the effect of a uniform void fraction on the virtual mass of individual bubbles. We can do a simple calculation which indicates that the effect of gradients in void fraction and relative velocity may be more important.

We consider the three bubbles shown in Figure 5.10. All three are moving with constant velocity through a stagnant liquid. In order for this motion to be maintained each bubble must have some force applied to it. This is because when spheres move along one in front of another they appear to repel each other. Considering the flow to be that of three dipoles we can calculate the force which must be exerted on sphere 2.

$$F = 6\pi\mu \left\{ \frac{a^6}{c_{12}^4} \dot{y}_1^2 - \frac{a^6}{c_{23}^4} \dot{y}_3^2 \right\}$$

Letting \dot{y} be a continuous function of y :

$$F = 6\pi\mu a^6 \left\{ \frac{1}{c_{12}^4} (\dot{y}^2|_2 + \frac{d\dot{y}^2}{dy}|_2 c_{12}) - \frac{1}{c_{23}^4} (\dot{y}^2|_2 - \frac{d\dot{y}^2}{dy}|_2 c_{23}) \right\}$$

$$F = 6\pi\mu a^6 \left\{ \dot{y}^2 \left(\frac{1}{c_{12}^4} - \frac{1}{c_{23}^4} \right) + \frac{d\dot{y}^2}{dy} \left(\frac{1}{c_{12}^3} + \frac{1}{c_{23}^3} \right) \right\}$$

by recognizing that $\frac{4}{3}\pi \frac{a^3}{c^3}$ is the void fraction and that in a more

general situation \dot{y} corresponds to $(v_g - v_L)$:

$$F = 9\rho a^3 \frac{d}{dy} [\alpha(v_g - v_L)^2]$$

In a more general situation the magnitude of the force will be different but we can say that it will have the same functional form.

So:

$$F = \beta \rho_L \sigma \frac{d}{dy} \{\alpha(v_g - v_L)^2\}$$

where β is some unknown positive constant. Since this force is required to maintain the motion it must be the net resultant of the other forces on the bubble. In the problem we have been considering this leads to a bubble equation of motion:

$$\begin{aligned} \frac{\partial v_g}{\partial t} + v_g \frac{\partial v_g}{\partial y} - 3 \left\{ \frac{\partial v_L}{\partial t} + v_L \frac{\partial v_L}{\partial y} \right\} \\ + 2\beta \frac{\partial}{\partial y} \{\alpha(v_g - v_L)^2\} + \frac{1}{\tau_v} (v_g - v_L - V_0) = 0 \end{aligned} \quad (5.33)$$

When this equation is used in our set of governing equations, the characteristics become:

$$\begin{aligned} \dot{Y} &= \frac{(1 - \alpha)v_g + 3\alpha v_L + 2\beta\alpha(v_g - v_L) \pm (v_g - v_L)\sqrt{f(\alpha)}}{(1 + 2\alpha)} \\ f(\alpha) &= (2\beta - 3)\alpha + (4\beta^2 - 6\beta + 3)\alpha^2 + 4\beta\alpha^3 \end{aligned} \quad (5.34)$$

If β is large enough $f(\alpha)$ can become positive for large α and our system may become hyperbolic.

If we perform our singular perturbation analysis again, using this new bubble motion equation, the results are exactly the same as before except that the diffusion coefficient ν is now given by:

$$\nu = \alpha_0 (1 - \alpha_0) (3 - 2\beta - 2\alpha_0) \quad (5.35)$$

For large enough β , ν can become negative and our system can be stable.

We conclude from this, that the type of term we would need to include in the bubble motion equation to account for interactions might possibly change the character of our equations for high void fraction and thus limit the growth of a disturbance. It is also interesting to note that the diffusion coefficient, ν , depends strongly enough on the interaction term, β , that one might possibly learn the magnitude of the interaction term from an experiment measuring the growth rate of a disturbance.

In any event, it is significant that our equations provide such a reasonable description of the system for low void fractions. This shows that although the resulting mathematical problem is not well-posed, it does not necessarily mean that we have modeled the physics of the problem incorrectly.

It is also of some interest to note that in the problem of choked flow through a contraction (which motivated this whole discussion), the bubble residence time is small compared with τ_v . Since the disturbances we have been considering here grow on a time scale proportional to τ_v , they will not have enough time to grow significantly during the time the bubbles actually reside in the

contraction. Hence, in that discussion we were correct not to be concerned about these disturbances and consider only steady flow.

REFERENCES

- 5.1 M. K. Likht and V. A. Shteinbert, "Stability of a Liquid Layer with Bubbling", Fluid Dynamics Volume 9, Number 4, July - August 1974, pp. 540 - 546.
- 5.2 P. R. Garabedian, "Partial Differential Equations", John Wiley and Sons, Inc. (Pub.), 1964, Chapter 4.
- 5.3 N. Zuber, "On the Dispersed Two-Phase Flow in the Laminar Flow Regime", Chemical Engineering Science Volume 19, 1964, pp. 897 - 917.
- 5.4 L. van Wijngaarden, "Hydrodynamic Interaction Between Gas Bubbles in Liquid", Journal of Fluid Mechanics Volume 77, Part 1, 1976, pp. 27 - 44.

Notation for Chapter 5

a	Ratio between self-preserving wave speed and bubble terminal velocity; bubble radius
$a_{\pm}(k)$	Real parts of $s_{\pm}(k)$
$b_{\pm}(k)$	Imaginary parts of $s_{\pm}(k)$
c	Distance between bubbles
c_g	Speed of sound in the gas
$F(k)$	Fourier transform
g	Acceleration of gravity
F	Force on a bubble
k	Wave number
L_0	Length scale of a long disturbance
p	Pressure
q_{\pm}	Functions formed from the Fourier transforms of initial data
$s_{\pm}(k)$	Exponents in Fourier transform solution of linearized equations
u_0	Self-preserving wave speed
v	Velocity
\dot{Y}	Characteristic speed
α	Void fraction
α_0	Undisturbed void fraction
β	Interaction term coefficient
γ	Undisturbed void ratio
ϵ	Ratio of relaxation length to disturbance length scale
η	Coordinate following a wave form
ν	Diffusion coefficient
ρ	Density

Notation for Chapter 5 (Cont'd.)

σ Stretched time coordinate; bubble volume

τ_v Viscous relaxation time

Subscripts

g Gas

L Liquid

TABLE 5.1

Pertinent Data on 1/32" Diameter
Air Bubbles Rising in Water

Relaxation Time = τ_v	=	0.0086 sec
Terminal Velocity = V_o	=	0.56 ft/sec
Relaxation Length = $V_o \tau_v$	=	0.058 inches
Reynolds Number	=	133
Weber Number	=	0.16
Expected Fractional Bubble Size Charge	=	0.0002

TABLE 5.2 Computed Values of the
Functions $a_{\pm}(k)$ and $b_{\pm}(k)$

GAMMA= 0.100

WAVE NUMBER	A-PLUS	B-PLUS	A-MINUS	B-MINUS
0.001000	0.000000	-0.000091	-0.846154	-0.000371
0.002000	0.000001	-0.000182	-0.846155	-0.000741
0.005000	0.000006	-0.000455	-0.846159	-0.001853
0.010000	0.000023	-0.000909	-0.846177	-0.003706
0.020000	0.000093	-0.001819	-0.846247	-0.007412
0.050000	0.000582	-0.004555	-0.846735	-0.018522
0.100000	0.002320	-0.009167	-0.848474	-0.036987
0.200000	0.009178	-0.018776	-0.855331	-0.073532
0.500000	0.053604	-0.053318	-0.899758	-0.177451
1.000000	0.181963	-0.132971	-1.028116	-0.328567
2.000000	0.527994	-0.337107	-1.374147	-0.585969
5.000000	1.730000	-1.016434	-2.576154	-1.291257
10.000000	3.813664	-2.168029	-4.659818	-2.447355
20.000000	8.015198	-4.475139	-8.861351	-4.755630
50.000000	20.647873	-11.398048	-21.494034	-11.678864
100.000000	41.711777	-22.936478	-42.557938	-23.217346
200.000000	83.843079	-46.013412	-84.689240	-46.294281
500.000000	210.239868	-115.244141	-211.085938	-115.525009

TABLE 5.3 Computed Values of the
Functions $a_{\pm}(k)$ and $b_{\pm}(k)$

GAMMA= 0.250

WAVE NUMBER	A-PLUS	B-PLUS	A-MINUS	B-MINUS
0.001000	0.000000	-0.000200	-0.714286	-0.000657
0.002000	0.000002	-0.000400	-0.714287	-0.001314
0.005000	0.000010	-0.001000	-0.714296	-0.003286
0.010000	0.000042	-0.002000	-0.714327	-0.006571
0.020000	0.000166	-0.004002	-0.714452	-0.013141
0.050000	0.001037	-0.010033	-0.715323	-0.032824
0.100000	0.004120	-0.020261	-0.718405	-0.065454
0.200000	0.016034	-0.041964	-0.730319	-0.129464
0.500000	0.086955	-0.122377	-0.801240	-0.306194
1.000000	0.267001	-0.297780	-0.981286	-0.559362
2.000000	0.706209	-0.703604	-1.420494	-1.010680
5.000000	2.148160	-1.979937	-2.862445	-2.305777
10.000000	4.607167	-4.121275	-5.321453	-4.450152
20.000000	9.548103	-8.406593	-10.262390	-8.736252
50.000000	24.389542	-21.263626	-25.103836	-21.593491
100.000000	49.131546	-42.692184	-49.845825	-43.022079
200.000000	98.617905	-85.549316	-99.332184	-85.879227
500.000000	247.078979	-214.120605	-247.793213	-214.450562

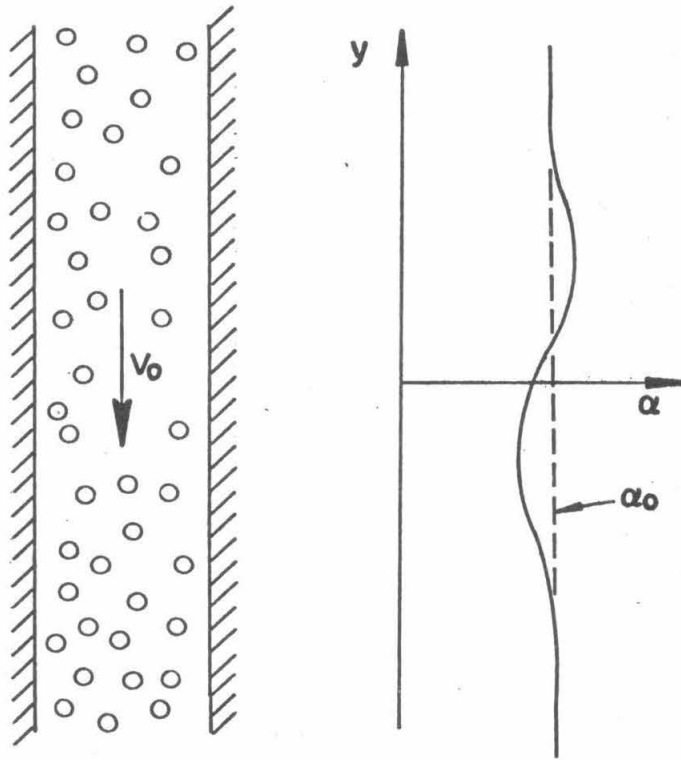
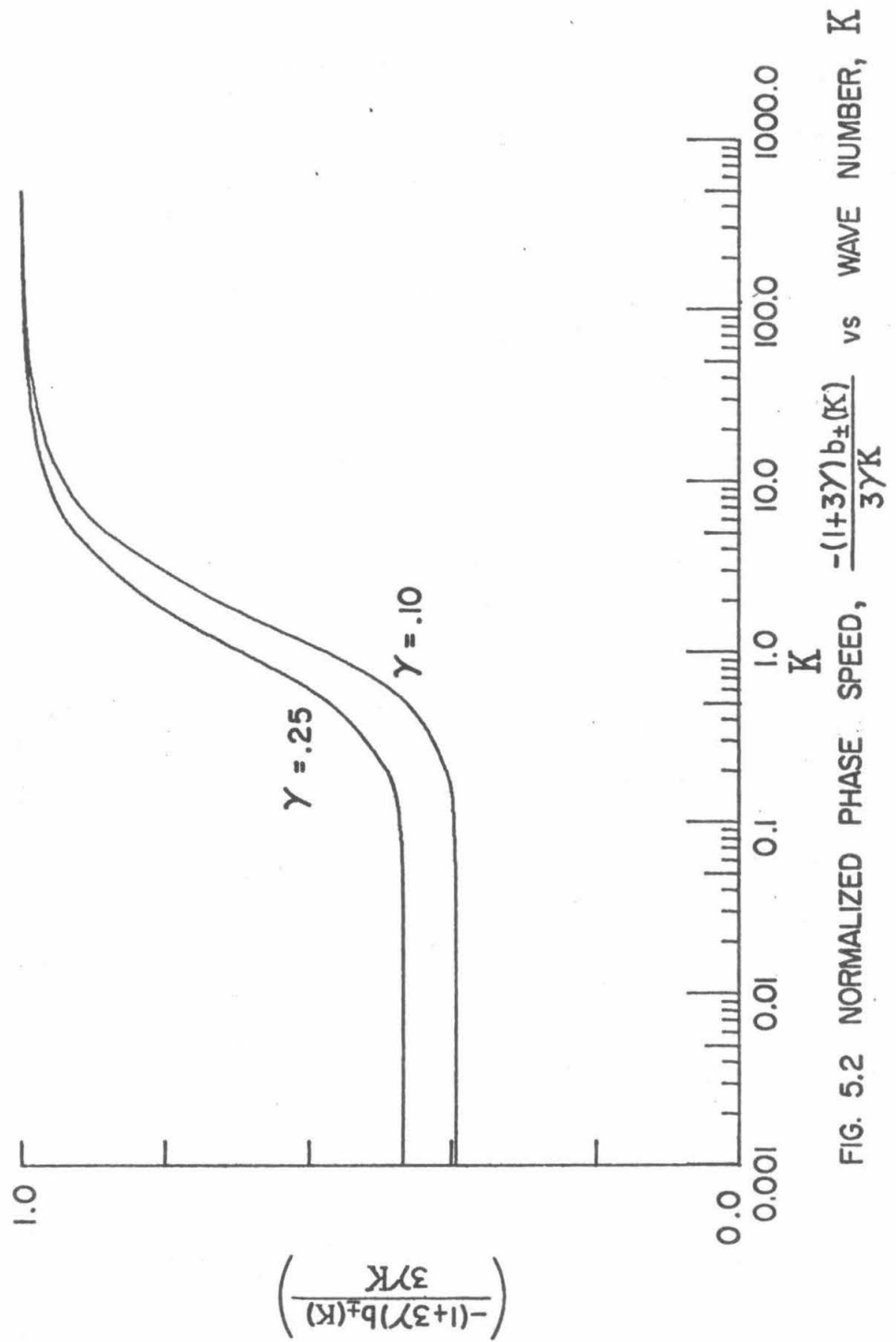


FIG. 5.1 GEOMETRY AND NOTATION FOR ONE-DIMENSIONAL ANALYSIS OF A DISTURBANCE TO A UNIFORM BUBBLE CLOUD



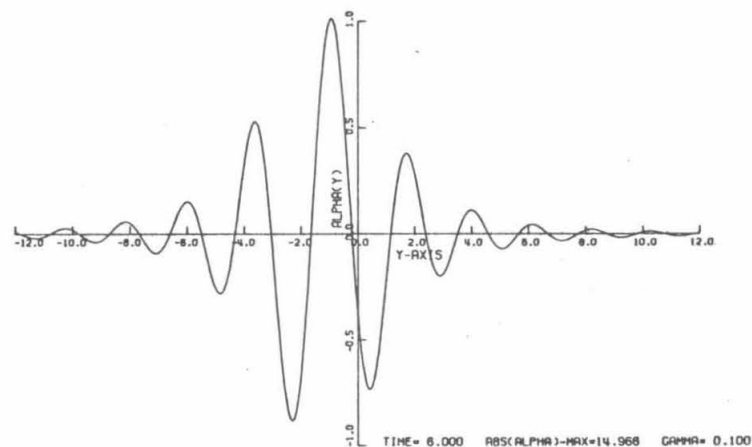
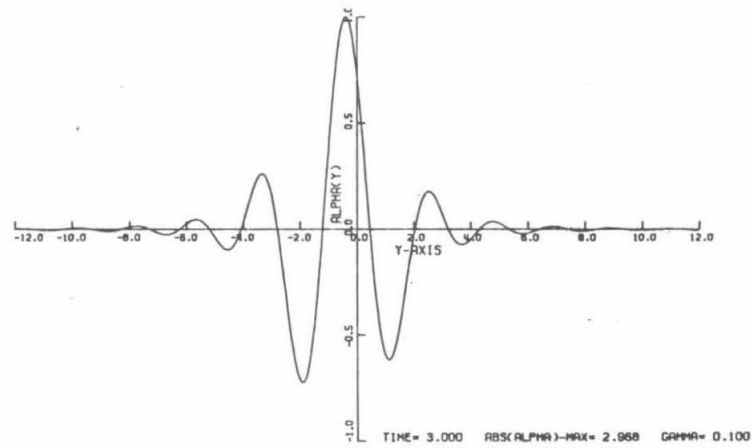
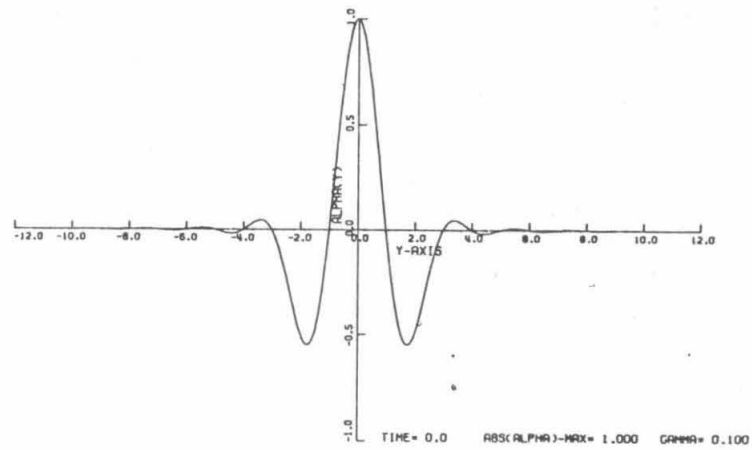


Figure 5.3 Solution of Linearized Equations for One-Dimensional Disturbance; Void Fraction Perturbation

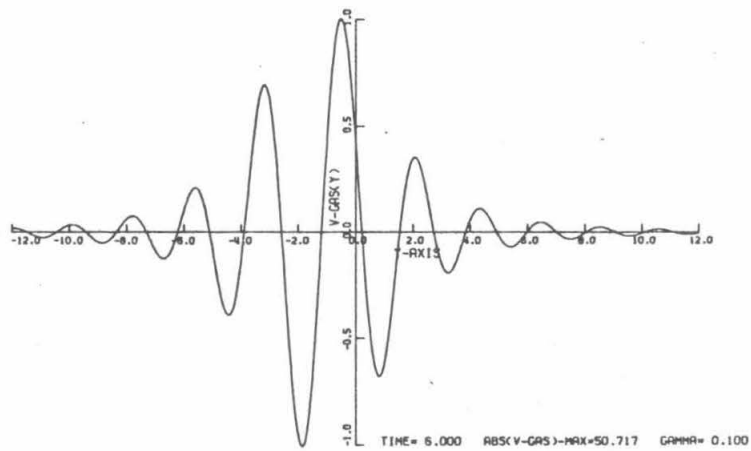
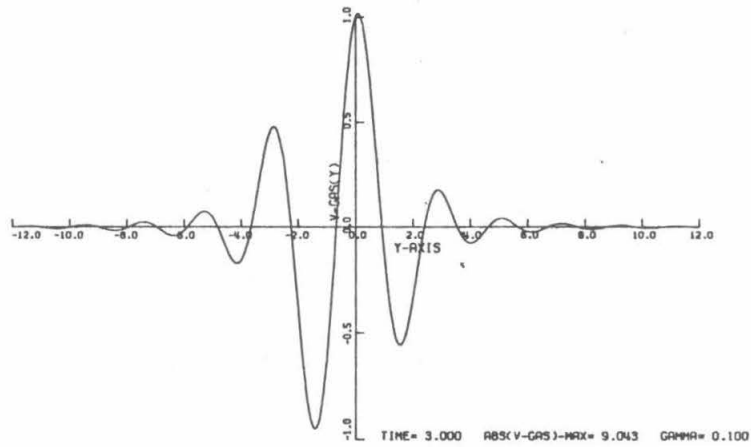


Figure 5.4 Solution of Linearized Equations for One-Dimensional Disturbance; Gas Velocity Perturbation

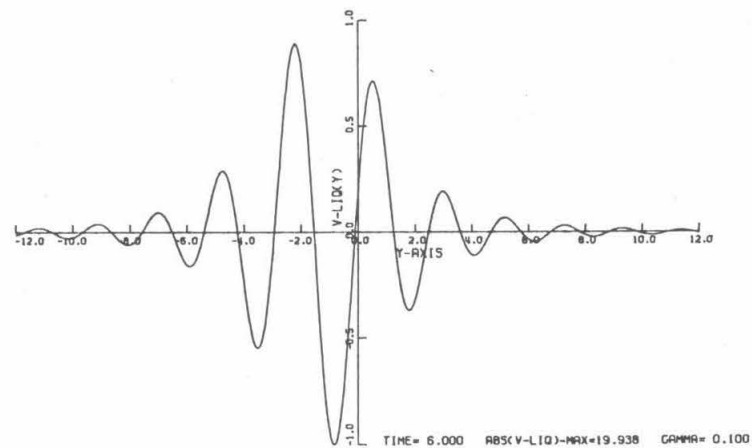
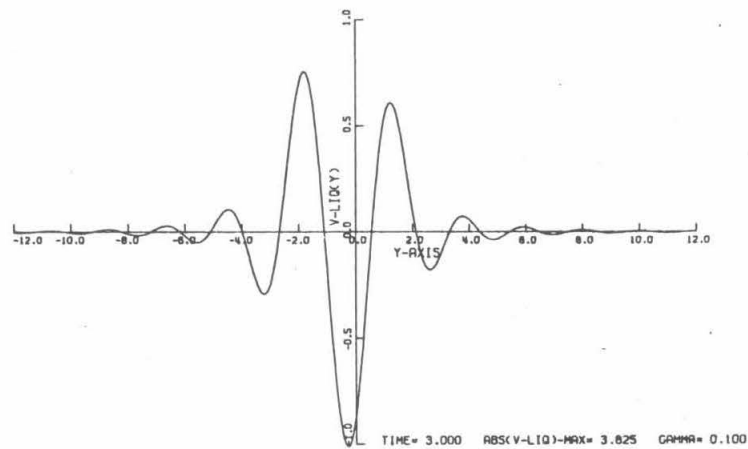
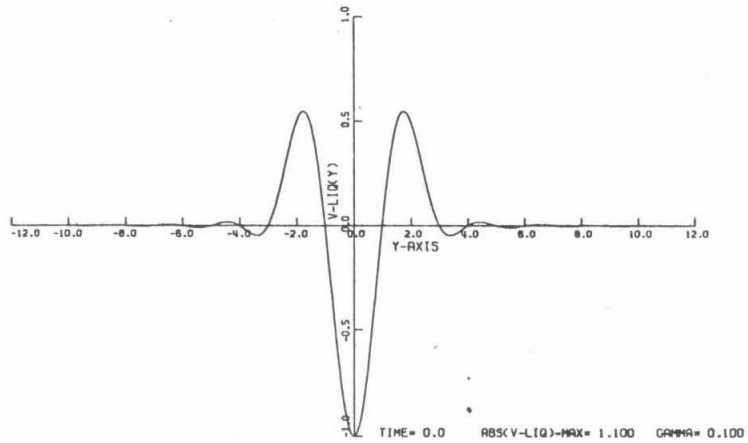


Figure 5.5 Solution of Linearized Equations for One-Dimensional Disturbance; Liquid Velocity Perturbation

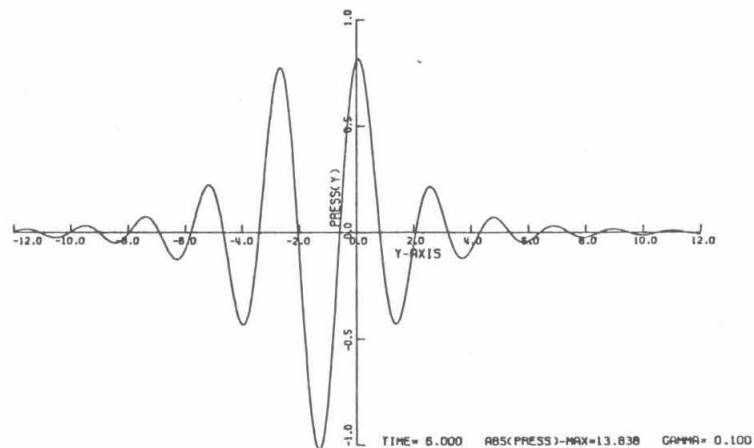
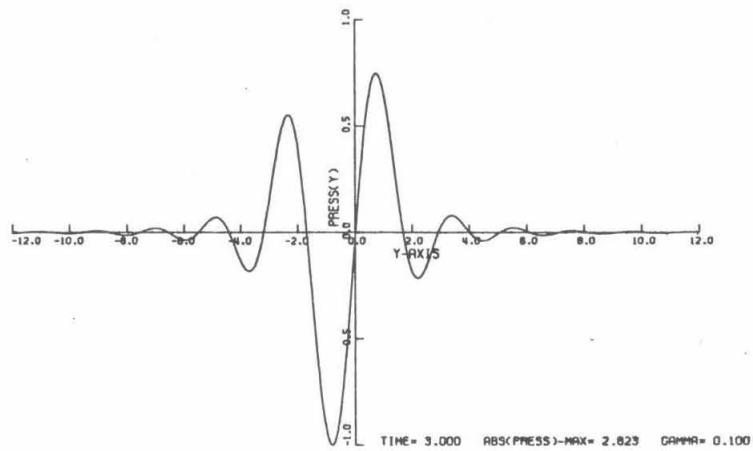
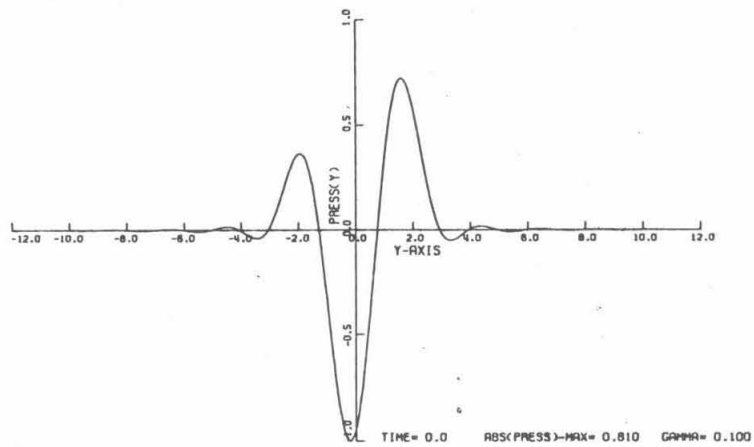


Figure 5.6 Solution of Linearized Equations for One-Dimensional Disturbance; Pressure Perturbation

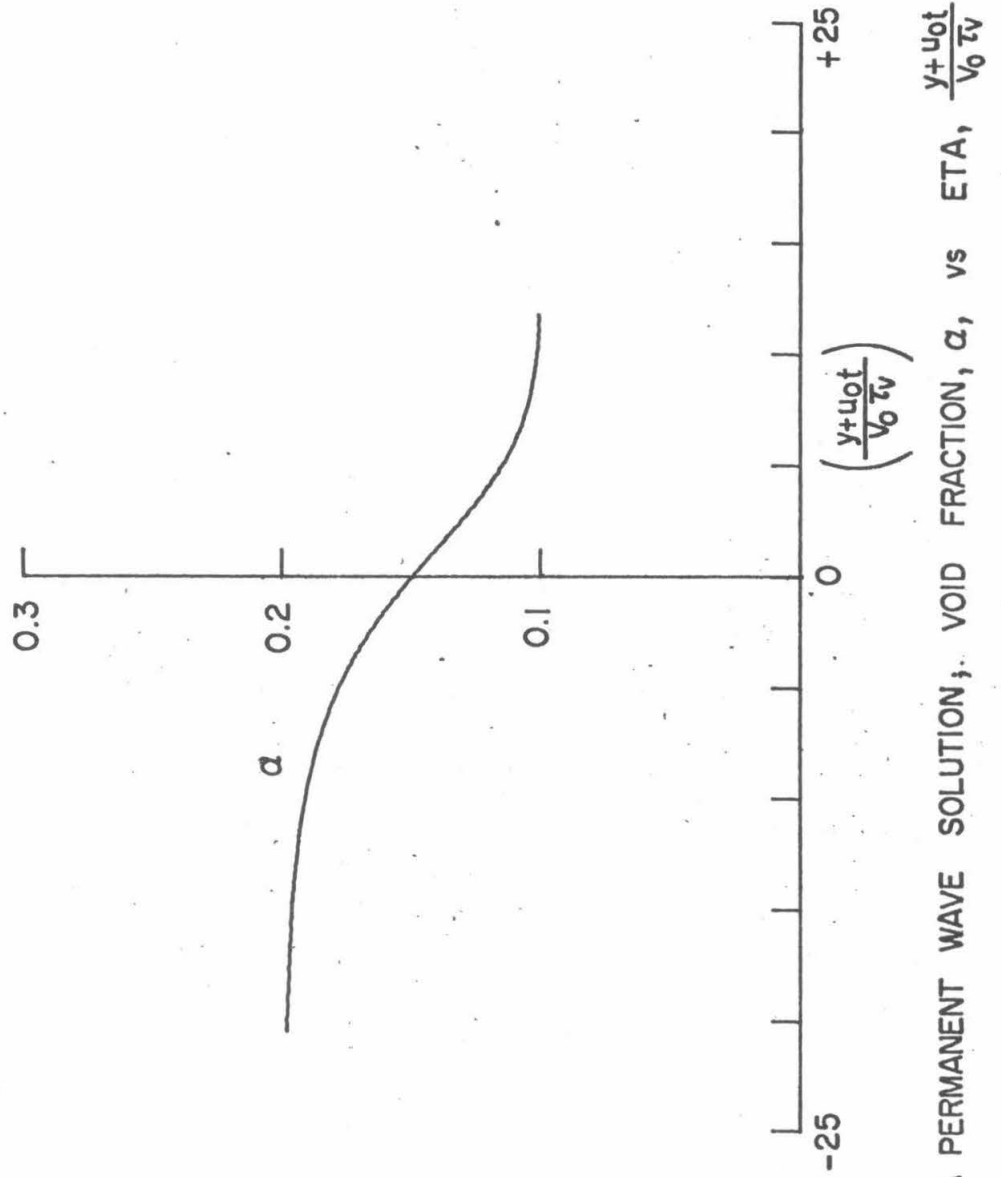
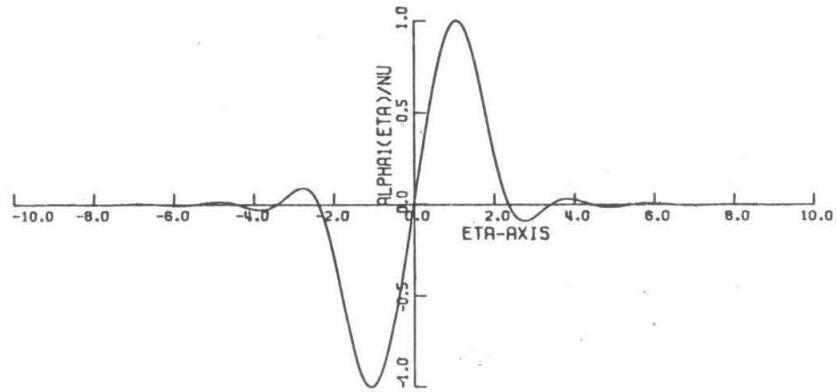
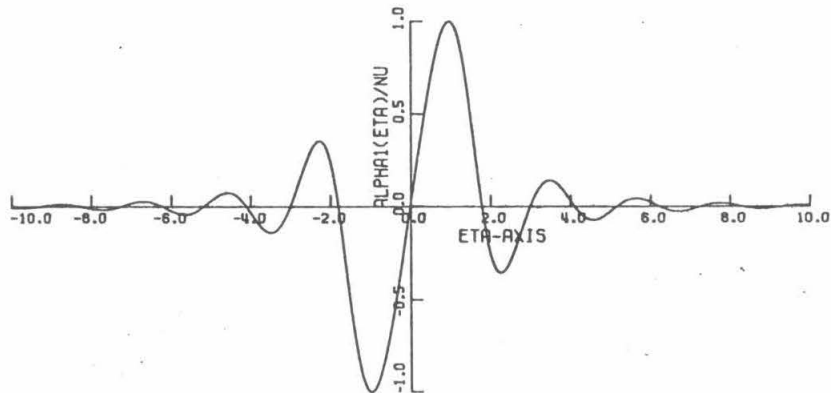


FIG. 5.7 A PERMANENT WAVE SOLUTION, VOID FRACTION, α , vs $\text{ETA}, \frac{y+u_0 t}{V_0 \tau_v}$



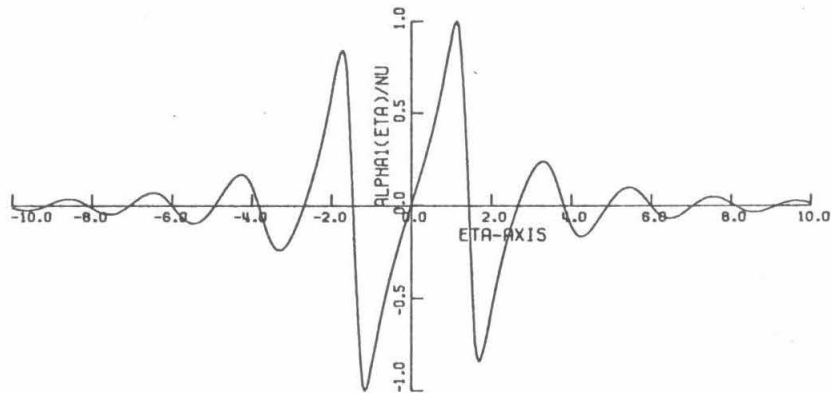
NU=SIGMA= 0.0

ALPHA1 SCALE= 0.30145



NU=SIGMA= 0.25000

ALPHA1 SCALE= 0.62136



NU=SIGMA= 0.54000

ALPHA1 SCALE= 3.42550

Figure 5.8 A Solution of the Burger's Equation for a One-Dimensional Disturbance

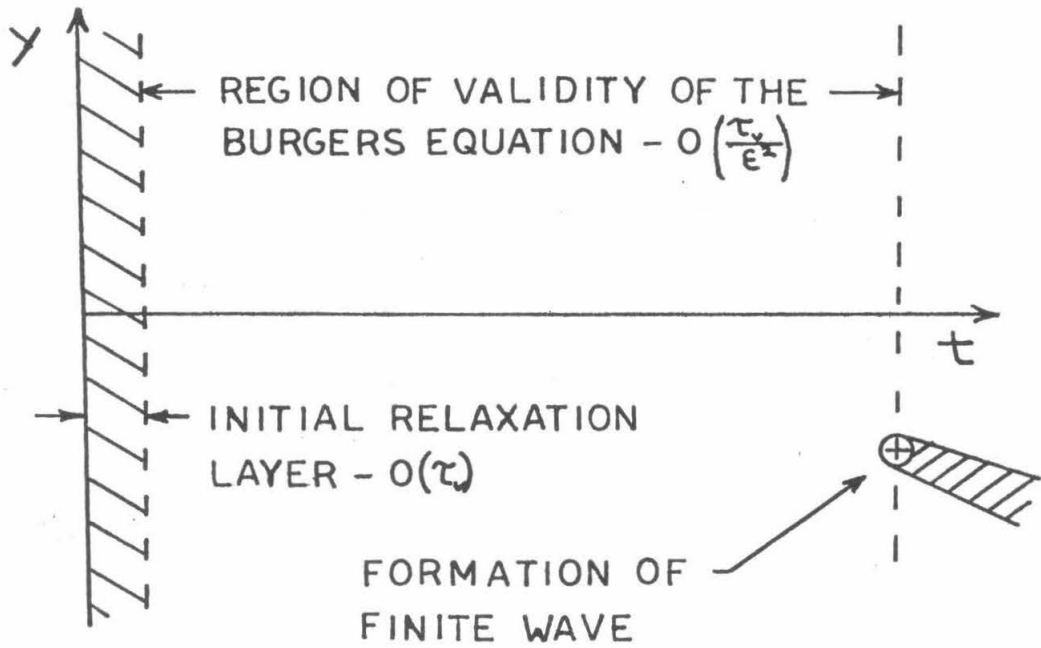


Figure 5.9a

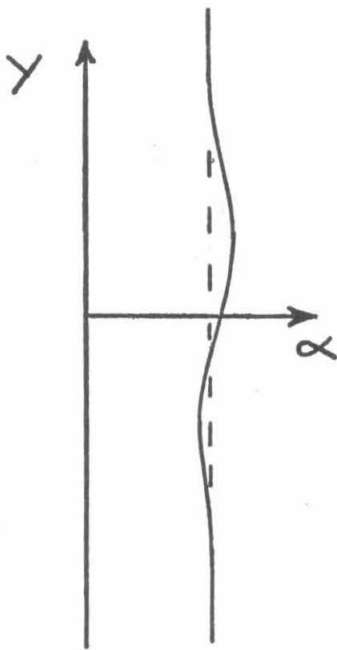


Figure 5.9b

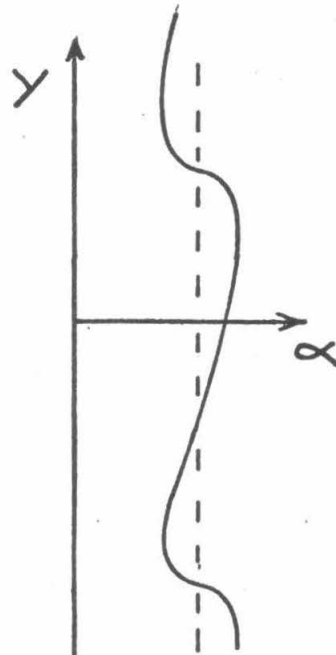


Figure 5.9c

Development of a Long Length Scale Disturbance

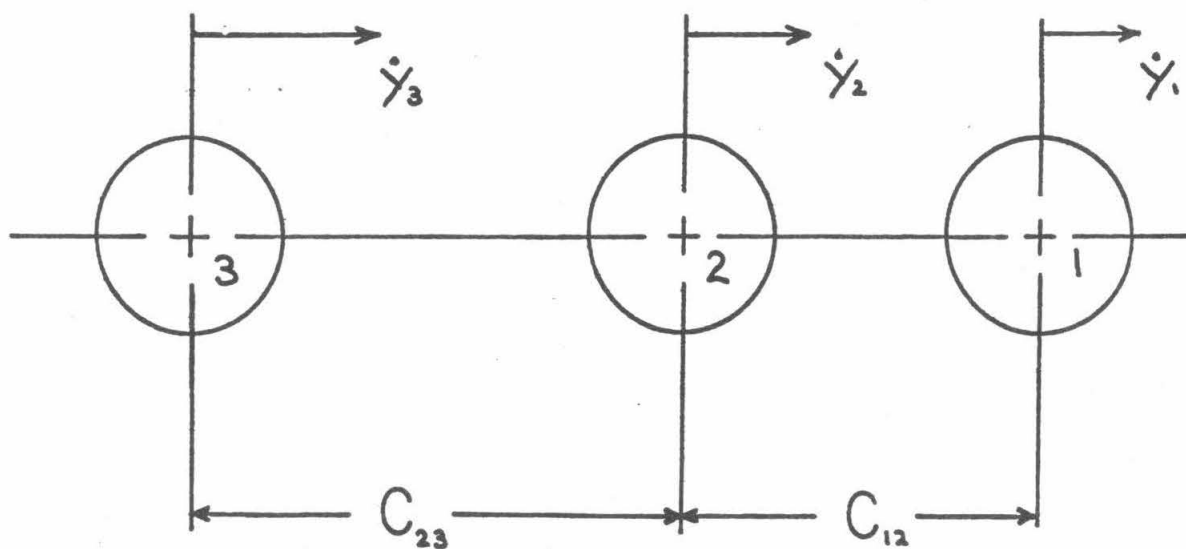


Figure 5.10 Geometry and Notation for Bubble-Bubble Interaction Calculation

CHAPTER 6

Bubbly Flow Over a Wavy Wall

The flow of fluid over a wavy wall, which is a classical problem in elementary fluid mechanics, serves also to illustrate some of the phenomena concerning the motion of a bubbly flow and in particular the phase separation that takes place when the flow deviates slightly from one-dimensional.

Consider the situation, depicted in Figure 6.1, in which a mixture of liquid and gas bubbles is flowing over a wavy wall. The height of the wall, η , is given by:

$$\eta = \epsilon \lambda \cos \frac{2\pi x}{\lambda} \quad (6.1)$$

The number, ϵ , is the ratio between the height of the wall and its wavelength. We expect considerable simplification of the problem when ϵ is small. The flow is then a small perturbation to the uniform rectilinear flow and we may solve the problem by linearizing the governing equations and boundary conditions.

We simplify the governing equations, (2.3, 2.4, 2.9 and 2.18) with the following assumptions:

- (I) That the inertia of the gas is negligible
- (II) That the liquid and gas behave isothermally
- (III) That the liquid is incompressible
- (IV) That the pressure in the gas bubbles is essentially the same as in the surrounding liquid
- (V) That the gas bubbles do not interact with each other and that their viscous interaction with the surrounding

liquid may be described by a linear drag law.

With these assumptions the governing equations take the following form:

Gas Conservation:

$$\frac{D}{Dt} (p\alpha) + p\alpha \nabla \cdot \vec{u}_g = 0 \quad (6.2)$$

Liquid Conservation:

$$\frac{d}{dt} (1 - \alpha) + (1 - \alpha) \nabla \cdot \vec{u}_L = 0 \quad (6.3)$$

Mixture Motion:

$$\rho_L (1 - \alpha) \frac{d\vec{u}_L}{dt} + \nabla p = 0 \quad (6.4)$$

Bubble Motion:

$$\frac{D\vec{u}_g}{Dt} - (\vec{u}_g - \vec{u}_L) \frac{1}{p} \frac{Dp}{Dt} - 3 \frac{d\vec{u}_L}{dt} + \frac{1}{\tau_v(p)} (\vec{u}_g - \vec{u}_L) = 0 \quad (6.5)$$

These equations apply to any bubbly flow obeying assumptions I through V. If, in addition, we assume that the flow is a small perturbation to a uniform flow in the x-direction we can then linearize these equations about that uniform flow.

$$\begin{aligned} \vec{u}_L &= U_o \hat{i} + \epsilon \vec{u}_L^{(1)} \\ \vec{u}_g &= U_o \hat{i} + \epsilon \vec{u}_g^{(1)} \\ \alpha &= \alpha_o + \epsilon \alpha^{(1)} \\ p &= p_o + \epsilon p^{(1)} \end{aligned} \quad (6.6)$$

Substituting this into Equations 6.2 through 6.5 we find that:

$$\left\{ \frac{\partial}{\partial t} + U_0 \frac{\partial}{\partial x} \right\} (\alpha_0 p^{(1)} + p_0 \alpha^{(1)}) + \alpha_0 p_0 \nabla \cdot \vec{u}_g^{(1)} = 0 \quad (6.7)$$

$$- \left\{ \frac{\partial}{\partial t} + U_0 \frac{\partial}{\partial x} \right\} (\alpha^{(1)}) + (1 - \alpha_0) \nabla \cdot \vec{u}_L^{(1)} = 0 \quad (6.8)$$

$$\rho_L (1 - \alpha) \left\{ \frac{\partial}{\partial t} + U_0 \frac{\partial}{\partial x} \right\} \vec{u}_L + \nabla p^{(1)} = 0 \quad (6.9)$$

$$\left\{ \frac{\partial}{\partial t} + U_0 \frac{\partial}{\partial x} \right\} (\vec{u}_g^{(1)} - 3 \vec{u}_L^{(1)}) + \frac{1}{\tau_v(p_0)} (\vec{u}_g^{(1)} - u_L^{(1)}) = 0 \quad (6.10)$$

These four equations enable us, with the help of appropriate boundary and initial conditions, to find $\vec{u}_L^{(1)}$, $\vec{u}_g^{(1)}$, $\alpha^{(1)}$ and $p^{(1)}$ as functions of space and time. It should be noted that we have not yet assumed the flow to be two-dimensional or steady, so (6.7) to (6.10) describe any small perturbation to a rectilinear flow. If we take the curl of Equation 6.9 we find:

$$\left\{ \frac{\partial}{\partial t} + U_0 \frac{\partial}{\partial x} \right\} (\nabla \times \vec{u}_L^{(1)}) = 0 \quad (6.11)$$

And by taking the curl of (6.10):

$$\left\{ \frac{\partial}{\partial t} + U_0 \frac{\partial}{\partial x} + \frac{1}{\tau_v(p_0)} \right\} (\nabla \times \vec{u}_g^{(1)}) = \frac{1}{\tau_v(p_0)} \nabla \times \vec{u}_L^{(1)} \quad (6.12)$$

Equation 6.11 tells us that to order ϵ the convective derivative of the vorticity of the liquid is zero. If we imagine that at some place far upstream the flow is completely uniform, then $\nabla \times \vec{u}_L^{(1)}$ will always be zero. In effect, we have a restricted form of the Kelvin Theorem for the liquid. Under these same conditions, Equation 6.12 tells us that to order ϵ the vorticity of the gas

will also be zero. We therefore also have the same restricted Kelvin Theorem for the gas. So, as a consequence of (6.11) and (6.12) we can state that in any flow, which is a small perturbation to the uniform flow, the gas and liquid velocity fields may be derived from potentials. In this respect our problem is similar to a gas-particle flow over a wavy wall which was studied in detail by Zung (6.1).

If we now define the potentials:

$$\begin{aligned}\vec{u}_L^{(1)} &= \nabla \phi_L \\ \vec{u}_g^{(1)} &= \nabla \phi_g\end{aligned}\tag{6.13}$$

we can integrate Equation 6.9 to find:

$$p^{(1)} = -\rho_L (1 - \alpha_0) \left\{ \frac{\partial}{\partial t} + U_0 \frac{\partial}{\partial x} \right\} \phi_L\tag{6.14}$$

Now, performing entirely algebraic manipulations on (6.7), (6.8) and (6.10), we can find a wave equation for ϕ_L :

$$\begin{aligned}\left\{ \frac{\partial}{\partial t} + U_0 \frac{\partial}{\partial x} \right\} \left[\frac{1}{c_o^2} \left\{ \frac{\partial}{\partial t} + U_0 \frac{\partial}{\partial x} \right\}^2 \phi_L - (1 + 2\alpha_0) \nabla^2 \phi_L \right] \\ + \frac{1}{\tau_v} \left[\frac{1}{c_o^2} \left\{ \frac{\partial}{\partial t} + U_0 \frac{\partial}{\partial x} \right\}^2 \phi_L - \nabla^2 \phi_L \right] = 0\end{aligned}\tag{6.15}$$

where $c_o^2 = \frac{p_0}{\rho_L \alpha_0 (1 - \alpha_0)}$

Equation 6.15 applies for a general, three-dimensional, time dependent, perturbation to the uniform flow, U_0 in the x-direction. The speed, c_o , is the speed of an acoustic wave propagating iso-

thermally and generating no relative motion. If we set $U_0 = 0$ we recover a wave equation which describes the acoustics of a stationary bubbly mixture.

$$\frac{\partial}{\partial t} \left[\frac{1}{c_0^2} \frac{\partial^2 \phi_L}{\partial t^2} - (1 + 2\alpha_0) \nabla^2 \phi_L \right] + \frac{1}{\tau_v} \left[\frac{1}{c_0^2} \frac{\partial^2 \phi_L}{\partial t^2} - \nabla^2 \phi_L \right] = 0 \quad (6.16)$$

From (6.16) it is clear that low frequency sound waves ($\omega \tau_v \ll 1$) travel at speed c_0 , while high frequency waves ($\omega \tau_v \gg 1$) travel at $\sqrt{1 + 2\alpha_0} c_0$. Waves of the type obeying (6.16) have been studied by Marble (6.2) in connection with their occurrence in dusty gases, and by Whitham (6.3) with regard to applications in magnetohydrodynamics.

Returning to the flow over the wavy wall, we can simplify Equation 6.15 for steady, two-dimensional flow:

$$\frac{\partial}{\partial x} \left\{ M_0^2 \frac{\partial^2 \phi_L}{\partial x^2} - (1 + 2\alpha_0) \nabla^2 \phi_L \right\} + \frac{1}{U_0 \tau_v} \left\{ M_0^2 \frac{\partial^2 \phi_L}{\partial x^2} - \nabla^2 \phi_L \right\} = 0 \quad (6.17)$$

in which ∇^2 is now a two-dimensional operator, and M_0 is the Mach number, (U_0 / c_0) .

To solve Equation 6.17 for ϕ_L we must offer certain boundary conditions. The physical conditions are these:

- 1) The liquid adjacent to the wall must follow the contour of the wall as it moves
- 2) The disturbance caused by the waves in the wall must disappear as we move far away from the wall.

These two conditions expressed mathematically, in linearized form, are:

$$\frac{\partial \phi_L}{\partial y} = U_0 \frac{\partial \eta}{\partial x} = \epsilon 2 \pi U_0 \sin\left(\frac{2\pi x}{\lambda}\right); \text{ on } y = 0 \quad (6.18)$$

$$\phi_L \rightarrow 0 \quad \text{as} \quad y \rightarrow \infty \quad (6.19)$$

It is convenient to find ϕ_L by solving (6.17) for the flow over a wavy wall whose height is complex. If we let the wall height, η , be given by:

$$\eta = \frac{2\pi\epsilon}{k} e^{ikx}; \quad k = \frac{2\pi}{\lambda} \quad (6.20)$$

It becomes particularly simple to solve the problem, and the solution to our original problem may be extracted by taking the real part of the quantity in question. This is a consequence of the linearity of our problem.

If η is given by Equation 6.20, then we have the mathematical problem:

$$\frac{\partial}{\partial x} \left\{ M_0^2 \frac{\partial^2 \phi_L}{\partial x^2} - (1 + 2\alpha_0) \nabla^2 \phi_L \right\} + \frac{1}{U_0 \tau_v} \left\{ M_0^2 \frac{\partial^2 \phi_L}{\partial x^2} - \nabla^2 \phi_L \right\} = 0 \quad (6.21)$$

$$\left. \frac{\partial \phi_L}{\partial y} \right|_{y=0} = i \epsilon 2 \pi U_0 e^{ikx}$$

$$\phi_L \rightarrow 0 \quad \text{as} \quad y \rightarrow \infty$$

The solution for ϕ_L is:

$$\phi_L = \frac{i \epsilon 2 \pi U_0}{s} e^{s y + ikx} \quad (6.22)$$

where s is given by the expression:

$$s = \left\{ \frac{(1 - M_0^2) + \gamma^2(1 + 2\alpha_0)(1 + 2\alpha_0 - M_0^2) + 2i\gamma\alpha_0 M_0^2}{1 + \gamma^2(1 + 2\alpha_0)^2} \right\}^{\frac{1}{2}} k \quad (6.23)$$

$$\gamma = k U_0 \tau_v$$

The square root in Equation 6.23 is taken so that $\text{Re}[s] \leq 0$, and thus $\phi_L \rightarrow 0$ as $y \rightarrow 0$.

Using Equation 6.10 we can find the potential for the gas velocity.

$$\phi_g = \frac{i \epsilon 2 \pi U_0}{s} \left\{ \frac{1 + 3i\gamma}{1 + i\gamma} \right\} e^{s y + i k x} \quad (6.24)$$

From (6.8) the void fraction perturbation is:

$$\alpha' = 2 \pi \epsilon (1 - \alpha_0) \frac{s^2 - k^2}{(s k)} e^{s y + i k x} + g(y) \quad (6.25)$$

in which integration with respect to x has introduced the function $g(y)$. This means physically that we can prescribe the void fraction as a function of y somewhere upstream of where the waves in the wall begin.

Using (6.14) we find the pressure perturbation:

$$p' = 2 \pi \epsilon \rho_L (1 - \alpha_0) U_0^2 (k/s) e^{s y + i k x} \quad (6.26)$$

Equations 6.22 through 6.26 give the solution for flow over a wavy wall of height, $\frac{2 \pi \epsilon}{k} e^{i k x}$. The solution for a real wall of height $\frac{2 \pi \epsilon}{k} \cos kx$ is found by taking the real parts of these expressions.

We can see from these expressions that the parameter, γ ,

is quite important in determining the character of the solution. This number has the physical significance of being the ratio between the viscous relaxation time, and the time a bubble will take in passing one wavelength of wall. Therefore, we can expect that if γ is small there will be very little relative motion between the phases, since viscosity will be effective in retarding this motion. If, on the other hand, γ is a large number, the bubbles will not have sufficient time to relax viscously and their motion will be almost entirely controlled by the dynamic forces on them. This is clearly seen when we realize:

$$\phi_g = \frac{1 + 3i\gamma}{1 + i\gamma} \phi_L \quad (6.27)$$

For $\gamma = 0$, the gas and liquid execute exactly the same motion. For large γ the gas moves in the same fashion as the liquid but with three times the amplitude. This is because the gas responds much more quickly to a pressure gradient than the liquid. For intermediate values of γ the combination of viscous and dynamic forces on the bubbles causes a phase difference between the liquid and gas motions. The gas executes a motion similar to that of the liquid but displaced upstream by an angle δ :

$$\delta = \tan^{-1} \left(\frac{2\gamma}{1 + 3\gamma^2} \right) \quad (6.28)$$

The phase difference has a maximum value of 30° when $\gamma = \frac{1}{\sqrt{3}}$.

It is interesting to note that the velocity calculated from the gas potential indicates that some of the bubbles will go in and out of the wall. Of course, in the actual physical situation, this does

not happen. What is happening here is that the liquid is executing a motion which forces bubbles alternately toward and away from the wall. When they get near the wall, interaction forces between the bubbles and the wall will become important. We have left these forces out of our equation of motion for the bubbles and therefore cannot expect our bubbles to detect the presence of the wall. After the mixture has flowed past many wavelengths of the wall we can expect that the function $g(y)$ (in Equation 6.25) will have adjusted itself so that there are no bubbles near the wall. By "near the wall" we mean in a layer as thick as the range of the bubble-wall interaction forces.

Another interesting quantity which we may calculate from our solution is the drag on the wall. We expect that there will be some drag, because there is viscous dissipation corresponding to the motion of the bubbles with respect to the liquid. The drag on one wavelength of the wall is:

$$D = \int_0^{\frac{2\pi}{k}} p' \Big|_{y=0} \cdot \left(\frac{d\eta}{dx} \right) dx \quad (6.29)$$

Performing the integration we find:

$$D = (2\pi\epsilon)^2 \rho_L (1 - \alpha_0) U_0^2 \operatorname{Im} \left\{ \frac{\pi}{s} \right\}$$

As we expect the drag will be zero for $\gamma = 0$ and $\gamma = \infty$, these two cases corresponding to no relative motion and free relative motion, respectively.

We have seen that the bubbly flow over a wavy wall may be solved by the use of potentials for both the gas and liquid velocity

fields. In solving the problem we are unable to enforce a boundary condition on the gas velocity at the surface of the wall. The result is that the gas velocity normal to the wall is not zero. The difficulty is alleviated when we realize that after flowing over many wavelengths of the wall the bubbles will rearrange themselves so that the void fraction is zero next to the wall. In a more practical problem such a flow around a corner or a bend in a pipe the bubbles would not have time to rearrange themselves and the non-zero gas velocity at the wall would correspond to a collection of bubbles there. If this occurred to a great extent, these bubbles might form a film of gas next to the wall and thus change the flow regime.

REFERENCES

- 6.1 L.B. Zung, "Particle Fluid Mechanics in Shear Flows, Acoustic Waves and Shock Waves", (Ph.D. Thesis, California Institute of Technology), 1967.
- 6.2 F.E. Marble, "Dynamics of Dusty Gases", Annual Review of Fluid Mechanics" Volume 2, 1970, pp. 397 - 466.
- 6.3 G.B. Whitham, "Some Comments on Wave Propagation and Shock Wave Structure with Application to Magnetohydrodynamics", Communications on Pure and Applied Mathematics Volume XII, 1959, pp. 113 - 158.

Notation for Chapter 6

c_o	Sound speed
D	Drag on one wavelength of wall
k	Wave number of wall
M_o	Mach number
p	Pressure
s	Exponent describing y dependence of solution
u	Velocity
α	Void fraction
γ	Dimensionless wave number of wall
δ	Phase angle
ϵ	Ratio of height of wall to its wavelength
η	Wall height
λ	Wavelength of wall
ρ	Density
τ_v	Viscous relaxation time
ϕ	Velocity potential

Subscripts

g	Gas
L	Liquid
o	Undisturbed state

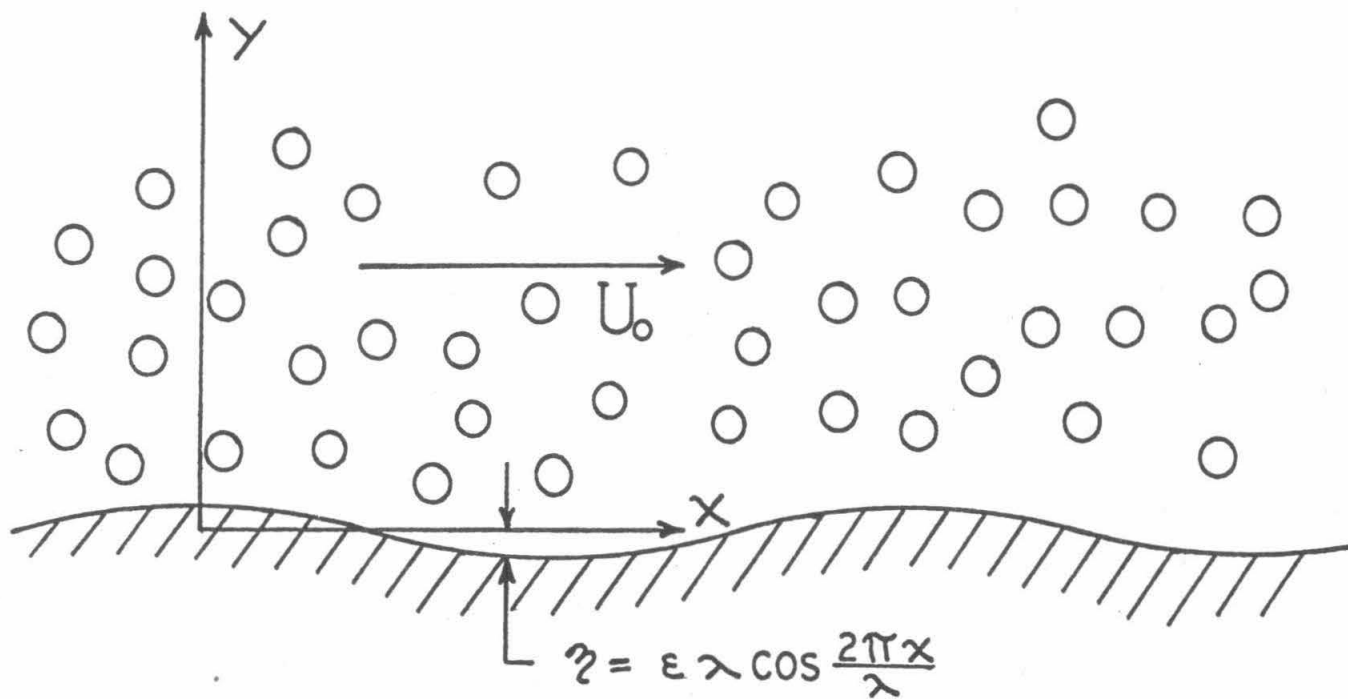


Figure 6.1 Geometry and Notation for Bubbly Flow over a Wavy Wall

CHAPTER 7

Concluding Remarks

It has been the aim of this thesis to develop a consistent set of equations which describe, under some limitations, the flow of bubbly gas-liquid mixtures and apply them in the solution of a few problems that bear on technological issues of nuclear reactor safety.

Interpreting these results, and applying them to the scaling of experimental results, the importance of the ratio of the viscous relaxation time to the characteristic time of the flow is evident. In the case of a choked flow through a contraction this parameter was the dimensionless number $(\frac{L_0}{U_0 \tau_v})$. Examination of this ratio led to the conclusion that in many cases of practical interest the dynamic, rather than viscous, forces on the bubbles almost wholly determine their motion. In analyzing the rise of a cloud of gas bubbles through a liquid, this parameter takes the form of the ratio between the relaxation length, $V_0 \tau_v$, and the characteristic length scale of a disturbance to the flow. Our analysis of the problem was considerably simplified when this ratio was small, and the viscous forces on the bubbles dominated their motion. In the flow of a bubbly mixture over a wavy wall, the important parameter was the ratio of the viscous relaxation time to the time it took the bubbles to pass one wavelength of the wall. The effect of this ratio on the motion of the gas bubbles was clearly demonstrated.

It has also become very clear that substantial extensions

of this work require accounting properly for the bubble interaction forces of both the bubble-bubble and bubble-boundary varieties. Our inability to take bubble-boundary interactions into account causes us not to be able to enforce boundary conditions on the gas velocity at a solid wall. This was shown in the flow over the wavy wall. Our lack of skill in accounting for bubble-bubble interactions renders our theoretical work inaccurate for void fractions higher than about .2. From our speculation in Chapter 5 on the effect of bubble-bubble interactions, it is evident that not only analytical but experimental work as well is required in this area.